ABSTRACT

HAMID HAMEDI, has Designed a Chitosan-based Thermoresponsive Bioadhesive Polymer Composite for Wound Dressing Applications (Under the direction of Profs. Alan. E. Tonelli and Martin. W. King)

Wound healing is one of the most critical issues in clinical care. Designing a safe and effective system that actively close the wound immediately and control bleeding could promote wound healing and reduce the death rate.

Chitosan (CS) is an excellent candidate for biomedical applications due to its biocompatibility, antibacterial, hemostatic and biodegradability properties. Moreover, chitosan could be a safe thermoresponsive biopolymer. Chitosan has some level of bio adhesion property; however, its strength is not good enough in wet condition for some special applications such as wound dressing and suture less surgery. In this study, we aim to design a thermoresponsive bioadhesive based on chitosan and catechol containing molecules extracted from natural resources. di-hydrocaffeic acid is one of our candidates as an adhesive agent. Lactic acid is used for chitosan protonation to provide more adhesive, soft and flexible polymer. Designing a flexible and soft chitosan polymer solution could be more favorable for this application especially when it is applied in some part of body that needs movement and contraction. Due to the presence of different functional group, this design would be an intrinsic self-healing polymer that is very helpful for wound dressing and suture less surgery application. Graphene oxide is applied in our design to take advantage of its special capabilities for improving mechanical, antibacterial and angiogenesis properties of the polymer.

In Chapter one, a brief introduction to this project is presented and some highlights and technology gap is explained. In chapter two, a literature review at current designs are presented. This chapter has two main parts. Part one a literature review on chitosan based bioadhesive. Chitosan/GO film and their application in wound dressing is studied in part two of this chapter. Chapter three, contains materials and methods used in this project. To evaluate polymer properties two main

characterization techniques are applied. First, physicochemical characterization, including: Rheological study, FTIR test, SEM, Nano Ct Scan, Swelling ratio and Water vapor transmission rate, second; In vitro tests like: Biodegradability, antibacterial assay, cell migration, cell cytotoxicity, cell morphology and RT- PCR. In chapter four all results are presented and they are discussed separately in different sections. Conclusion and recommendations are presented in chapter five.

In this project the effect of different additives with different molar ratio and volumetric concertation are studied. Presence of these additives enable us to take advantage of their chemical and physical properties to improve different aspects of this design. In general, our study showed a chitosan based thermoresponsive bioadhesive polymer could be a great candidate for wound dressings. This design also opened some new avenues for biomedical applications of chitosan based thermoresponsive bioadhesive for other biomedical applications like suture-less surgery, localized drug delivery and gene delivery.

Design a Chitosan based Thermoresponsive Bioadhesive Polymer Composite for Wound Dressing Applications

by
Hamid Hamedi

A dissertation or thesis submitted to the Graduate Faculty of
North Carolina State University
in partial fulfillment of the
requirements for the degree of
Doctor of Philosophy

Raleigh, North Carolina
2022

APPROVED BY:

_____	_____
Professor Marin W. King Committee Chair	Professor Alan. E. Tonelli
_____	_____
Professor Samuel M. Hudson	Professor Saad Khan

_____
Professor Ashley Brown

DEDICATION

I dedicate my dissertation work to my parents and my pretty wife Sara Moradi and many great friends.

BIOGRAPHY

Hamid Hamedi is a PhD candidate majoring in Fiber and Polymer science and minoring in Chemical and Bio molecular engineering at North Carolina State University. He received his M.Sc. in the chemical engineering from Iran University of science and Technology (IUST) and BSc. in Chemical engineering From Arak Azad University. Prior to his PhD program, he was research assistant in Prof. Tonelli's lab for a year. As a research assistant, he was working on preparing 3D hydrogel networks based on biopolymers such as chitosan, alginate and polyvinyl alcohol for biomedical applications (wound dressing and drug delivery). In his PhD project, Hamid developed a chitosan based thermos-responsive bio adhesive polymer for biomedical engineering applications focused on wound dressings.

ACKNOWLEDGMENTS

First and foremost, I would like to express my sincere appreciation to my Co-advisor Prof. Alan Tonelli who has provided this opportunity for me to pursue my dream in science and engineering since I joined his lab as a visiting researcher. I appreciate the opportunities and mentorship I received to pursue my Ph.D. degree in his labs and am thankful for his support, help, patience, and guidance throughout my Ph.D. studies.

I would like to thank Prof. Martin King for accepting me in his biomedical research group. I really appreciate his help in teaching me how to conduct scientific research and his useful guidance in Biological studies. He also provided many suggestions for my career and personal life, which was an enormous help.

I also want to thank Dr. Jessica Gluck for her generous support on In vitro tests, and cell culture and PCR training. I also want to thank Prof. S. Hudson, Prof. S. Khan, and Prof. A. Brown for being on my committee and thank them for their valuable time and suggestions in the fields of Polymer, rheology and wound dressings.

I am so grateful for the instrument training, resources, and coaching from laboratory managers of Department of Textile Engineering, Chemistry and Science (TECS), Wilson College of Textiles, and AIF, NC State University. Ms. Judy Elson provided SEM and Ms. Teresa White provided physical testing facilities.

Lastly, I want to thank the most important people in my life. Thanks to my parents, my wife for unconditioned love and support. They always encouraged me, whatever problems I confronted. Lastly, I would like to thank my best friends in the BMT group for their friendship and the Wilson College of Textiles staff for their help and kindness. With them, I will never feel alone during my study abroad. Love you all forever.

TABLE OF CONTENTS

LIST OF TABLES

LIST OF FIGURES

1. CHAPTER ONE: INTRODUCTION

1-1 Highlight and Contribution

Wound healing includes hemostasis, inflammation, proliferation, contraction, and remodeling steps [1]. Chitosan based hydrogels could improve wound healing process in all steps. [2] Most wound healing strategies focused on biochemical improvement of wound dressings. This improvement could be on traditional or modern dressings. Developments on traditional wound dressings include gauze, lint, plasters, bandages (natural or synthetic) and cotton wool that are dry and used as primary or secondary dressings for protecting the wound. Modern wound dressings include foam, film, hydrogels and hydrocolloids acting as a barrier against penetration of bacteria to the wound environment and preparing an appropriate environment for wound healing [3]. Current improvements on modern wound dressings focus on biochemical and biological modification of the wound site including delivery of biologically active agents such as growth factors and cells from the dressing materials. These designs are associated with high cost product, drug side effects, fabrication difficulties and lack of drug release control. [4]

Designing a thermoresponsive bioadhesive is a demanding injectable hydrogel for different applications of wound dressing [5], suture less surgery [6], effective cancer therapy [7], cell delivery [8] and injectable nerve regeneration [9]. In our current design, we aim to develop a thermoresponsive bioadhesive as a wound dressing to be able to close the wound immediately and provide an appropriate environment to accelerate wound healing. Due to the unique properties of chitosan such as biocompatibility, biodegradability, antibacterial properties, low toxicity and immune-stimulatory activities, it is an excellent candidate as a basic polymer for designing a thermoresponsive bioadhesive for wound dressing application. [10], Chitosan also has been used in commercial wound dressings such as ChitoSam, ChitoGauze XR pro and Axiostat®.

There are a few thermoresponsive bioadhesives for wound dressing applications. However, these current thermoresponsive bioadhesive designs for wound dressings have some disadvantages listed below:

- One of the main problems with current bioadhesives is the lack of mechanical properties that is essential to provide cohesiveness to bioadhesive polymers.
- Lack of adhesive properties in wet (bloody) conditions; as presented in the literature review there are some bioadhesive designs that have good adhesive properties in dry condition, due to the presence of blood and exudate in the wound site having good adhesive properties in wet condition is very important.
- Lack of self-healing properties; Self-healing properties would be very helpful when wounds are in a place that needs movement and there is a chance for wound dressing rupture. This property gives us more flexibility for wound dressing application.
- Lack of angiogenesis property; Most of current design do not have angiogenesis property. This property could provide better vessel formation in wound site and provide nutrient and oxygen that are essential for cells.

In this project, we aim to overcome these issues by designing an effective thermoresponsive bioadhesive. In the following parts aims and more details of different steps of this project are presented.

1-2 Aims:

The ultimate goal of this project is designing a safe and effective thermoresponsive bioadhesive polymer for wound dressing to accelerate the wound healing progress. This project is designed in two objectives; basic objective and detail objective. Each step has specific aims.

Basic objective:

- **Specific aim:** Prepare a first design based on chitosan that has both thermoresponsive and bioadhesive properties. Its adhesive properties should be higher than pure chitosan polymers. In addition, Its gelation time should be acceptable in comparison with current design.

Detail objective:

- **Specific aim:** Find efficient compositions of chitosan and other additives that have as high as possible adhesive properties with better biocompatibility (in vitro) and wound healing properties.

2. CHAPTER TWO: LITERATURE REVIEW

2-1 Introduction:

The basic concepts of wound healing, thermoresponsive materials and bio-adhesive polymers are presented in two main different sections. In the first section, different types of chitosan bioadhesives with or without external stimuli responsive properties are presented. Different mechanisms of adhesion are also explained with some examples that have chitosan as an adhesive agent or main component in their structure. This part of the literature review is published in Carbohydrate polymers journal [11].

In the Second section, Graphene oxide as an additive to chitosan is studied. Different Graphene oxide properties like biocompatibility, toxicity and biomedical properties are presented. In addition, Presence of Graphene Oxide in chitosan hydrogel and its effect on wound healing is reviewed in this paper. This literature review is published in Applied Material journals [12].

2-2 Chitosan based Bioadhesives for Biomedical Applications: A Review

2-2-1 Abstract

Due to the promising properties of chitosan for biomedical engineering applications like biodegradability, biocompatibility, and non-toxicity, it is one of the most interesting biopolymers in this field. Therefore, Chitosan and its derivatives have attracted great attention in vast variety of biomedical applications. In the current paper, different types of chitosan-based bioadhesives including passive and active and their different types of external stimuli response structure such as thermo, pH and Light responsive systems are discussed. Different bioadhesives mechanisms with chitosan as an adhesive agent or main polymer component and some examples were also presented. Chitosan based bioadhesives and their potential biomedical applications in drug delivery systems, suture less surgery, wound dressing and hemostatic are also discussed. The results confirmed

wound healing, hemostatic and bioadhesion capabilities of the chitosan bioadhesives and its great potential for biomedical applications.

Keywords: Chitosan, Bioadhesives, Drug delivery, Wound dressing, Suture less surgery

Abbreviation list: GLP-1: Glucagon-like peptide-1, HPMCP: Hydroxypropyl methylcellulose phthalate, LMWH: Low-molecular weight heparin, CSLC: Cancer Stem Like Cell, pNIPAM: poly(N-isopropyl acrylamide), HEC-CS: 2-hydroxyethyl cellulose/chitosan, DOPA: L-3,4-dihydroxy phenylalanine, PVP: Poly vinyl pyrrolidone, TPGS: d-α-tocopheryl glycol succinate 1000, HPMC: Hydroxypropyl methylcellulose, CIP: Ciprofloxacin, LA: Lactic Acid, AA: Acetic acid, AdMSCs: Adipose-derived mesenchymal stem cells, HTCC: N-(2-hydroxypropyl)-3-trimethylammonium chitosan chloride, GRGDS: Glycine-arginine-glycine-aspartic acid-serine, PEG-2000: Polyethylene glycol, CSS: Chitosan succinate, BCI: Blood-clotting index, BFG: Bael fruit gum, TNX: Tenoxicam, GBTI: Gingival bleeding time index, LCST: Lower critical solution temperature, FITC : Fluorescein isothiocyanate, APTT: Activated partial thromboplastin time, VEGF: Vascular endothelial growth factor, FGF: Fibroblast growth factor, EGF: Epidermal growth factor

2-2-2 Introduction

Bioadhesive polymers are a class of polymers to adhere two surfaces where at least one of them is a living tissue. These polymers are drawing attention in different applications from Effective drug delivery, replacement for the surgical sutures and wound dressings. An ideal tissue adhesive should: 1) be safe, sterilizable, nontoxic, easy to prepare and apply to desired area; 2) rapidly solidify in situ to minimize bleeding and surgery time; 3) adhere to tissue strongly and prove hemostatic, tissue healing and regeneration properties, and can control infection; 4) have sufficient mechanical properties; 5) be degradable and absorbable in reasonable time period; and 6) be affordable [13]. Several mechanisms for bioadhesion have been explained in literatures which can be assorted in four categories: mechanical interlocking, chemical bonding, diffusion theory, and electrostatic theory [13, 14]. The interaction between adherent and adhesive substrate are mainly combination of these mechanisms which are described in detail in following section.

Among different candidates for bioadhesive polymers [15], chitosan could be one of the best due to its unique properties such as biodegradability, low toxicity, low immunogenicity, antibacterial and antifungal activities and biocompatibility [16, 17]. Chitosan is a diacetylated derivative of Chitin [18]. Chitin can be soluble in aqueous acidic media when the degree of deacetylation is about 50% or higher and then is called chitosan [19]. Chitosan is most important derivatives of chitin in terms of application as it is abundant, biodegradable, and nontoxic [19]. Resources of chitin can be insects (cuticles) and crustaceans (skeletons) such as crab, shrimp, and lobster. Chitin is also extracted from the exoskeleton of cephalopod species, such as squid, cuttlefish and octopiand [20, 21, 10]. Chitosan preparation from fungal cell walls with fermentation technology has become an alternative economical way to produce this polymer. It can be found in the cell wall of certain groups of fungi, particularly zygomycetes [22]. The most important advantage of this method is that the cell wall of zygomycetous fungi contains a large quantity of chitosan and by managing the parameters of fermentation process, chitosan with desired physicochemical properties can be accessible [10]. Sufficient amounts of chitosan have also been identified in *Mucor rouxii, phycomyces, saccharomyces, R.miehei* and *M.racemosus* [23, 24, 25].

Chitosan bioadhesives have been wildly used in various biomedical applications such as drug delivery, wound dressings, hemostatic and sutureless surgery. Chitosan-based buccal bioadhesive were designed by Kumria et al. [26] for delivery of zolmitriptan in the treatment of migraine. It was observed that the chitosan buccal film could be used in both prophylaxis and acute treatment of migraine, however further *in vivo* and clinical tests are needed. Guyot et al. [27] developed an Injectable bioadhesive catechol-chitosan hydrogels using sodium bicarbonate as a gelling agent. Bioadhesive chitosan coated PLGA nanoparticles were developed by Ameeduzzafar et al. [28] for improvement of ocular efficacy of Levofloxacin in the treatment of conjunctivitis which is a

common infection of ocular surfaces. Pardeshi et al. [29] synthesized N,N,N-trimethyl chitosan film for regulating bioadhesive and nasal membrane permeation properties.

In this review study, different types of chitosan bioadhesives with or without external stimuli responsive properties are presented. To the best of our knowledge, there is not a comprehensive review paper about different biomedical applications of chitosan-based bioadhesive systems. There are some review papers about biomedical applications of bioadhesives but not specifically chitosan-based. Some of the main applications of these chitosan based bioadhesives in biomedical engineering are discussed. Different mechanisms of adhesion are also explained with some examples that have chitosan as an adhesive agent or main component in their structure. The outcome of this review paper can help researchers and even industrial community to realize recent studies done in the field of biomedical applications of chitosan bioadhesives for further investigation and/or commercialization.

2-2-3 Chitosan

Chitosan is a linear polysaccharide composed of randomly distributed (beta-1-4) N-acetyl-D-glucosamine materials. It produces from deacetylation of chitin and its properties are strongly dependent on degree of deacetylation, polydispersity, and molecular weight. Chitosan is one of the most widely used materials for biomedical applications such as wound dressings [30, 31, 32, 33]. It has excellent biocompatibility, low toxicity and immune-stimulatory activities which was described in detailed in our previous review paper about applications of chitosan hydrogels on wound dressings [10].

2-2-4 Chitosan-based bioadhesives

Bioadhesive systems have attracted many interests owe to their ability to localize drug delivery along with controlled release. A liquid adhesive is characterized by three values: surface tension,

viscosity, and penetration on the material support. The surface tension allows the surface of a liquid to resist an external force and viscosity is a measurement of liquid resistance to gradual deformation such as spreading [14]. Bioadhesives are made of synthetic or natural polymers. Most of the current synthetic bioadhesive polymers are polyacrylic acid or cellulose derivatives. (semi) natural bioadhesive polymers include chitosan and various gums such as guar, gellan, pectin, and alginate [34].

Tissue adhesion ability of cationic chitosan hydrogels is limited, probably because chitosan hydrogels weakly interact with tissues which is mainly due to charge interactions without forming mutually entangled chains between the two contacting interfaces [5]. Several studies have tried to improve bioadhesive properties of the chitosan by conjugating different adhesive agents to chitosan backbone. Due to variety of proteins in body tissues, different adhesive agents are needed, but most of the studies have focused on wound healing and mucoadhesive applications of bioadhesives. Balakrishnan et. al [6] developed an in situ bioadhesive including chitosan and dextran. Adhesive strength was in the range of 200–400 gf/cm^2 which is about 4–5 times of fibrin glue at comparable setting times. The adhesive showed burst strength in the range of 400–410 mm of Hg which can be applied in many surgeries for controlling bleeding even at high blood pressure. The prepared adhesive also was effective as a drug delivery device. Lih et. al [35] fabricated chitosan/polyethylene glycol/tyramine bioadhesive hydrogels which were rapidly formed in situ using horseradish peroxidase and hydrogen peroxide. The hydrogels showed adhesiveness ranging from 3 to 20 times of fibrin glue (Greenplast®). Chitosan hydrogels formed very fast within 5s after contact with the skin of rats. Some other adhesive conjugated agents on the chitosan and their applications are presented in Table 2-1.

Table 2-1 Adhesive conjugated agents on chitosan

Adhesive agents	Applications	Tested site	Dry Adhesion strength	Wet adhesion strength	Biocompatibility	Biodegradability	Ref.
Dextran	Wound dressing and suture less surgery	Defatted rat (Wistar male) skin	20-40 kPa	-	95-100% after 24 hrs	50 % after 45 days	[6]
Polyethylene glycol / tyramine	Wound dressing and suture less surgery	Porcine skin	17–97 kPa	-	N.R.	N.R.	[35]
ε-polylysine	Tissue sealants, hemostatic and drug delivery	Glass costed by layer of gelatin matrix	80-90 kPa	-	100-120% after 72 hrs	N.R.	[36]
Catechol	Drug delivery depots, tissue engineering hydrogels, tissue adhesives, Hemostasis application	Mouse subcutaneous tissue	7-15 kPa	-	N.R.	0-40% after 30 days	[5]
	Hemostasis application	Defatted porcine skin	1-5 kPa	3-4 kPa	100-140 % after 72 hrs	N.R.	[37]
	Biomedical applications	Mouse subcutaneous tissue	5-35 kPa	-	50-98 % dose dependent	N.R.	[38]
	Mucoadhesive film	Rabbit small intestine	0.25-1 kPa	-	N.R.	N.R.	[39]
	Biomedical adhesive	Glass	40-400 kPa	50-500 kPa	N.R.	N.R.	[40]

N.R. (Not Reported)

Bioadhesives can be categorized into two main groups; passive and active (which also called external-responsive) bioadhesives which are explained in detail in the following sections.

2-2-4-1 Passive chitosan-based bioadhesive

Passive bioadhesives do not respond to the external stimuli. Loratadine-loaded Chitosan/ethyl cellulose composed microspheres were prepared by spray-drying of simple dispersion, emulsion and suspension methods and compared with chitosan microspheres for nasal delivery system [41]. Composed microspheres improved loratadine entrapment. Tensile test showed that increasing chitosan concentration increased bioadhesive properties of the microspheres and effect of suspension method on bioadhesive properties of the microspheres was more than emulsion method. Chitosan was combined with hydroxypropyl methylcellulose, sodium carboxymethyl cellulose or guar gum to produce fluconazole vaginal tablets [42]. Among the different combinations, chitosan: guar gum: PVP at 1:2:1 ratio had higher antifungal activity, longer bioadhesion time, and was safe to vaginal mucosa. Shalaby et al. [43] developed and optimized insulin-loaded cationic liposomes coated with bioadhesive chitosan for oral delivery. Release of insulin was very low release (18.9%) in simulated gastric fluid in comparison with intestinal fluid (73.33%) after 48 hours. After one hour of oral administration of chitosan-coated liposome, a significant decrease was observed in glucose level (129.29± 3.15 mg/dl) which continued until 8 hours.

2-2-4-2 Active chitosan-based bioadhesives

External-responsive bioadhesives can change their chemical and/or physical properties such as swelling, structure and mechanical properties upon exposure to external stimuli like temperature, pH, light, ionic strength, electric or magnetic field.

2-2-4-3 Thermo-responsive chitosan-based bioadhesive

Hydrophilic and hydrophobic groups present a great balance in the structure of thermo-responsive polymers. Most of thermo-responsive polymers have hydrophobic group such as methyl, ethyl, and propyl which their interactions with water molecule in different temperature present their thermo-responsive properties [44]. Due to the balance between hydrophilic or hydrophobic groups, a small change in the temperature of the polymer solution can lead to a new adjustment of the hydrophilic and hydrophobic interactions between the polymer blocks and water molecules [45] (Figure 1A). As presented in this figure by increasing temperature above lower Critical Solution Temperature (LCST), aqueous polymer solution start to phase transfer (one phase or soluble state toward two-phase or phase separation).

Thermo-responsive polymers could be classified in three main groups; 1) include hydrophobic and hydrophilic repeat units on their backbone and do not need any gelling agents (Copolymer), Poloxamer is an example that Polyethylene oxides are two hydrophilic groups and Poly propylene oxide is a hydrophilic group on a polymer structure (Figure 2-1B,a), 2) include hydrophobic and hydrophilic groups as a separate functional groups (Copolymer) but need a gelling agent to form a thermo-responsive polymer. Chitosan is an example with acetyl glucosamine repeat unit as a hydrophobic and glucosamine as a hydrophilic group which can show thermo-responsive property by adding a polyol such as beta glycerophosphate (Figure 2-1B,b), and 3) have both hydrophobic and hydrophilic groups on a single repeat unit and do not need any gelling agent (Figure 2-1B,c).

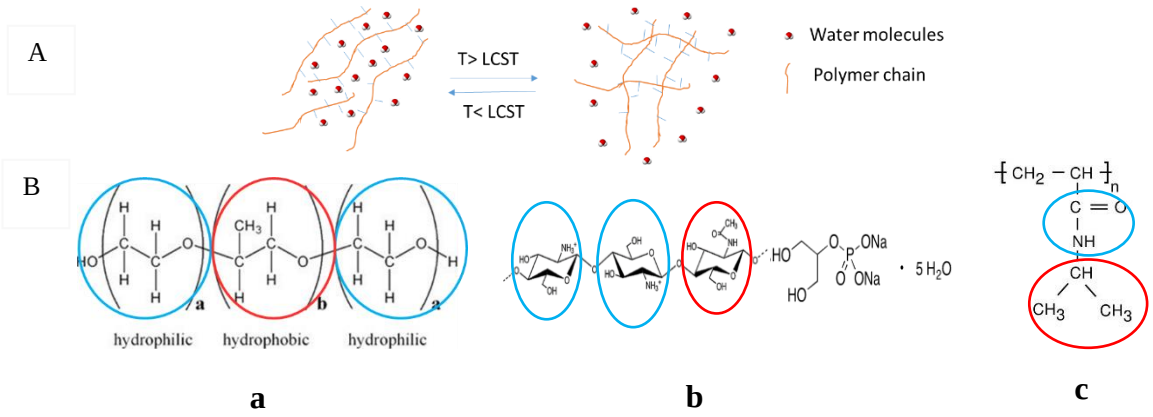

Figure 2-1 A) Hydrophobic and hydrophilic interaction in thermoresponsive polymers and B) a) first group of thermo-responsive polymers that have hydrophobic ( ) and hydrophilic ( ) functional group in different repeat units, b) Second group of thermo-responsive polymers that needs gelling agents) third thermo-responsive polymers that has hydrophobic group in a single repeat unit (no need to gelling agent)

Catechol-hydroxy butyl chitosan was prepared as a thermo-responsive bioadhesive. In this polymer structure, Dopamine as a catechol group is an adhesion part and Hydroxy butyl is a thermo-responsive or gelling group. The thermo-responsive ability of the hydrogels was based on the changes of intramolecular/ intermolecular hydrogen bonds and hydrophobic interactions generating from hydroxy butyl groups as is shown in Figure 2-2. The amino groups on chitosan backbones and the catechol groups introduced by amidation reaction made the hydrogel attach firmly to tissues by multiple interactions, including hydrogen bond, π–π stacking, cation–π interactions, and synergistic interplay. The bioadhesives were thermosensitive, injectable, biodegradable, biocompatible, and wound hemostatic [37].

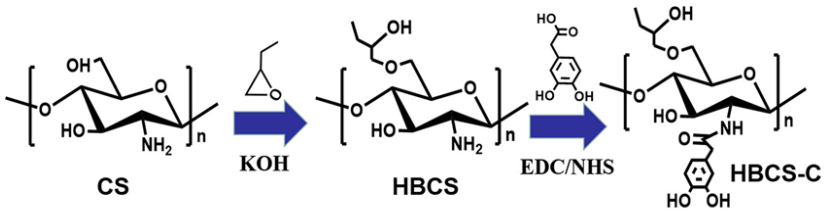

Figure 2-2 Chemical reaction of the Catechol-hydroxy butyl chitosan hydrogels (HBCS-C) [37]

Ryu et. al [5] developed catechol-conjugated chitosan and thiol-terminated Pluronic bioadhesive hydrogels for drug delivery, tissue adhesives, and antibleeding applications. The hydrogels were

thermosensitive and injectable with great mechanical properties and stability in vitro and in vivo. They could form adhesive gels to the tissue immediately after injection which may be a good potential for biomedical applications.

In the following table different functionalities of the chitosan as a thermo-responsive or bioadhesive part in the thermo-responsive- bioadhesive system has been presented.

2-2-4-4 pH-responsive chitosan-based bioadhesive

Most pH-sensitive hydrogels have a high density of separable acidic or alkaline groups with the ability of ionizing at a certain pH [46]. As Chitosan is a cationic polyelectrolyte and soluble in the acidic medium, would show a liquid–gel transition around pH 6.5, when pH changes mildly from acidic to neutral. Increasing the pH-neutralizes cationic chitosan and generates three-dimensional structure owe to the formation of hydrogen bonds [47] (see Figure 2-3). Dudhani et. al [48] prepared and characterized bioadhesive chitosan nanoparticles with or without catechin. Fluorescein isothiocyanate (FITC)/chitosan were synthesized to investigate mucoadhesion properties. They studied the effect of pH on the nanoparticle size and adhesion and showed that at pH 4.5, the size of chitosan nanoparticles was larger than those prepared at pH 5.5. The ionic crosslinking process for the formation of chitosan nanoparticles is pH-responsive which can be applied for the modulating of the chitosan nanoparticle's properties. At higher pH more cross-linked particles are formed in comparison with lower pH. pH is also an important factor for entrapment efficiency, loading capacity and yield of the loaded drug. Entrapment efficiency and yield at pH 4.5 were higher than those at pH 5.5 except for loading capacity. pH may have a remarkable role during particle formation and in the encapsulation of bioactives. Chitosan nanoparticles loaded with catechin had higher mucoadhesion. It may be due to the presence of catechin in the structure which decreased the particle size notably. Shrestha et al [49] developed a

mucoadhesive and pH-responsive nano-system based on chitosan for advanced oral type 2 diabetes mellitus therapy. Glucagon-like peptide-1 (GLP-1) was used as a model peptide for dual protein-drug oral delivery. GLP-1 is an antidiabetic peptide which increases insulin secretion in a glucose-dependent manner. The system showed controlled drug delivery, enhanced mucoadhesion and improved intestinal permeability which exhibited a high potential for synergistic therapy.

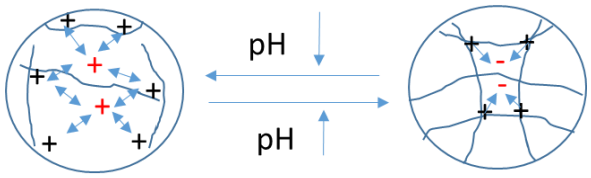

Figure 2-3 effect of pH on sol-gel formation of chitosan polymer

Fan et al. [50] developed pH-responsive and mucoadhesive thiolated chitosan and hydroxypropyl methylcellulose phthalate (HPMCP) nano-system for oral bioavailability of low-molecular weight heparin (LMWH). The intestinal mucoadhesive property improved compared to the control group which is based on the immobilization of thiol groups on chitosan. APTT assay was used for investigating the coagulating effect of nanoparticles on plasma through single oral administration of different samples in rats. The LMWH-loaded nanoparticles had enhanced anticoagulant effects indicating that prepared nanoparticles could promote drug absorptions due to the synergistic effects between the pH-sensitivity of HPMCP and permeation ability of thiolated chitosan.

Cell adhesion of pH-responsive chitosan bioadhesives has been investigated by several studies [51, 52, 53]. Yena et. al [54] applied chitosan-based pH-responsive system to isolate Cancer Stem Like Cell (CSLC) from A549 cells via integrin β4. The pH-dependent cell isolation on chitosan could serve as a label-free platform and the isolated subpopulation with low adhesiveness had superior cancer stem-like cell hallmarks compared to those with high-adhesiveness. Injectable mucoadhesive and pH-responsive hydrogels including chitosan/dihydrocaffeic acid/oxidized

pullulan were fabricated for localized drug delivery by Liang et al. [55]. Anti-cancer drug, doxorubicin, was used as a drug model for investigating the pH-sensitive drug release behavior of the hydrogels. The hydrogels had good drug release, effectively killing colon tumor cells (HCT116 cells) and good antibacterial properties against *E. coli* and *S. aureus.*

2-2-4-5 Light-responsive chitosan-based bioadhesive

Two main categories of the light-responsive bioadhesives are explained here. Photothermal-responsive polymers in which light (mostly near infrared laser) is altered to the heat as a stimulus agent to induce polymer solution to respond [7]. Platinum nanoparticles [56], organic compounds [57], Gold nanoparticles [58], graphene oxide nanosheets [59], and carbon nanomaterials [60] are some of the photothermal agents that apply inside of polymer structure to provide near infrared-responsive polymer solutions. Second group includes mostly UV-responsive polymer solution that provide a crosslinking due to the UV shining.

2-2-4-6 Photothermal-responsive chitosan-based bioadhesive

Matteini et. al [61] introduced a novel combination of Gold Nano rods as a photothermal agent and chitosan in form of biocompatible film with improved mechanical properties, and effective laser-activatable adhesion via photothermal conversion and H-bonds formation. when this colloid exposed to near-infrared laser light, the Gold Nano rods carry out efficient photothermal conversion activating the polar groups of chitosan strands and mediating functional adhesion with a biological tissue. In another study, they worked on the effect of pulse power and duration on adhesive properties to find the optimal condition to decrease detrimental superheating [62]. Xu et. al [63] developed a chitosan light-responsive based on the Fe_3O_4 as a photothermal agent. In this study, Fe_3O_4 NPs doped inside of chitosan–catechol–pNIPAM, resulting to remotely controllable thermo-responsive adhesion/detachment behavior over the skin upon near-infrared laser

irradiation. The wet adhesion and lubrication properties of the chitosan–based bioadhesives could be controlled due to its temperature responsiveness where the wet adhesion increased from 0.63 to 3.18 kPa by increasing the temperature from 10 to 40 °C.

2-2-4-7 UV-responsive chitosan-based bioadhesive

In these polymers, a photosensitive agent is conjugated on the chitosan backbone (mainly to its amine groups) and are classified as photo-crosslinking polymers. Stoyneva et. al [64] developed a cryogel from chitosan and 2-hydroxyethyl cellulose (HEC-CS) was prepared by UV irradiation. Resultant gel showed pH-responsivity and good bioadhesive properties. Their result indicated that pure HEC did not have adhesive property, while HEC-CS treated by UV (azide and lactose moieties as photo-crosslinkable derivative) had better adhesive property. Increasing the amount of crosslinker significantly enhanced the elastic modulus of the bioadhesive [65]. Ono et. al [66] conjugated azide and lactose on the chitosan structure to take advantages of photo crosslinkable agents and bioadhesive property of the chitosan for designing a UV-responsive chitosan based bioadhesive for surgery applications. Chitosan hydrogel prepared with UV irradiation could stop the bleeding about 1 minute quicker than fibrin glue while hydrogels prepared without UV irradiation were unable to block the bleeding. Also, applying chitosan-based hydrogel with UV irradiation for 90 seconds could stop air leakage from the lung and further evaluation exhibited full expansion of the sealed lungs.

2-2-5 Mechanisms of Chitosan Bioadhesives Performance

Mechanism and theories of bioadhesion could be classified in four main categories [13, 14]. Electronic theory, mechanical interlocking, intermolecular/interatomic bonding (adsorption theory) and Chain entanglement (interdiffusion theory) [67, 68] . The interaction between adherent and adhesive substrate mainly are a combination of these mechanisms. Electrostatic interactions

(electronic theory) and hydrogen bonding (adsorption theory) are two common mechanism of chitosan adhesion. Hydrogen bonding sites (in case of adsorption theory) and protonation site (in case of electronic theory) for chitin and chitosan are presented in

Figure 2-4. Lee et. al [69] studied interactions of protonated chitosan (in acidic medium) in aqueous solution, their results showed that due to the electrostatic interactions between positively charged chitosan and negatively charged surface, it adheres to the surface well. They also observed hydrogen bonds and van der Waals forces between d-glucosamine and hydrated surface or adherent which play a main role in adhesion process. The chitosan interactions decreased with increasing buffer pH, which is proposed to be mainly due to the reduction in solubility of chitosan molecules as they are not protonated at higher pH. The mechanisms of bioadhesives are explained in detailed in the following.

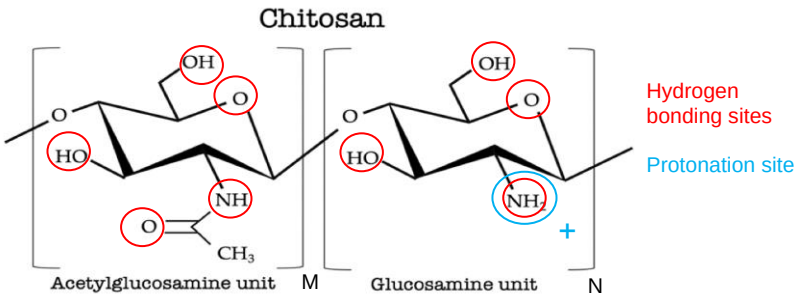

Figure 2-4 Protonation sites and Hydrogen bonding sites in case of chitin (M>N) or chitosan (N>M)

2-2-5-1 Mechanical interlocking

In the mechanical interlocking, adhesive substrate penetrates the pores and rough surfaces and fills them, consequently the wettability of the adhesive substrate plays main role (Figure 2-5a). Better wettability leads to better adhesion. Van der Leeden et. al [70] reported that in lower wettability, surface roughness may play negative role and reduce the adhesive property owe to decrease in available contact surface, lower surface adhesive interaction and less adhesion. Ruprai et al [71] showed that possible bonding mechanisms for porous oligomer chitosan/L-3,4-dihydroxy

phenylalanine (DOPA) films on tissue without green light exposure is mechanical interlocking. Depan et. al [72] dispersed graphene oxide in chitosan matrix instead of covalently linked and showed that the nanoscale roughness would be likely to contribute to mechanical interlocking with the macromolecular chains of chitosan.

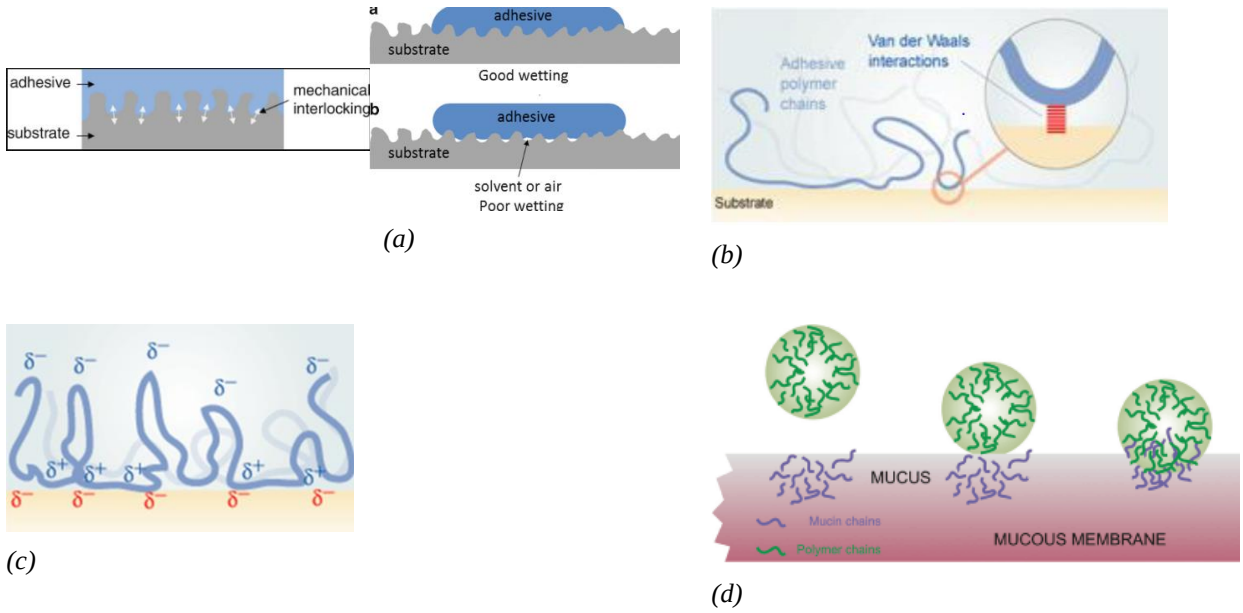

Figure 2-5 Bioadhesive mechanisms

2-2-5-2 Intermolecular/ interatomic bonding

This mechanism attributes the formation of an adhesion bond to surface chemical forces. Hydrogen, covalent, and ionic bonds are some of the strong intermolecular/interatomic interactions (Figure 5b). Covalent (150–950 kJ mol^{-1}) and ionic (400–800 kJ mol^{-1}) bonds have much more stronger interactions compared to hydrogen bonds (10–40 kJ mol^{-1}) and van der Waals forces (2–15 kJ mol^{-1}) [14]. Due to the presence of amine group, chitosan can form hydrogen bonding with different proteins and amino acids of human body for topical applications. There are several studies that used DOPA for improving adhesive property of the chitosan [39, 5]. Ai et al. [73] reported that DOPA can play two main roles in adhesion process: one as a catecholic anchor which absorb chemically to the surfaces through various mechanisms like hydrogen bonding. Other one is that

it can easily be oxidized enzymatically or chemically to form DOPA-quinone to act as a covalent crosslinking unit. Mucoadhesion polymers based on chitosan is another example of the intermolecular/ interatomic interactions which is composed of attractive bonds like Van der Waal forces and hydrogen bonding [74, 75].

2-2-5-3 Electrostatic theory

In electrostatic theory forces in the form of an electrical double layer are produced at the adhesive–adherent interface (Figure 5c). These forces are primarily dispersion forces arising from the interaction of permanent dipoles. Such interactions are only effective on a very short range (less than 0.5 nm), and their effectiveness decreases with the sixth or seventh power of the distance of separation [76]. Mechanistic studies of chitosan and mucin have shown that the electrostatic interaction between the positively charged amines on the polymer chains and the negative sialic acid residues on the mucin glycoprotein play a role in the mucoadhesive properties of chitosan [77]. He et. al [63] indicated that mucoadhesive property of chitosan is due to electrostatic interactions between sialic acid and chitosan.

2-2-5-4 Chain entanglement or interdiffusion theory

This theory is based on the ability of adhesive and adherent to penetrate inside of each other (mainly penetration of adhesive to adherent) (Figure 5d). The penetration rate depends on the diffusion coefficients of both interacting polymers, and the diffusion coefficient is depended on molecular weight, cross-linking density, segment mobility, and flexibility of the bioadhesive polymer [34]. Interfacial tension has been shown that is proportional to $\chi^{1/2}$, where χ is the Flory polymer–polymer interaction parameter. Lower amount of χ leads to better polymer-polymer interaction (diffusion) and an increased miscibility [78]. Based on this theory, the larger chain length, the better chain entanglement and bioadhesion. There is no individual bioadhesive theory

that could be able to explain all aspects of an adhesion phenomena, so the polymer interactions are considered as combinations of all these theories. Suknunthat et. al [79] evaluated the mucoadhesion of chitosan, polyvinylpyrrolidone (PVP), and chitosan/PVP using various techniques and showed that mucoadhesion is a complex phenomenon needing combination of different theories to explain it. The diffusion theory is one of these theories. It could explain the interpenetration and physical entanglement of the mucus and the mucoadhesive.

2-2-6 Biomedical applications of chitosan based bioadhesives

Different types of cationic, anionic, and nonionic polymers can be used in designing mucoadhesive systems, however, cationic polymers have higher mucoadhesive power in comparison with other polymers [80]. Chitosan is one of the most widely used cationic biopolymers in preparation of the bioadhesive delivery systems. It is reported that coating micro- and nanoparticles with chitosan can increase drug adsorption to mucosal surfaces, particularly in nasal drug delivery. Beside its hydration in the nasal cavity, interaction of the positively charged amino groups with the negatively charged sites on the mucosa surface helps to mucoadhesion [81]. But chitosan is insoluble at neutral and basic environments like large intestine and colon. So, it can't be used as a penetration enhancer. To overcome this problem, chitosan's solubility can be increased by trimethylating its primary amino groups [82]. Chitosan can be easily modified by adding different chemical groups into its structure, particularly to the C-2 position. Such modifications allow researchers to resolve pharmaceutical challenges by applying chemically modified chitosan in mucoadhesive delivery systems [80, 82].

Chitosan as a cationic polysaccharide with the ability to bioadhesion to the corneal surface has been vastly used in the ophthalmic preparation. It is because of the chitosan electrostatic attraction

and penetration-enhancing property which is mostly owe to the opening of the tight junctions in epithelial cells leading to the increase of absorption across the mucosal [83].

Lectins are other examples of materials used to develop bioadhesives systems. They are chemically proteins with the ability to bind with carbohydrate residues. Lectin-based bioadhesive can be applied in targeted delivery of bioactive molecules. However, lectins can be toxic and show immunological problems. Also, lectin-induced antibiotics can block interaction between lectin-based drug delivery systems and bioadhesive surface [80].

2-2-6-1 Drug delivery

Tan et al. [83] developed a colloidal system containing timolol maleate chitosan coated liposomes as a potential carrier for ocular drug delivery. Prepared structure had an extended drug release, significant mucin adhesion and increased permeability coefficient (Papp) in comparison with commercial eye drops, resulting in a significant enhancement of corneal permeation. The ocular irritation study indicated that the developed liposomes produced no significant irritant effects. Their results indicated that the prepared chitosan bioadhesive can be beneficial for improving ocular retention time, corneal permeability, and bioavailability of timolol maleate in comparison with commercial timolol maleate drops.

In Plapied et al. [84] study, chitosan was used to encapsulate a plasmid DNA coding for a reporter gene. Prepared nanoparticles had a high association of DNA and protected the plasmid against nuclease degradation. Fungal trimethylchitosan was also tested but the complexes interactions were too strong to induce transfection in vitro. Quantification seemed to show that more DNA was associated with the cells when incubated with chitosan nanoparticles and that the presence of M cells slightly influenced DNA uptake when complexed with chitosan. It was found that this

chitosan nanocarrier can be a promising candidate for oral gene delivery and oral DNA vaccination.

In another study, the ability of using chitosan (different molecular mass and viscosity) as a vaginal mucoadhesive gel for evaluation of release of econazole nitrate and miconazole nitrate was evaluated [85]. One of the important parameters for vaginal gel compatibility is pH of the formulation. The results showed that type of chitosan did not have significant effect on pH of the gels but adding econazole nitrate and miconazole nitrate into the structure remarkably reduced values of the pH. It was found that chitosan gels with medium molecular weight had high mucoadhesive, suitable mechanical and release properties with good vaginal retention and may be applied as an antifungal agent for treatment of vaginal candidiasis. Other examples of chitosan bioadhesives applications in drug delivery systems are presented in Table 2-2.

Table 2-2 Applications of chitosan bioadhesives in drug delivery systems

Ingredients	Potential Applications	Type of adhesive	Type of Structure	Ref.
Chitosan/alginate	Controlled release of theophylline	Mucoadhesive	Beads	[86]
Chitosan	Buccal delivery of metformin	Mucoadhesive	Discs	[87]
TPGS[1]-chitosan	Brain targeted drug delivery	Bioadhesive pH- sensitive	Micelles	[88]
Chitosan	Oral delivery of insulin	Mucoadhesive pH-sensitive	Microparticles	[74]
Chitosan/HPMC[2]	Intestinal drug delivery	Mucoadhesive	Hydrogel Particles	[89]
Chitosan/PVA	Buccal delivery of zolmitriptan	Mucoadhesive	Film	[26]
Chitosan/pectin	Antipsychotic drug delivery	Mucoadhesive pH-sensitive	Nasal inserts	[90]
Catechol-chitosan	Buccal drug delivery	Mucoadhesive	Hydrogel	[91]
lyophilized chitosan	Protein drug delivery via buccal mucosa	Mucoadhesive	Wafer	[92]
Chitosan/ hyaluronic acid	Controlled release of lidocaine	Bioadhesive pH- sensitive	Film	[93]
Chitosan	Nasal Delivery of Insulin	Bioadhesive	Gel	[94]

[1]d-α- tocopheryl glycol succinate 1000

[2]Hydroxypropyl-methylcellulos

2-2-6-2 Wound dressings

A bioadhesive wound dressing film based on weisocyanate/dendronized PVP/crosslinked chitosan loaded with ciprofloxacin (CIP) was developed by Garcia et. al [95]. Ciprofloxacin is a fluoroquinolone with high antibacterial effects and is used for various topical applications. The prepared films could inhibit the growth of *S. aureus* and *P. aeruginosa* (Gram-positive and Gram-negative) bacteria. The irritation results (scores lower than 2) showed that films are non-irritant. Biocompatibility and bioadhesion tests on the eyes of male rabbits showed that the films have the ability to be applied for topical applications.

Wittaya-areekul and Prahsarn [96] prepared a chitosan-based bioadhesive film with corn starch and dextran for wound dressing application. In this study propylene glycol was added to the polymer structure to improve the film flexibility which had negative effect on bioadhesive property of the film. They chitosan/dextran films with added propylene glycol showed the lowest and very homogeneous detachment forces in comparison to the pure chitosan films and the chitosan/corn starch films. Addition of dextran and corn starch did not affect the bioadhesive properties very much. The prepared bioadhesives could protect against microbial penetration proofing their ability to be used as wound dressing.

Khan et. al [97] studied the effect of chitosan solvent on bioadhesion and wound healing process. They developed chitosan-based wound dressings with two different solvents: acetic acid and lactic acid and compared with a commercial product, Omiderm®. Their study indicated that chitosan dissolved in Lactic Acid (Chitosan-LA) had better bioadhesion than that of dissolved in acetic acid (Chitosan-AA) (detachment force 0.71 vs. 0.47 N), however it had lower tensile strengthen. Chitosan-LA did not have irritant effect on skin and did not cause any skin allergic reaction. The irritation index of chitosan-LA and Omiderm were almost close, but the irritation index of

chitosan-AA was about 16 times higher. They concluded that Chitosan-LA is more adequate for managing of wound healing and skin burn. Some other examples of application of chitosan bioadhesives in wound dressings are given in Table 2-3.

Table 2-3 Applications of chitosan bioadhesives in wound dressings

Materials	Tested site	Dry Adhesion strength	Wet Adhesion strength	Biodegradability	Cell viability	Ref.
Chitosan/Laponite	Pig ear skin	0.35-0.71 N	-	N.R.*	95-100%	[98]
Chitosan/Fucoidan	Chicken back skin	-	405.0- 7162.0 (mN/cm2)	N.R.	N.R.	[99]
Chitosan/Eudragit RS 30D	Pig's intestine	-	0.49-0.74 N	N.R.	N.R.	[100]
Chitosan/Alginate	Mouse skin	-	0.166-0.383 N	N.R.	0.124- 0.829 (O.D at 570 nm, 24 hrs)	[101]
Chitosan/Collagen	Mouse skin	0.26-0.35 N	-	+30 days	N.R.	[102]
Chitosan/Curcumin/Deformable Liposomes	Human skin	0.17-0.23 N	-	N.R.	N.R.	[103]
Chitosan/ hydrocaffeic acid/ Hydrophobically modified chitosan	Pig skin	-	4.0-8.0 KPa	4 weeks	1.25 (O.D at 570 nm, after 5 days)	[104]
Azide Chitosan/lactose	Mouse skin	117.0 - 304.0 mN/cm^2	-	N.R.	N.R.	[105]
Oxetane-grafted chitosan/ polyurethane	Pig skin	373-415 kPa	-	< 25% after 55 days	40-85% after 7 days	[106]
Silk fibroin/ polylysine/ chitosan	Rat skin	60-75 kPa	-	35-40% after 10 days	95-105%	[107]

* Not Reported (N.R.)

2-2-6-3 Replacement for surgical suture

Nerve regeneration and re-innervation are usually difficult after peripheral nerve injury. Compared to the direct suture method, chitosan conduits have showed good clinical recovery with small gaps (2 mm) [108]. Ruprai et. al [109] fabricated porous chitosan adhesive with the ability of supporting stem cells by photochemical tissue bonding technique. This surgical technique can avoid risk of thermal tissue injuries and use of sutures to maintain strong tissue connection. Porous adhesive films (pore diameter ∼110 μm) could keep similar tissue bonding strengths (13−15 kPa) compared to that of the nonporous adhesives when photoactivated. The porous film could be seen in SEM photos to conform to tissue, and it may be hypothesized that the porosity of the adhesive increases tissue interlocking, leading to higher bonding strength.

Lauto et. al [110] designed a chitosan-based strip bioadhesive that can adhere two side of separated Sciatic nerve. This laser active strip can adhere Sciatic nerve well (11.0 KPa) by shining a light with 808 nm wavelength for 54 second. The laser irradiation led to the mild coagulation of the tissue under the chitosan adhesive, but there were no signs of tissue charring, ablation, or vacuoles in the histology test. The nerve anastomoses were complete and chitosan bioadhesive kept the nerve tight 3 days after the operation. There were no gaps between the nerves, and they were continuous. In comparison with other surgical glues, the chitosan bioadhesive has the advantage of being insoluble in physiological fluids, while fibrin glues and albumin solders are soluble. The chitosan bioadhesive is flexible and does not break or fold during applying the force. Another chitosan-based sutureless scaffold has been designed by Lauto [111], which is able to adhere small intestine submucosa (SIS) to tissue like a bioadhesive (shear stress 9.6 kPa). Suturing is a common technique for this purpose, but it may damage the structure of the extracellular matrices and create technical difficulties, especially during laparoscopic procedures. Due to the presence of low conductive biopolymer in the structure of this laser active scaffold, the

temperature of wound site does not increase above 30°C. Consequently, proteins (collagen, fibronecting and laminen) or growth factors (such as VEGF, FGF, EGF and TGF-b) can be avoided from irreversible thermal denaturation.

Shokrollahi et al. [112] developed a dual functional Polypropylene mesh with antibacterial and anti-adhesion properties on the front and adhesion properties on the backside for hernia repair. The backside of mesh was coated with polycaprolactone nanofibers modified by L-DOPA bioadhesive and the front side was made of polycaprolactone /carboxyethyl-chitosan /polyvinyl alcohol nanofibers with various ofloxacin concentrations. Coating backside of the mesh with Dopa was because of fixing the polycaprolactone meshes during the sutureless surgery, improving the regeneration of new tissue and cell growth that helps repairing of damaged hernia. Prepared meshes with ofloxacin less than 20wt% had better Adipose-derived mesenchymal stem cells (AdMSCs) adhesion prevention, cell viability and great antibacterial activity. DOPA could increase the surface properties of the polycaprolactone mesh, and improve spreading, adhesion, and proliferation of cells. There are some other studies about the applications of chitosan bioadhesives which are shown in Table 2-4.

Table 2-4 Applications of chitosan bioadhesives in surgical suture replacement

Materials	Application	Dry Adhesion strength	Wet Adhesion strength	Leak pressure	Biodegradability	Ref.
Chitosan/Poloxamer	Ocular mucoadhesion	-	0.1007- 0.1275 N		N.R.	[113]
Chitosan/chromophore ICG	corneal and sclera incisions	-	-	233 mmHg	15-30% after 30 days	[114]
Chitosan/Rose Bengal	Median nerves repair	0.37 N	-	-	N.R.	[115]
Periodate/oxidized chitosan/polyethylene glycol/tyramine	Wound sealant	75-105 KPa	-	-	N.R.	[116]
Polyethylene glycol diacrylate/quaternized chitosan/tannic acid	sutureless surgical material	12.0-22.0 N	-	20-65 KPa	100% after 6 weeks	[117]

Not Reported (N.R).

2-2-6-4 Hemostatic Applications

Lih et. al [35] fabricated chitosan/polyethylene glycol/tyramine bioadhesive hydrogels which were rapidly formed in situ using horseradish peroxidase and hydrogen peroxide. The hemostatic ability of the hydrogels was evaluated on the basis that bleeding from liver defects was significantly arrested by the combined effect of the adhesiveness of the hydrogels and the hemostatic property of the chitosan materials. chitosan could form hydrogel rapidly after 5 seconds of contact with rat skin by enzymatic crosslinking technique. Histology test showed great healing progress in rat skin in comparison with fibrin glue, suture, and cyanoacrylate.

Singh et al. [118] developed a hydrogel dressing made of quaternized and phosphorylated chitosan with tannic acid as a hemostat agent and crosslinker for controlling of hemorrhage/ bleeding. Adding poly-Ɛ-lysine improved elastic and adhesive properties of the system adhesion strength. The adhesion strength was calculated 0.00915 MPa which was two times higher than that of gelatin and three times higher than commercial Axiostat. The hematological and serum biochemistry test indicated no inflammation and toxicity to the rats. The animal in vivo test confirmed better hemostatic efficacy of the prepared hydrogels in comparison with commercial Axiostat (clotting time~225s).

Discharge plasma technology was applied for developing a gallic acid/chitosan bioadhesive hydrogel to be used in biomedical applications such as wound healing and hemostatic. The capability of the hydrogel to improve wound healing and hemostasis were evaluated using in vivo rat and the results showed fast blood clotting at the injury site same as famous hemostatic gelatin sponge’s performance. Hydrogels exhibited fast adhesion properties with no external pressure need to assist wounds [119]

Table 2-5 Hemostatic applications of chitosan bioadhesives

Materials	Tested area	Adhesion strength	Clotting time	Biocompatibility	Biodegradability	Ref.
Catechol-hydroxybutyl chitosan	Rat-liver	1-4.5 kPa	30 s	100% after 9 days	>100% after 3 days	[37]
HTCC/polydextran aldehyde [1]	Mice-liver/	4-7.5 kpa (Porcine skin)	3 min	N.R.	N.R.	[120]
CSS/ PEG-2000/GRGDS [2]	Rat-liver	-	1.5 min	N.R.	N.R.	[121]
Chitosan/Gallic acid	Porcine skin	51-53 kPa	BCI~82.19[3]	N.R.	N.R.	[122]
Catechol-conjugated glycol chitosan	Rat-liver	610 Pa	3 min	N.R.	40-100% (dose dependent)	[123]

[1] HTCC: N-(2-hydroxypropyl)-3-trimethylammonium chitosan chloride

[2] GRGDS: Glycine-arginine-glycine-aspartic acid-serine, PEG-2000: Polyethylene glycol and CSS: Chitosan succinate

[3] BCI: Blood-clotting index

Not Reported (N.R.)

2-2-6-5 Other Biomedical Applications of Chitosan Bioadhesives

A catechol-conjugated chitosan hydrogel with hemostasis and bone regeneration properties was prepared by Huang et al. [124] which can be injected into bleeding sites and bone defective areas. This self-healing hydrogel can then be changed to an integrated hydrogel filling the defective sites and stop bleeding during surgery. Hydrogels showed much more hemostasis properties in the mouse liver injury and tail amputation in comparison with gauze and gelatin sponge as they could self-heal very fast (about 2 minutes) and stick to the bleeding surface. Also, platelets and red blood cells can adhere to the surface of the hydrogel leading to blood coagulation. Injection of the hydrogel into a defective bone site in rabbit ilium defect group had better hemostatic effect compared to bone wax and because of good absorbability and biocompatibility of the hydrogel, didn't interface with bone regeneration.

Gene transfer has been considered as a new method for the treatment of chronic ocular diseases such as corneal dystrophies, and dry eye. For example, in a study a DNA nanocarrier composed of hyaluronan and chitosan was designed for topical ophthalmic gene therapy [125]. After topical administration to rabbits, nanoparticles with low molecular weight chitosan could enter to the conjunctival epithelial and corneal cells and become assimilated by the cells. They also were able to deliver the associated plasmid DNA inside the cells, proving their potential as a gene therapy device.

The Nanocomposite composed of bioadhesive bael fruit gum (BFG), nano-hydroxyapatite and chitosan were developed for bone tissue engineering [126]. Loading BFG into the structure enhanced the compressive modulus and strength, biodegradability, adsorption of protein, swelling and antibacterial activity. BFG-loaded nanocomposite showed better cell adhesion and proliferation. The biomineralization capability is an important factor to increase bone bonding

and osteogenic capacity of the bone regenerating materials. A remarkable increase in apatite layer was observed after 30 days of incubation of bone mineral on the prepared scaffolds in simulated body fluid (SBF). It is because BFG enhanced calcium phosphate formation on the surface through absorbing more calcium ions from the medium. Table 2-6 summarized some more examples of other biomedical applications of chitosan bioadhesives.

Table 2-6 Other biomedical applications of chitosan bioadhesives

Ingredients	Potential Applications	Type of adhesive	Biocompatibility	Dry adhesive strength	Ref.
Chitosan/ oxidized dextran or starch	Bone glue	Bioadhesive	95-100%	0.18-0.41 MPa	[127]
Chitosan/ cyclodextrin ICs	Increase oral bioavailability of doxorubicin	Bioadhesive	N.R.	-	[128]
Chitosan	Oral DNA delivery	Mucoadhesive nanoparticles	N.R.	-	[84]
Chitosan/gold nanorod	Tissue repair	Bioadhesive	N.R.	12.3 kPa	[61]
Chitosan	Bone-adhesive joint	Bioadhesive	N.R.	0.2-0.24 MPa	[129]
Chitosan	Peripheral neurosurgeries	Bioadhesive	95-110%	68.9-88.8 mN	[130]
Mono N-carboxymethyl chitosan/ N-trimethyl chitosan nanoparticles	Non-invasive vaccine delivery (mucosal immunization)	Mucoadhesive	N.R.	-	[131]
Polyurethane/ polyols*/ hexamethylene diisocyanate/ chitosan	External biomedical tissue adhesives	Bioadhesive	60-98%	4.5-5.8 MPa	[132]

***** Derived from castor oil (chemically modified and unmodified)

Biodegradability was not reported for above literature.

Not Reported (N.R.)

2-2-7 Clinical Studies

There are some clinical studies of applying chitosan-based bioadhesives which some of them are explained in following. In a study by Abd-Allah et al. [133], chitosan nanoparticles loading the nutraceutical nicotinamide were prepared and clinically tested on patients suffering from acne vulgaris. Due to the barrier properties of stratum corneum, there are challenges for topical delivery. Bioadhesive chitosan nanoparticles are selected for this aim as they can enhance the drug permeation through the skin, open the tight junctions of the dermal cells, and interact electrostatically with the negatively charged dermal cells. Chitosan nanoparticles showed strong skin adhesion and high nicotinamide deposition in different skin layers. The clinical test was involved twenty patients (male and female) suffering from mild or moderate acne vulgaris. The results exhibited a notable reduction in the amount of total acne lesions and inflammatory ($P<0.05$) with no remarkable decline in the amount of comedones ($P>0.05$) in comparison with untreated ones. No local irritation, dermatitis or burning was observed during the treatment period.

Ashri et al. [134] fabricated a buccal mucoadhesive tenoxicam (TNX) local delivery system composing chitosan and polyvinyl pyrrolidone for the treatment of chronic periodontitis. The adhesion capacity and in vivo TNX release of the mucoadhesive films was tested in six healthy female volunteers aged between 18 and 40 years. The results showed that prepared chitosan films did not cause discomfort (however taste was a bit bitter). No extreme irritation, salivation, and mouth drying was observed. The in vivo TNX release was tested over 6 h after applying into the buccal cavity and the films were kept in the buccal cavity even after its detachment. The salivary TNX release was fast and continuous. The authors concluded that the chitosan mucoadhesive film can be a candidate for treatment of the chronic periodontitis instead of current oral therapy.

In another study, the clinical influence of chitosan gel alone and combined with metronidazole in the treatment of chronic periodontitis was evaluated [135]. Due to the bioadhesive and antimicrobial properties of the chitosan, the application time of the gels was selected twice a week. All patients received the standard phase 1 periodontal therapy, and the treated teeth were single rooted. significant improvements were observed in clinical parameters such as probing depth, the amount of gingival recession, attachment level, plaque, and gingival index. In the long-term evaluations, chitosan gel groups had lower GBTI scores (bleeding from each site was evaluated by the gingival bleeding time index) in comparison with those of the control group showing the inflammatory properties of the chitosan. It was found that chitosan and its combination with metronidazole is effective in the treatment of chronic periodontitis.

Efficacy of a nasal chitosan/morphine formulation for pain relief of patients with cancer was investigated by Pavis et al. [136]. Morphine is defectively absorbed nasally because of its hydrophilicity nature which can be solved by combining it with chitosan, a bioadhesive polymer that slows the mucociliary clearance of morphine, letting more time for absorption. Nasal symptoms, dizziness, sedation, nausea, and pain scores were recorded in 14 patients (men and women) at specific intervals up to 4 hours after dosing. The formulation was bearable to patients, well tolerated, and had an onset of pain relief 5 minutes after administration. The results showed that the nasal formulation of chitosan/morphine is more rapidly effective and convenient than the oral route.

Aksungur et al. [137] developed a chitosan-based occlusive system for treatment of oral mucositis. Nystatin, a prophylactic agent for oral mucositis, was selected as a drug model. Topical application of chitosan gel and suspension to the oral mucosa in six healthy volunteers remarkably decreased the severity and rate of oral mucositis and had a notable healing. Comparing to the suspension

formulation, chitosan gel had slower release and a longer retention time owe to its bioadhesive properties. The results of this study indicated ability of chitosan for treatment of oral mucositis and delivery of the therapeutic compounds. due to its antimicrobial property, it also has an advantage over suspension.

A bioadhesive system composed of chitosan and hyaluronic acid was designed for transdermal delivery of lidocaine. The prepared bioadhesives could be easily removed from human skin and caused almost no irritation after 24 hours of application onto human skin while in some previous studies, the skin damages through application of transdermal film were reported from mild to serve. The release profile of a 30 and 60 days-kept chitosan/HA bioadhesive was similar to a newly prepared bioadhesive [93].

Based on above literature review, almost all the studies reached to this conclusion that the chitosan bioadhesives systems are able to be applied in different biomedical applications such as drug delivery, wound dressings, hemostatic, sutureless surgery and so on. Almost all the prepared chitosan-based systems could deliver drug to the targeted organ and were non-toxic or low-toxic to the cells with minor or mild irritation for optimum formulation. However, lack of sufficient animal and clinical tests for confirmation of the results can be observed which can be a perspective for future investigations and studies. There are some in vivo tests but the number of clinical tested done is limited.

2-2-8 Conclusions

Bioadhesives are gaining increasing attention in recent years. for example, due to the technical limitation for suturing in laparoscopic surgery, bioadhesives could be a good candidate for suture less surgery. There are some bioadhesives with great adhesive properties, but their applications for internal use are limited due to their low biocompatibility. Therefore, chitosan based bioadhesives

are taking more attentions from researchers and surgeons, because of promising properties of chitosan for internal use. Also, several studies have shown great properties of chitosan for wound dressing making it a very good potential for topical applications. External stimuli responsive chitosan based bioadhesives could provide a new avenue for bioadhesives. As discussed in this review, Thermo, pH and light responsive bioadhesives are more common for suture less and wound dressing applications.

2-3 Chitosan/Graphene Oxide Composite Films and Their Application in Wound Dressings and Drug Delivery Systems: A Review

2-3-1 Abstract

The healing of wounds is still one of the challenging clinical problems for which an efficient and fast treatment is needed. Therefore, recent studies have created a new generation of wound dressings which can accelerate the wound healing process with minimum side effects. Chitosan, a natural biopolymer, is an attractive candidate for preparing biocompatible dressings. The biodegradability, non-toxicity and antibacterial activity of chitosan have made it a promising biopolymer for treating wounds. Graphene oxide has also been considered by researchers as a non-toxic, inexpensive, and biocompatible material for wound healing applications. This review paper discusses the potential use of chitosan/graphene oxide composite films and their application in wound dressing and drug delivery systems.

Keywords: Chitosan, Graphene oxide, Wound dressings, Drug delivery

2-3-2 Introduction

The creation of smart wound dressings that work proactively with the human body to speed up the wound healing process and prevent infection has received more attention recently, particularly for individuals with chronic wounds. Due to the need for a new generations of smart wound dressings with the ability to accelerate the wound healing process and prevent infections, various kinds of

dressings with novel materials and structures have been prepared and studied. Biopolymers in particular have attracted more interest due to their biocompatibility and low or non-toxicity.

Chitosan is one of the most attractive biopolymers for wound dressing applications. It is a linear polysaccharide derived from chitin, which is the second most abundant biopolymer after cellulose. It has antimicrobial, anticoagulant, antibacterial, antifungal, anti-tumor, and haemostatic properties [10]. Due to these excellent characteristics, chitosan has been a potential biomaterial for biomedical applications such as wound dressings [138], drug delivery systems and tissue engineering scaffolds [139]. Graphene oxide (GO), is one of the most important derivatives of graphene. In recent years it has been considered as a suitable material for biomedical applications. Owing to its large surface area and functional groups, such as carboxyl and hydroxyl, GO is hydrophilic in nature, and so it can be dispersed in aqueous solutions via electrostatic repulsion [140]. GO can be applied to reinforce natural polymers such as chitosan, and some reports have indicated that chitosan/GO composites can capitalize on the advantages of both chitosan and GO materials [141]. Therefore there are several studies regarding the preparation and characterization of chitosan/GO composite films and their application in different biomedical fields such as wound dressings and drug delivery systems.

This review highlights the applications of chitosan/GO composites as wound dressings and drug delivery systems. First, the individual properties of chitosan and graphene oxide are described. Then, different hybrid chitosan/GO structures such as hydrogels and electrospun nanofibers are discussed.

2-3-3 Chitosan

The general term chitosan describes a range of poly-(beta-1-4) N-acetyl-D-glucosamine materials (Figure 2-6) whose properties are highly dependent on the degree of deacetylation, average

molecular weight, polydispersity, morphology and chemical structure. Chitosan is one of the most widely used materials for biomedical end-uses including wound dressing applications [30, 31, 32, 33]. It has excellent biocompatibility and low toxicity, and can stimulate a positive immune response as described in our previous review paper about applications for chitosan hydrogels as wound dressing materials [10].

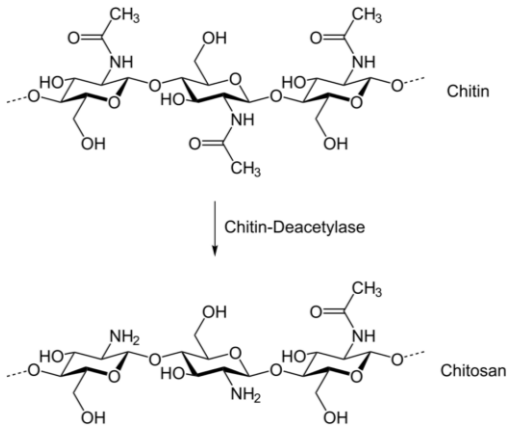

Figure 2-6 Chitosan structure [10]

2-3-4 Graphene Oxide

Graphene, also known as graphite, consists of a single layer of carbon atoms arranged in a two-dimensional honeycomb lattice. Graphene oxide is composed of carbon, oxygen, and hydrogen in variable ratios, obtained by treating graphene with strong oxidizing agents (Figure 2-7). The structure and properties of graphene oxide depend on the method of synthesis and the degree of oxidation. It usually maintains the single layer structure of graphene, but the layers are buckled and the space between the layers is about two times larger (~0.7 nm) than that of graphene. Graphene oxide can be considered a promising candidate for biological and biomedical applications because of its amphiphilicity, aqueous processability, ease of surface functionalization, and its capacity for fluorescence quenching [142].

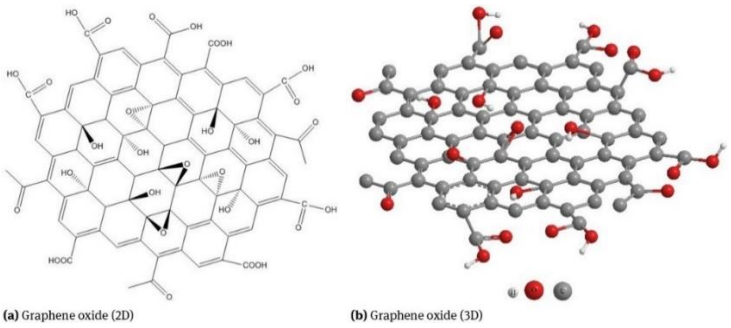

Figure 2-7 Graphene oxide [143]

2-3-4-1 Toxicity

The toxicity of graphene oxide (GO) has been studied by several researchers. In a study undertaken by Chang et al. [144] evaluating of toxicity of GO on A549 human lung cells, it was shown that GO does not enter the A549 cell and causes no evident cytotoxicity. But based on the applied dose, it can lead to oxidative stress in cells and some loss of cell viability at high concentrations. LiQiang et al. [145] showed that GO has a moderate level of toxicity to human bone marrow neuroblastoma cells and human epithelial carcinoma cells. When studied with zebrafish (Danio rerio) embryos, a 20% inhibition of cell growth was observed. And when a high dosage of 50 mg/L was used, this caused a delay in the hatching of the zebrafish embryos, but it did not increase apoptosis significantly.

Majidi et al. [146] synthesized GO-chitosan nanohybrid films for wider biomedical applications and characterized the film's structure, antibacterial activity and cytotoxicity. The results of the antibacterial tests showed that GO-chitosan hybrids had greater antibacterial activity compared to that of pure GO. Also, the attachment of graphene sheets to GO decreased the level of cytotoxicity and in some cases led to increased cell proliferation.

In another study Liao et al. [147] evaluated the cytotoxicity of GO and graphene sheets with different sizes and oxygen levels on human red blood cells and adherent skin fibroblasts using WST-8 viability and hemolysis assays. The results of the WST-8 assay and hemolysis data proved

that compact graphene sheets were more toxic to mammalian fibroblasts than the less dense graphene oxide. Also, the graphene sheets produced more reactive oxygen species on the surface of the dermal fibroblasts. They concluded that the toxicity of graphene and graphene oxide depends on the exposure environment, such as the level of aggregation, and the type of cell interaction (i.e. cell suspension versus adherent cells).

Exposure of reduced graphene oxide (rGO) particles with a diameter between 100–110 nm and a thickness between 3–5 nm to human PC12 neuronal cells increased the activation of caspase-3, the release of lactate dehydrogenase, and the generation of reactive oxygen species. However, rGO had a moderate effect on protein levels during contact with human HepG2 hepatoma cells [148]. According to the literature, the toxicity of GO and rGO is strongly dependent on their concentration and increases with the amount of GO or rGO. For instance, a GO concentration of greater than 50 μg/mL showed toxicity to human fibroblasts, decreased the amount of cell adhesion and promoted cell apoptosis [149].

H. J. Majidi et. al [146] showed introducing GO in Chitosan polymer could decrease cytotoxicity effect. Chitosan would blunt the edges of CS-functionalized GO from the other side, eventually, results in the lower cell membrane damage. In addition, hybridization of GO with CS decreased the hydrophilicity of nano-hybrid particles compared to the pure GO which may decrease the affinity of cells to the nano-hybrids, leading to the lower possibility of cell-killing.

2-3-4-2 Biocompatibility

As mentioned above, Liao et al. [147] investigated the blood compatibility of GO and graphene sheets on human red blood cells and adherent skin fibroblasts. The observed level of hemolysis for the GO samples was strongly dependent on the extent of exfoliation of the injured dermal tissue and the particle size. Smaller-sized GO particles had a higher hemolytic activity compared to larger

sized GO particles. Their results demonstrated that the size, shape and density of the graphene particles and the oxygen content and electrostatic charge on the surface of the particles strongly affected the toxicological and biological response by the red blood cells. They also found that covering GO with chitosan removed any hemolytic activity. Zhang et al. [150] investigated the biocompatibility and distribution of GO in mice. The results showed that GO did accumulate in the lungs over an extended period of time. GO also contributed to a slower blood circulation time, with 5.3 + 1.2 hours half-life compared to other carbon nanomaterials. When the mice were exposed to 1 mg kg^{-1} body weight of GO for 14 days, no pathological changes were observed in the examined organs. GO exhibited good biocompatibility to red blood cells. The conclusions recommended that GO in low doses is an acceptable candidate for biomedical applications, but when the dosage exceeds 10 mg kg^{-1} body weight, some pathological changes, such as pulmonary edema, chronic inflammation, and granuloma formation are likely to occur.

Based on a review report by Kiew et al. [151], after incubation for 3 hours, the micro-sized (3μm) graphene sheets (10% hemolysis at 100 μg/mL) caused less hemolysis than nano-sized GO (350 nm) particles (70% at 25 μg/mL). The superior hemocompatibility of the smaller-sized graphene oxide sheets was no doubt due to the limited overall surface area available for interaction with red blood cells.

2-3-4-3 Biomedical Properties

The study of Mukherjee et al. [152] showed that the activation of inflammasomes does not depend on the lateral dimensions of the GO sheets. Inflammasomes, are receptors/sensors of the innate immune system, that regulate the activation of caspase-1 and are responsible for the activation of inflammatory responses, such as IL-1β. Mukherjee et al. also showed that when GO sheets (small and large) are exposed to primary human macrophages, they are not cytotoxic for primary human

macrophages and do not trigger a typical Th1 cytokine (i.e., TNF-α, IL-6, or IL-1β) or Th2 cytokine (i.e., IL-4, IL-5, and IL-13) response in macrophages. From these observations, it was concluded that endotoxin-free GO is biocompatible and proinflammatory [20].

GO can be gradually degraded through enzyme induced oxidization by, for example, horseradish peroxidase (HRP). Because of the remote possibility of toxicity to macrophages, coating GO with biocompatible macromolecules can be a method to reduce its level of cytotoxicity. But at the same time, coating can limit the degradability of GO due to steric hindrance. So more recent studies have attempted to design a surface modified GO carrier that will degrade and provide drug delivery functionality while maintaining an acceptable level of toxicity [153, 154].

Gurunathan et al. [155] investigated the antibacterial activity of GO and reduced graphene oxide (rGO) against *P. aeruginosa*. The rGO sample was synthesized from GO using betamercapto-ethanol (BME) as a novel reducing agent, which is known to be less cytotoxic than hydrazine. The results showed that both GO and rGO had significant antibacterial activity in a concentration- and time-dependent manner. They also realized that oxidative stress is a key mechanism for antibacterial activity of GO and rGO. In another study by Liu et al. [156] the antibacterial activity of GO sheets with different sizes and shapes was evaluated against *Escherichia coli*. The results indicated that the antibacterial activity of GO depended on the specimen's lateral size. Larger-sized GO sheets had more antibacterial activity compared to smaller-sized ones. They also had different time- and concentration-dependent antibacterial activities. The antibacterial activity of different graphene-based materials, including graphite (Gt), graphite oxide (GtO), graphene oxide (GO), and reduced graphene oxide (rGO), were investigated against *Escherichia coli*, and the results showed that GO had the highest antibacterial activity, followed by rGO, Gt, and GtO [157].

Angiogenesis is another key property to accelerate the wound healing process. Ozkan et al. demonstrated that GO and rGO have promising angiogenesis properties [26]. A combination of GO and other polymers, such as GelMA [158] and chitosan [159], provides an attractive method to accelerate the wound healing process by promoting angiogenesis. Reactive oxygen species (ROS) in biological systems play an important role in angiogenesis. Both GO and rGO can increase the concentration of the ROS. And ROS can also act as signaling molecules as part of the growth factor-mediated physiological response to cell proliferation and wound healing. [158]

2-3-4-4 Electrical Conductivity

Graphene also has unique optical, electrical, and thermal characteristics, which make it suitable for a range of different applications, such as biosensors, transparent conductors, and drug diagnostics. Both GO and rGO have residual functional groups leading to faster heterogeneous electron transfer on the surface and better biocompatibility, dispersibility and charge transfer than is possible with pure graphene [160]. Several studies have demonstrated the effect of electrical conductivity of GO in combination with other polymers and its applications. Ozkan et al. prepared chitosan/rGO nanocomposites with appropriate levels of conductivity, stability, charge density, and electrochemical properties for designing molecular detection systems [160]. In another study, chitosan and reduced graphene oxide sheets with a high conductivity of 1.28 S m^{-1} were fabricated for various biological applications, such as biosensors and tissue engineering scaffolds [161]. Electrically conductive chitosan/GO based scaffolds have been prepared for cardiac tissue engineering end-uses [162, 8]. And the electrical conductivity of GO has been found to be highly desirable for use as biosensors [163, 164], supercapacitors [165, 166] and cardiovascular tissue engineering scaffolds [167, 168].

2-3-5 Chitosan/Graphene Oxide Films for Wound Dressing Applications

Because of its electronegativity, graphene oxide can easily interact with cationic polymers, such as chitosan, which may lead to a reduction in toxicity and enhanced mechanical properties of the composite structure. With respect to the specific properties of chitosan/graphene oxide blends, there are a series of different wound dressing studies with alternative techniques for the preparation of the chitosan/GO composites, which are classified and discussed in the following sections.

2-3-6 Chitosan/Graphene Oxide Hydrogels

Hydrogels are cross-linked and three-dimensional structures which can absorb water and biological liquids without dissolving or losing their 3D network. They are able to absorb and hold high levels of exudate and can be separated from the wound's surface with minimal pain. Fan et al. [169] prepared composite hydrogels from oxidized konjac glucomannan (OKGM) and carboxymethyl chitosan (CMCS) with different concentrations of graphene oxide (GO) as a nano-additive. The hydrogels had a stable 3D structure with a fast gelation time, good water retention capacity and a high swelling ratio. The compressive modulus and strength were significantly enhanced by adding GO, which was due to the increased hydrogen bonding between the polymer chains and the GO. An *in vitro* cytotoxicity assay showed that the samples loaded with GO had better biocompatibility compared to those without GO, from which it was concluded that the prepared hydrogels could be considered as potential wound dressings.

Another type of wound dressing was developed by loading polyhexamethylene guanidine (PHMG)-modified graphene oxide (mGO) into a polyvinyl alcohol/chitosan (PVA/CS) matrix [139]. The dressings had good mechanical properties, less swelling time, higher water vapor transmission rate (WVTR), faster cell proliferation and greater antibacterial activity compared to those without mGO. The average wound closure time for the films loaded with mGO was 8.2 ±

0.4 days, which was significantly shorter than the Vaseline gauze control and the hydrogels without mGO (Figure 2-8). An *in vivo* trial confirmed that this novel composite PVA/CS/mGO film had the ability to accelerate wound healing and therefore showed promise in wound dressing applications.

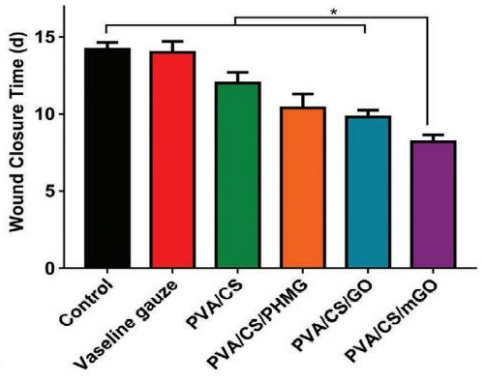

Figure 2-8 Wound closure time of hydrogels with GO [139]

Layered nanocomposite hydrogel films containing chitosan and GO were prepared for use in biomedical applications by Zhang et al. [170]. The resultant hydrogels had superior mechanical properties and a pH-driven shape memory effect. Shape memory polymers are stimuli-responsive materials that can maintain a temporary deformed shape, but then return to their original permanent shape when exposed to external stimuli. In this study, the initial shape of the CS and CS/GO hydrogels were straight strips. After 5 minutes of immersion in pH 3 solution, the films could be easily deformed and bent into a "U" shape by an external applied stress, and kept in that shape at pH 12 aqueous solution for 10 min. The deformed and bent films were then transferred back to pH 3 solution, and as can be seen from Figure 2-9, the CS/GO hydrogel reverted to its original shape in 9 minutes whereas the CS hydrogel strip did not returned to its original straight shape in more than 15 minutes. The shape fixity ratio of the hydrogels with 5 wt% GO was about 99% compared to 86% for the pure CS film. These results demonstrated that the prepared films could be combined with hydrogels for biomedical applications such as wound dressings.

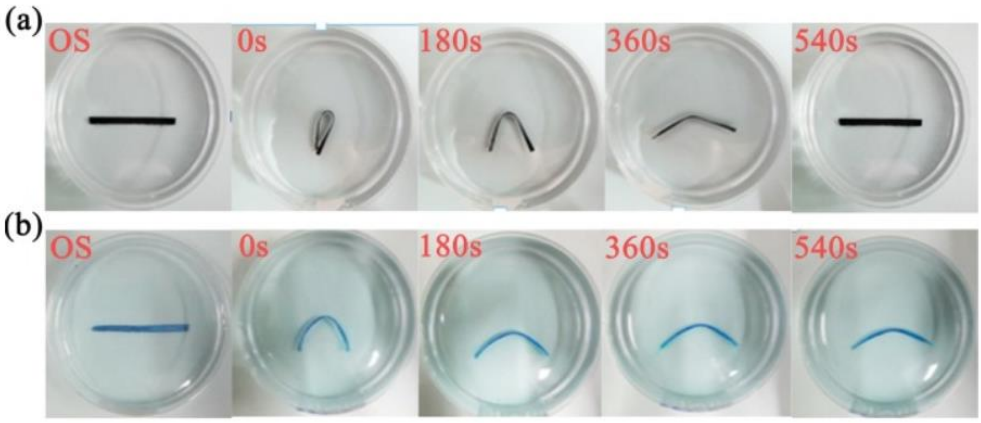

Figure 2-9 Photographs of pH-driven shape memory polymer samples a) CS/5 wt% GO and b) pure CS. The CS strip was coated with methylene blue for improved visibility. OS: original sample [170].

Several other studies which involved the preparation of chitosan/GO hydrogels are listed in Table 2-7.

Table 2-7 Chitosan/GO hydrogels and their biomedical applications

Ingredients	Potential Applications	Characterization	Ref.
Chitosan/GO/curcumin	Wound dressings	Improved Young's modulus.	[171]
		Improved antibacterial activity and *in vitro* release after addition of curcumin	
		Greater proliferation of NIH/3T3 fibroblast cells	
		GO/curcumin increased hydrophilic properties	
Chitosan/iron oxide/GO	Biomedical Applications	Improved thermal and mechanical properties	[172]
		Significant antimicrobial activities	
		Non-cytotoxic	
Chitosan/GO and Chitosan/reduced GO	Tissue engineering	Improved Young's modulus (rGO was soft and easy to bend)	[173]
		Improved structural, thermal, surface, and mechanical properties	
Carboxymethyl chitosan/GO/polyacrylamide	Bioengineering and drug delivery systems	Excellent mechanical performance	[174]
		Biocompatible	
		Fast recovery	
Quaternary chitosan/ cyclodextrin/GO	Wound dressings	Similar conductivity with that of skin and rapid self-healing behavior	[175]
		Superior antibacterial property	
		Accelerated *in vivo* wound healing	
		Good biocompatibility	
Carboxymethyl-hexanoyl chitosan/GO/cellulose nanocrystals	Wound dressings	Excellent biocompatibility	[176]
		Superior antibacterial properties	
		High water absorption capacity and water retention capability	
		GO/cellulose increased hydrophilic properties	
Poly(p-phenylene sulfide)/ chitosan/rGO	Wound Tissue Engineering	Acceptable biocompatibility and cell attachment	[177]
		Swelling ratio and WVTR* decreased by adding PPS**/rGO	
		Improved mechanical properties	

* Water vapor transmission rate
** Poly(p-phenylene sulfid

2-3-7 Chitosan/Graphene Oxide Nanofibers

Because of the similarity of the structure to extracellular matrix, electrospun chitosan/graphene oxide nanofiber webs can promote cell adhesion, proliferation and migration, and as a result, they can be considered as an attractive candidate for wound dressing applications. They can act as a barrier to the contamination of open wounds from exogenous microorganisms, and they can maintain a moisture of wound surface to promote the wound healing process. Electrospun nanofibers have a high surface area, which makes them ideal for use in drug delivery systems [178].

Yang et al. [178] prepared chitosan/polyvinyl alcohol/graphene oxide (CS/PVA/GO) nanofibers loaded with antibiotic drugs, such as ciprofloxacin and ciprofloxacin hydrochloride, by using an electrospinning technique. The drug release results showed a controlled release without an initial burst. Adding GO moderately improved the drug release ratio. The drug-loaded nanofibers had significant antibacterial activity against both gram-negative and gram-positive bacteria, as well as cytocompatibility with melanoma cells. In another study, by increasing the GO content in the electrospun antibacterial CS/PVA/GO nanofibers was found to decrease the thermal stability of the hybrid composite nanofibers [179]. The nanofiber web had effective antibacterial activity against both Gram-negative and Gram-positive bacteria, suggesting that the electrospun nanofiber web could be used as a wound dressing. The natural garlic extract, allicin, with its strong antibacterial activity, was loaded into the electrospun chitosan/polyvinyl alcohol/GO nanofibers, and the release study showed that the amount of allicin released could be controlled by the GO content. The drug-loaded nanofibers had effective antibacterial activity against *Staphylococcus aureus*, and the nanofibers containing GO had superior antibacterial activity compared to those without GO. The drug-loaded nanofibers also had a significant moisture-retention capacity and

hygroscopicity, and as a result these nanofibers were considered to be potential candidates for wound dressing and tissue engineering applications.

In another study, multi-component nanofiber webs loaded with various antibacterial agents, such as silver nanoparticles (Ag), graphene oxide (GO), curcumin (CUR) and chitosan (CS), were prepared [138]. First, PEGylated GO was used as the template to synthesize a series of PEGylated GO/Ag/CUR nanocomposites by incorporating them into CS/polyvinyl alcohol nanofibers (Figure 2-10). The results from an antibacterial test indicated improved effectiveness compared to other formulations. The GO increased the mechanical properties of the nanofibers, with a tensile strength of 25 MPa compared to 7.2 MPa, and a Young's modulus of 364 MPa compared to 73 MPa. A cell viability assay also confirmed the biocompatibility of the nanofiber web, indicating that the prepared nanocomposites had potential for use as wound dressing materials.

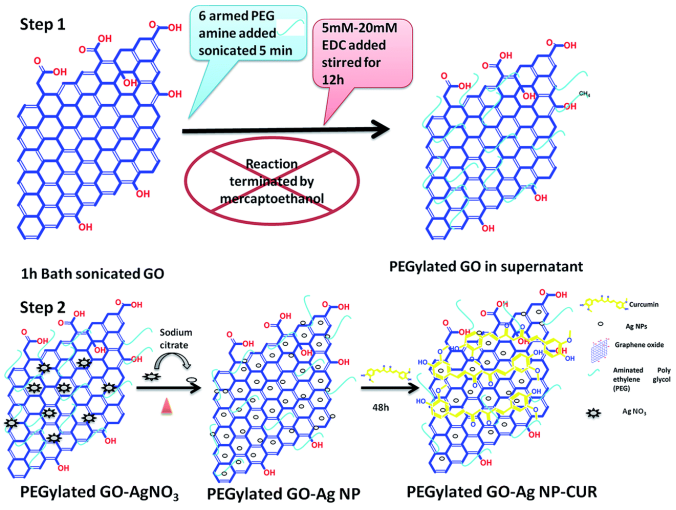

Figure 2-10 Schematic of synthesis of PEGylated GO and the PEGylated-GO-based nanocomposites [138]

Some other preparations are also listed in Table 2-8.

Table 2-8 Chitosan/GO nanofiber webs and their biomedical applications

Ingredients	Potential Applications	Characterization	Ref.
Chitosan /polyvinyl pyrrolidone /polyethylene oxide /GO	Wound dressings	Enhanced elastic modulus and tensile strength Controllable water permeability Biocompatible Accelerated *in vivo* wound closure rate	[180]
Chitosan / levorotatory poly-L-lactide/ GO	Wound dressings	Excellent antimicrobial activity Promoted proliferation of pig iliac endothelial cells Improved *in vivo* wound healing	[181]
Polyvinyl alcohol/ chitosan/ GO	Tissue engineering, wound healing, and drug delivery systems	Improved mechanical properties Effective antibacterial activity	[182]
Chitosan/bacterial cellulose/ GO	Skin tissue engineering and wound dressing	Adding GO reduced nanofiber size Water vapor permeability and hydrophilicity decreased by adding GO	[183]
Polylactide-co-glycolide/ chitosan/ GO/ silver nanoparticles	Biomedical applications	Improved wettability of nanofibers Enhanced antimicrobial function	[184]
Chitosan/ gelatin/ GO-silver	Tissue engineering, nanomedicine	Improved tensile strength and Young's modulus Enhanced antimicrobial activity Improved thermal stability	[185]

2-3-8 Other Types of Chitosan/Graphene Oxide Composites

Shao et al [186] fabricated biocompatible graphene oxide nanocomposite membranes cross-linked with chitosan which can be used for different applications. A schematic diagram of the reaction is shown in Figure 2-11. The tensile strength of the membranes was significantly improved with the incorporation of GO. By adding 1 wt% GO the tensile strength improved from 43.2 MPa to 104.2 MPa, an increase of 141% which can be explained by the formation of covalent bonds formed during the chitosan/GO cross-linking reaction. The authors claimed that by controlling other physicochemical properties of GO, such as the density of the functional groups and the particle size, superior nanocomposite properties can be achieved.

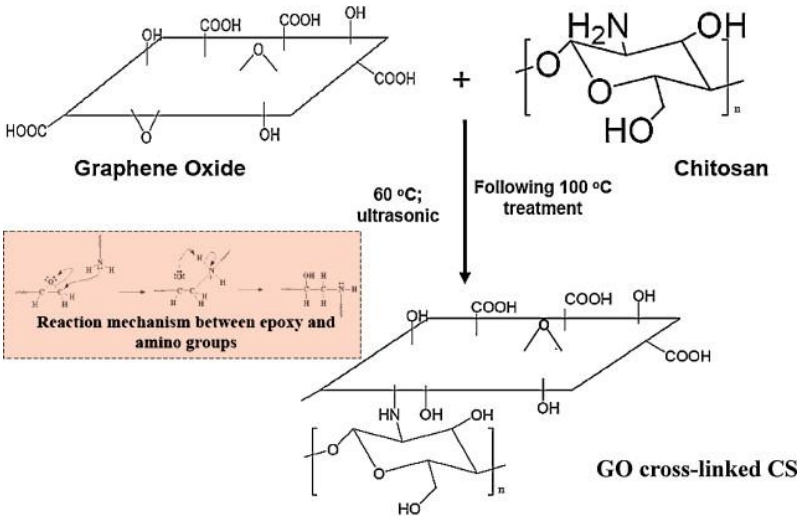

Figure 2-11 Cross-linking reaction between GO and CS to form nanocomposite membranes [186]

Chitosan/GO and chitosan/reduced GO (rGO) hybrid nanocomposites were fabricated by Kosowska et al. [173]. Reduced graphene oxide was synthesized by "green" reducing agents such as L-ascorbic acid (LAA), grape extract, and green tea extract. Among these three reducing agents, the nanocomposites prepared with rGO-LAA had good wettability and a regular, homogeneous microstructure, indicating that such nanocomposite materials may be considered as potential tissue

engineering scaffolds. The composites prepared from grape and green tea extracts were less homogenous and formed visible agglomerates.

Chitosan/hyaluronic acid wound dressings were prepared with GO/copper using sodium trimeta-phosphate (STMP) as the crosslinking agent followed by vacuum freeze-drying [187]. The reason for using copper was that it is a cheaper antimicrobial agent with the ability to kill pathogens on its metallic surface. The prototype dressings had excellent antimicrobial activity against two strains of *Staphylococcus aureus*, usually found in wound infections, and good cytocompatibility when cultured with NIH/3T3-L1 mouse fibroblasts. The wound dressings loaded with copper provided a significantly faster rate of wound healing together with controlled inflammatory infiltration and improved angiogenesis in the regenerated surrounding granulation tissue. No adverse pathologies were observed when the tissues of other organs, such as the heart, lung, liver and kidney, were examined.

A series of chitosan and graphene oxide (CS/GO) aerogels were developed as hemostatic agents by incorporating proanthocyanidins such as flavan-3-ols obtained from grape seed and skin extracts [188]. The aerogels were produced from solutions at two different pHs: acidic and alkaline. When exposed to whole blood the acidic aerogels reached total absorption within the first 30 s and the alkaline aerogels within 60 s. But the structure of acidic aerogels was found to be unstable due to capillarity forces, which caused them to dissolve in the media. Therefore the alkaline aerogels were considered more suitable as hemostatic agents due to their rigidity, porosity, superficial charge, PBS and blood absorption capacities as well as their stability in physiological media. These CS/GO aerogels promoted the accumulation of red blood cells through electrostatic interactions. The loaded aerogels showed slight cytotoxicity; however, the use of skin instead of grape seed extract increased the cell viability, making them acceptable for hemostatic applications.

However, the authors mentioned that additional studies are needed to realize the mechanisms which promote coagulation. Finally, they concluded that the prepared CS/GO aerogels could be considered for use as hemostatic agents in wound management.

2-3-9 Chitosan/Graphene Oxide as Drug Delivery Device

Justin et al. prepared chitosan/graphene oxide (CS/GO) nanocomposites, such as microneedle arrays, that were designed for transdermal drug delivery. The hybrid nanocomposite was found to provide faster, and more effective drug release compared to pure chitosan, and the drug delivery profile was dependent on the ratio of the loaded drug. The drug release of these particular nanocomposites were also pH sensitive, with 48% less release under acidic conditions compared to a neutral environment. In another study, chitosan/sulfonated graphene oxide nanohybrid scaffolds were designed for drug delivery and as a tissue engineering scaffold [189]. Greater hydrophilicity and improved mechanical properties were observed compared to chitosan alone. These nanohybrid prototype scaffolds had a uniform porous structure which facilitated the sustained release of an antimicrobial drug, tetracycline hydrochloride. In addition, they were highly biocompatible.

A genipin-crosslinked chitosan/graphene oxide (CS/GO) composite was prepared using a solution casting method [190]. The presence of the GO decreased the expansion ratio of the composite film when exposed to physiological conditions and increased the resistance to *in vitro* degradation by lysozymes. A cell culture study using mouse MC3T3-E1 pre-osteoblasts showed positive adhesion and cell proliferation, and the prototype films were considered attractive candidates for tissue engineering and drug delivery applications. In another study chitosan-functionalized graphene oxide hybrid nanosheets were synthesized and demonstrated that the experimental nanosheets significantly improved the solubility of the GO in aqueous acidic media [191]. They also provided

controlled release of drugs, such as ibuprofen and 5-fluorouracil, and exhibited long-term biocompatibility, suggesting that these CS/GO functionalized devices were suitable for biomedical applications such as drug delivery. Table 2-9 presents some other examples of the application of CS/GO films to serve as drug delivery device

Table 2-9 Application of chitosan/GO films to serve as drug delivery systems

Ingredients	Potential Applications	Characterization	Ref.
Chitosan/reduced GO	Transdermal drug delivery	Enhanced electrical conductivity	[192]
		pH dependent release behavior	
		rGO reduced biodegradation rate	
		Improved mechanical properties	
Chitosan/modified GO	Drug carrier	Stability in aqueous acidic and physiological solutions	[193]
		Biocompatible	
		Excellent dispersibility	
Aldehyde-conjugated chitosan/GO	Controlled chemical release	Improved mechanical properties	[194]
		Time-dependent aromatic release	
Chitosan/hydroxyethyl cellulose/GO	Drug delivery application	Stability over all pH ranges	[195]
		Biocompatibility	
Chitosan/GO	Delivery of Proanthocyanidins * (Ext.)	Nontoxic to kidney cells	[196]
		Thermostable	
		Biocompatibility of Ext. increased	

***** Obtained from grape seed extrac

2-3-10 Clinical and Pre-clinical Studies

To the best of our knowledge, there are not as yet any published reports describing clinical studies of using chitosan/graphene oxide (CS/GO) hydrogels as wound dressings. There are some pre-clinical *in vitro* and *in vivo* studies in this field. For example, in one study superior acute-wound healing was observed when CS/GO nanofibers were implanted in adult male rats [197]. The CS/GO nanofiber webs were prepared without any surfactants and organic solvents to make sure that the fibrous structure had excellent biocompatibility. *In vitro* evaluations with human skin fibroblasts indicated that the addition of GO improved cell viability with enhanced bactericidal capacity. *In vivo* wound healing studies on rat's skin demonstrated faster healing and full recovery of a 1.5×1.5 cm^2 open wound within 14 days. It is therefore recommended that these experimental CS/GO nanofiber webs have potential use in biomedical applications.

Other experimental wound dressings have been fabricated by incorporating polyhexamethylene guanidine and modified graphene oxide (mGO) into a polyvinyl alcohol/chitosan film [139]. In this *in vivo* study, cytotoxicity and wound healing were evaluated by applying HaCaT immortalized human keratinocyte cells to murine-infected full-thickness skin wounds. The results of the cytotoxicity test demonstrated good biocompatibility and the films generated rapid wound healing through faster re-epithelialization. However, by increasing the concentration of mGO up to 1 wt%, the proliferation of the HaCaT cells was prevented and lower cytotoxicity was observed. In another *in vivo* study rapid healing of dermal wounds was observed by using a prototype wound dressing made of chitosan/L-polylactic acid/GO nanofibers [181].

Reports in the literature have shown that collagen/chitosan/graphene oxide films with the addition of basic fibroblast growth factor (bFGF) have been studied for wound healing applications [198]. The bFGF was observed to provide continuous release for at least 28 days. No cytotoxic effects

were found by adding GO to the films, and in fact the addition of GO actually improved the cytocompatibility. This *in vivo* murine wound study confirmed that the GO prototype films were capable of accelerating the wound healing process in comparison with the control group.

Alkylated chitosan/GO sponges have also been studied for their hemostatic effects which can be used in wound healing applications [199]. The results of a rabbit femoral injury study showed higher hemostatic efficacy and promoted the adhesion of erythrocytes and platelets compared to the control samples. And by increasing the concentration of GO, blood clotting efficiency, platelet activation levels and the release of intracellular Ca^{2+} all increased.

2-3-11 Conclusions

Wound healing involves the replacement of damaged or injured tissue of living organisms by newly regenerated tissue. Due to the complexity of the wound healing process, much effort has been focused on new approaches to wound management, such as fabricating a new generation of wound dressings. This review summarized chitosan/graphene oxide composite films and their potential applications as wound dressings and drug delivery devices. Chitosan is an attractive candidate due to its biodegradability, non-toxicity and biocompatibility. Graphene oxide (GO) can be a substitute for carbon nanotubes or similar materials because of its lower price, low-toxicity, and ability to enhance the mechanical properties. In addition, it promotes nerve regeneration in the case of deep wounds, due to its excellent electrical conductivity. Composite or hybrid films composed of chitosan and graphene oxide can benefit from the advantages of both components which makes them promising candidates for drug delivery and wound dressing applications.

3. CHAPTER THREE: MATERIALS AND METHODS

3-1 Introduction

Wound healing is one of the most critical issues in clinical care. Designing a safe and effective system that actively close the wound immediately and control bleeding could promote wound healing and reduce the death rate. Moreover, wound healing acceleration could decrease the chance of chronic wound formation and its consequences. Chitosan (CS) is an excellent candidate for biomedical applications due to its biocompatibility, antibacterial, hemostatic and biodegradability properties. Moreover, chitosan could be a safe thermoresponsive biopolymer. Chitosan has some level of bio adhesion; however, its wet strength is not good enough for some special applications such as wound dressings and suture-less surgery. In this study, we aim to design a thermoresponsive bioadhesive based on chitosan and catechol containing molecule that are extracted from natural resources. Dihydrocaffeic acid (HCA) is used as an adhesive agent. Lactic acid is used for chitosan protonation to provide a more adhesive, soft and flexible polymer. Due to the presence of different functional groups, this design is an intrinsic self-healing polymer. Graphene oxide (GO) is applied in our design to take advantage of its special capabilities for improving mechanical and hemostatic properties of the polymer. In this project, we aim to introduce a safe design of thermoresponsive bioadhesive polymer to close the wound by biomechanical and biochemical means. In this design, a thermoresponsive polymer is injected to the wound site and due to the resulting contraction converted by phase transition and transferring this contraction to the wound site by the adhesive property it could decrease the size of the wound (see Figure 3-1). Due to the simplicity of the preparation technique that is presented in this project, it could have a potential for mass production and scale up. Here, we aim to take advantage of the high polarity of catechol groups. Highly polar catechol groups are able to form hydrogen bonds

with other functional groups of the polymer solution. This simplification could be helpful to avoid using other chemical agents as chemical cross linkers to make this design simple and more biocompatible. As mentioned before one of the main problems of bioadhesive polymers is low cohesiveness. Addition of Graphene oxide will improve mechanical properties and cohesiveness in our design. GO will improve angiogenesis [160] and hemostatic properties [200] of the thermoresponsive bioadhesive polymer [12]. A graphical abstract of this project is presented in Figure 3-1.

In this chapter, we will discuss materials and sample preparations following with several polymer characterization techniques as well as in vitro assays. Polymer characterizations include; rheological study, FTIR, lap shear test, degradation, water vapor transmission rate, swelling ratio and morphology. In vitro tests include; Cell cytotoxicity, cell migration, cell morphology, polymeric chain reaction, clotting time and whole blood clotting.

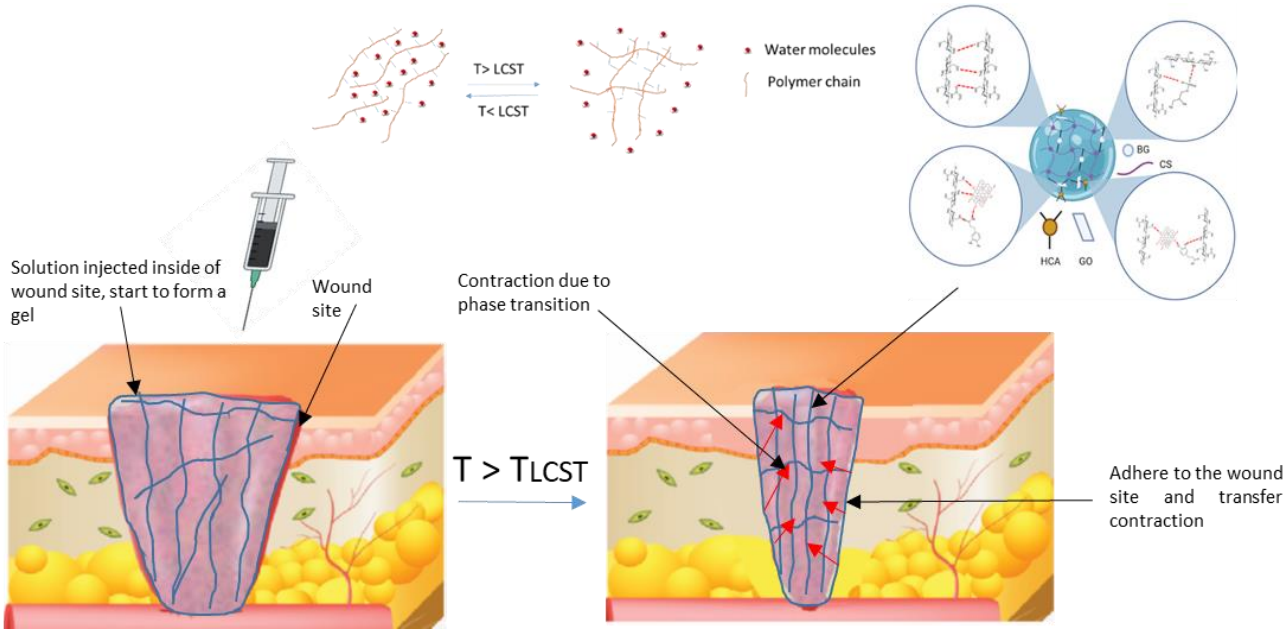

Figure 3-1. Graphical abstract

3-2 Materials for sample preparation

Chitosan with degree of deacetylation of 95% with Mw (by GPC) 300 kDa and 500 kDa (Heppe, Germany). Lactic Acid 85% (Sigma Aldrich), graphene Oxide (ACS, single layer, H method), Beta glycerol phosphate (sigma Aldrich) and 3, 4-Dihydroxyhydrocinnamic acid (HCA) 98% (sigma Aldrich).

3-2-1 Chitosan/Graphene oxide preparation (CS/GO)

0.05 gr GO was dispersed in 10 ml DI water by sonication for 30 minutes. 2 ml of GO solution dissolved in 5 ml water and 0.1 gr Chitosan were added to this solution. Then 0.037 ml Lactic acid was added to protonate chitosan and dissolve it in the GO-water solution. The solution was stirred for 8 hrs.

3-2-2 Chitosan/Graphene oxide/Beta glycerol phosphate/di-hydrocaffeic acid preparation (CS/GO/BG/HCA)

66% w/v of beta-glycerol phosphate (BG) in 9 ml water is prepared and filtrated to remove any impurities and unsolved particles. Then 1.5 ml of BG solution was added to the CS/GO at 4°C and stirred for 5 minutes to reach to pH of 6.8-7.0. lastly appropriate amount of HCA was added to the solution. The reason for adding BG before HCA addition is the effect of more alkaline condition on improvement of HCA oxidization and accordingly better adhesive property. In Table 3-1 samples compositions are presented.

Table 3-1. Composition of different samples

	CS: HCA molar ratio	GO concentration (V/V %)
1: 0.5, 0.5	1: 0.5	0.5
1: 1, 0.5	1:1	0.5
1:0.5, 1	1:0.5	1

Table 3-1 continued

1:1, 1	1:1	1
1: 0, 0.5	1: 0	0.5
1: 0, 0	1: 0	0.0

3-3 Polymeric Characterizations

3-3-1 Rheological study:

In the rheological study gelation time and self-healing properties of the polymer were analyzed using a discovery HR 20 rheometer (TA instrument, USA) with a 40 mm diameter parallel plate geometry. Time sweep experiments were carried out at strain 1%. The storage moduli (G′) and loss moduli (G″) of the hydrogels were analyzed at 1 Hz. Self-healing properties of the hydrogels were evaluated by the rheological analysis of network break and recovery in high and low strains, respectively. Cyclic step strain measurements at 1 Hz frequency were carried out for each sample at alternating 1 and 500% dynamic strains for 120 s in each step.

3-3-2 Contact angle:

Static water contact angle measurement was done by a contact angle measuring system at room temperature. A drop of distilled water (5 μL) was deposited on the surface of the dried hydrogel and images of the drop profile were converted by a computer.

3-3-3 FTIR:

FTIR spectra were recorded on a Nicolet iS10 spectrometer (Thermo-Fisher, USA) from 4000 to 600 cm^{-1} with an average of 64 scans at 4 cm^{-1} resolution. Interactions between additives inside of the hydrogel are traced by this test using different polymer combinations.

3-3-4 Lap shear test:

Lap shear tests were designed to measure the tissue-polymer adhesiveness. Two defatted pig skins were cut into the same rectangular shape by scalpel, and different combinations of hydrogel precursor solution was injected into the overlapped area (25 mm × 25 mm) between the two pigskins at room temperature. Subsequently, the lap joint was slightly pressurized with paper clips and put in the phosphate buffer solution (PBS, pH= 7.4) and at 37 °C for 20 min to simulate wet environment of the human body. All tests were repeated 3 times and the same procedure was obtained in the dry condition at 37 °C in the oven to measure the adhesive property of the polymer in dry condition. After 20 minutes or 24 hrs. (based on the experiment) two ends of the pig skins were clamped to the tensile machine. The shear velocity was 2.6 mm/min until two pigskins wholly separated. The pick loads were reported as a detachment force.

3-3-5 Degradation:

The hydrogels were weighed and then dried in the oven and weighted again. Initial weight was noted as W_i, and incubated in 1X PBS at 37 °C for different time intervals 1, 2, 3, 5 and 10 days. After the respective times were completed, the hydrogels were surface blotted with filter paper and dried out in oven at 40 °C and weight again. The weight of the hydrogels were recorded as W_f. The rate of degradation was then calculated by the mentioned formula.

$$Degradation\ \% = \left(\frac{W_i - W_f}{W_i}\right) * 100$$

3-3-6 Water Vapor Transmission Rate (WVTR):

The moisture permeability of the hydrogel were determined by measuring the water vapor transmission rate (WVTR) according to the ASTM standard. Gels having a diameter of 15 mm were prepared and mounted on the mouth of cylindrical cups (13 mm diameter) containing 10 mL water. In our previous study we used Teflon tape to seal our samples and cup connection surface,

while in this case we don't need Teflon tape because our samples adheres to the cup surface and seal it well. Our samples were kept at 37 °C and 35% relative humidity in an incubator. The cups were weighed at regular time intervals and the WVTR were calculated from the slope of the weight loss versus time plot, using the equation: [31]

$WVTR\ (gr\ m^{-2}\ day^{-1}) = \frac{Slope \times 24}{B}$ (B is area of cup mouth in m^2)

3-3-7 Swelling Ratio:

Swelling ratio of the bioadhesive hydrogel was measured by classical gravimetric method. Each sample (n = 3) of lyophilized hydrogels was weighed (W_d) and immersed into the distilled water at room temperature. At appropriate intervals (15, 30 min, 1, 2, 24, 48 and 72 hrs.), samples were removed, and the excess water on the surface was dried by filter paper and weighed again (W_w). The water uptake ratio (E_u) at each interval was calculated as below:

$$E_u\% = \left[\frac{W_w - W_d}{W_d}\right] * 100$$

3-3-8 Morphology:

Morphology and cross linking of samples were studied by using a Scanning Electron Microscope (Phenom G1 desktop SEM). Before SEM, all samples were lyophilized for 48 hrs. and sputter-coated with gold (SC7620 Mini Sputter Coater).

3-4 In vitro assays

3-4-1 Sterilization techniques:

For in vitro tests all samples must be sterilized. Due to the different properties of different components in the sample and their interaction with each other, it is not possible to use a single sterilization technique. At the beginning, CS/GO solution was sterilized by a hot steam sterilization

technique. Then BG solution was sterilized by sterilizing filter (VWR vacuum filter, 0.2 µm PES filter unit). HCA powder was sterilized by UV exposure. Then these sterilized components were added to each other as explained in the preparation section.

3-4-2 Antibacterial assay

The antibacterial activities of the samples against Escherichia coli (E. coli, ATCC# 25922, Microbiologics, LOT 335-503-1, gram-negative bacteria) and Staphylococcus aureus (S. aureus, ATCC# 6538, Microbiologics, 485-1002-4, gram-positive bacteria) were measured by the serial dilution technique. Briefly, E. coli and S. aureus were cultured seperately in a Tryptic Soy Broth medium (Remel, LOT 165803, REF R455052) to reach optical density of 0.2 (about 2×10^7 Bacteria). Optical densities were measured by spectroscopy (spectronic 200, Thermo Scientific). 150 µl of dried samples were soaked in 1 mL bacteria/TSB medium and inoculated for 24 h in a 37 °C shaker. After incubation, 100 µL of the bacteria/TSB medium was added to 900 µL of sterilized broth solution to prepare several decimal dilutions and then 10 µL of the diluted bacteria/TSB solutions were gently spread on a plate containing Tryptic Soy Agar (TSA agar). Plates were incubated at 37 °C for 24 h and the number of bacteria was counted. A pure bacteria solution was used as the control. Each test was repeated 3 times and the average value was reported.

3-4-3 Cell cytotoxicity:

The alamarBlue® assay was used to assess the level of cell metabolic activity and proliferation without damaging the scaffolds or the living cells. This technique has been explained by M. V. Deshpande et. al [201] Briefly, the ready-to-use, non-toxic alamarBlue® cell viability reagent from Invitrogen (Thermo Fisher Scientific, Eugene, OR, USA) was used to evaluate the cell metabolic activity on the hydrogel samples (sample size 150 µl) at Day 1and day 3 according to the standard

protocol recommended by the manufacturer. In this assay for all samples, we use the same passage of cells and similar number of cells ($1.5 * 10^5$) and samples were sterilized before use. A medium containing (85 % DMEM (Corning), 14% FBS (Millipore), 1% Pen strep (gibco)) with no scaffold and no cells was used as the negative control and fibroblast cells were seeded directly in the culture well with no scaffold used as the positive control. The fluorescence was measured using Gen5 software on a Biotek Model Synergy HT multi-mode microplate reader at excitation/emission wavelengths of 540/590 nm. The percentage of activity in each sample was calculated according to the following Equation:

$$A = \left(\frac{S - N}{P - N}\right) * 100$$

In this equation S, N and P stand for Sample, Negative control and Positive control respectively.

3-4-4 Angiogenisis assay on HUVEC:

In order to investigate the angiogenesis property of samples, $5*10^4$ endothelial cells (HUVEC: human umbilical vein endothelial cells) were incubated on the samples (sample size 150 µl) in a 24 well plate. Results are compared with HUVEC in EGM-2 medium (Lonzo, US) without sample as a positive control and EGM-2 without cell and sample as a negative control. Cell activity at 3 days is evaluated by alamarBlue® assay (Thermo Fisher Scientific, Eugene, OR, USA). The fluorescence was measured using Gen5 software on a Biotek Model Synergy HT multi-mode microplate reader at excitation/emission wavelengths of 540/590 nm. The percentage of activity in each sample was calculated according to the following Equation:

$$A = \left(\frac{S - N}{P - N}\right) * 100$$

In this equation S, N and P stand for Sample, Negative control and Positive control respectively.

3-4-5 Cell migration:

In vitro cell migration is an easy and well- developed technique. This protocol is explained by C. C. Liang et. al [202]. Briefly, $3*10^5$ NIH 3T3 cells were cultured in 24-well plate in NIH 3T3 medium (85 % DMEM (Corning), 14% FBS (Millipore) and 1% Pen strep (gibco)). Whenever confluency reached 90%, a scratch was formed by a 10ml serological pipet on the bottom of the well. Then detached cells were washed with PBS, aspirated and the size of scratches were measured (D_i). Finally, samples are placed on the scratch line and incubated (5 % CO_2, 37 °C). After 12 hrs. The size of scratches are measured (D_f) and compared with initial size. Percentage of the scratch closure was calculated by the following equation:

$$Percentage\ of\ scratch\ closure = \left(\frac{D_i - D_f}{D_i}\right) * 100$$

Three replications were considered for each sample and measurements are done on three different places of each scratch line.

3-4-6 Cell Morphology:

Samples were placed in a 24-well plate and washed with PBS three times. NIH 3T3 medium (85 % DMEM (Corning), 14% FBS (Millipore), 1% Pen strep (gibco)) was added on the samples surface and incubated for 24 hrs. $1.5 * 10^4$ cells (in 1 mL of medium) were seeded into each well, and then plate were incubated at 37 $^{\circ}$C and 5% CO_2 for 3 days. Then each well was washed three times with PBS, and fixed with paraformaldehyde solution and 4% PBS (thermos scientific) two times for 30 min. After thorough washing, the cells were dried with 30, 50, 70, 95 and 100% ethyl alcohol followed by a critical point drying. Cell attachment and cell morphology were observed by a Scanning Electron Microscopy.

3-4-7 Quantitative real-time polymerase chain reaction PCR

The gene expression analysis by real time RT-PCR was used for evaluation of the three important genes related to the cell migration and cell proliferation. Briefly, based on protocol that is presented in 3-4-5 (cell migration assay), after reaching 80-90% confluency of cells in each well, the bottom of wells were scratched by a 10 ml serological pipette. After day 1, and day 7. RNA is extracted and purified based on protocol provided by NORGEN BIOTEK (Cat. 35300). Concentration and purification of the RNAs are measured by spectrophotometry (NonoDrop One, Thermo Scientific). Then cDNA reverse transcription is done by high capacity cDNA reverse transcription kit (applied biosystems, Thermo fisher Scientist, Lot 00754387, REF 4368814). Thermal cycles for cDNA synthesis includes 10 minutes at 25 °C, 120 minutes at 37 °C and 5 minutes at 85 °C. MiniAmp Thermal Cycler (appliedbiosystem) conducted all thermal cycles for cDNA synthesis. Finally quantitative PCR is done by PowerTrack SYBR Green Master Mix (appliedbiosystems, Lot 01244277, REF A46109) and analyzed by QuantStudio 3 Real-Time PCR instrument (appliedbiosystems, Thermo Fisher Scientific). Cycling parameters were set for enzyme activation phase at 95 °C for two minutes in one cycle, denature phase at 95 °C for 15 seconds in 40 cycles and anneal/extend phase at 60 °C for 60 second in 40 cycles. Fluorescence data captured during the extension phase of each cycle. Table 3-2 shows primers used in PCR test.

Table 3-2 Primer Sequences Used for Validation by QRT-PCR

Gene/Oligo name	Oligo sequence
ACTR2 Forward	CTAAATGACGGGCGGAG
TGFβ1 Forward	CAATTCCTGGCGATACCTCAG
bFGF Forward	CAATTCCCATGTGCTGTGAC

Table 3-2 continued

ACTR2 Reverse	ATATCCACACTTCACAAACCC
TGFβ1 Reverse	GCACAACTCCGGTGACATCAA
bFGF Reverse	ACCTTGACCTCTCAGCCTCA

3-4-8 Clotting time:

A whole blood clotting time measurement was carried out by X. Sun [203]. Briefly, blood was taken from a horse (male, 10 years old) with a medical vacuum collective tube containing anticoagulant (3.8% sodium citrate: blood = 1:9). 100 µl of this sample was added to 1 ml citrated whole blood, then 100 µl of $CaCl_2$ (0.1 M) added to activate citrated blood. Immediately after that the sample was transferred to the hot water bath at 37 °C and time recorded. The tube was tilted every 10 s to observe if the blood was gelatinized.

3-4-9 Whole blood clotting kinetics:

The whole blood clotting kinetics of samples was carried out according to a reported procedure by X. Sun [203]. Briefly, 50 µl of sample was added to 100 µl of activated horse whole blood (1ml citrated blood activated with 100ul of $Cacl_2$ 0.1M). At different time intervals (5, 10, 35 and 50 min) 3 ml of DI water was added for 5 min to lyse red blood cells (RBCs) which were not trapped within the blood clot. After five minutes, 200 µL of remaining lysed RBCs was added to a 96 well plate in triplicates for each sample and time point. The absorbance at 540 nm was recorded by a BioTek Synergy HT type microplate reader. Because the absorbance is indicative of RBCs not trapped within the clot, it is inversely related to the clot size. Two controls were considered, the citrated blood and activated blood that were treated without sample and three replicates were performed for each sample.

3-5 Statistical analysis:

P values were determined by t-test and analysis of variance (ANOVA) by Microsoft Excel software. Values below 0.05 were considered statistically significant. Error bars in the graphs are Standard Error Mean (SEM) that are calculated by following equation:

$$SEM = \frac{\delta}{\sqrt{n}}$$

Where σ is standard deviation and n is number of samples.

4. CHAPTER FOUR: RESULTS AND DISCUSSION

4-1 Introduction:

Designing a thermoresponsive bioadhesive injectable hydrogel for different applications of wound dressing [5], suture less surgery [6], effective cancer therapy [7], cell delivery [8] and injectable nerve regeneration [9] is demanding. In the current design, we aim to develop a thermoresponsive bioadhesive as a wound dressing able to close the wound immediately and providing an appropriate environment to accelerate wound healing. As discussed in previous chapter due to the unique properties of chitosan such as biocompatibility, biodegradability, antibacterial properties, low toxicity and immune-stimulatory activities, it is an excellent candidate as a basic polymer for designing a thermoresponsive bioadhesive for wound dressing application. [10]. Our results indicate this design could improve wound healing process in different ways. As presented in previous chapter different Cs: HCA molar ratios and GO concentrations were studied. In this chapter, results of characterization of different samples are presented. We will discuss the effect of different additives on chitosan based thermoresponsive bioadhesive polymer properties.

4-2 Rheological study:

The changes of viscoelastic moduli, including storage modulus (G′) and loss modulus (G″), during the gelling process of hydrogels are demonstrated in supplementary data (Figure 7-1). Regarding the cross point of G′ and G″, the gelation times of all samples are presented in Table 4-1. Samples containing more HCA have higher gelation time. HCA and chitosan have repulsive interactions and it may separate chitosan chains and allow them to move easily and consequently increase gelation time. Meanwhile, increase in GO concentration decreases gelation time. It could be explained by hydrogen bonding between GO and chitosan amine groups that enable chitosan chains to interact with each other more closely and improve hydrophobic interactions at higher

temperature converting our samples to form gel due to hydrophilic - hydrophobic interactions (from solution at room temperature to gel at 37 °C).

Table 4-1 Gelation time for different samples extracted from rheological study (cross point of G′ and G″)

sample	Gelation time (s)
1:1, 0.5	250
1:0.5, 0.5	94
1:1, 1	84
1:0.5, 1	9

Structural breakdown and self-healing of the gels were evaluated through time-dependent dynamic experiments at a constant frequency of 1%. Sample microstructures were broken by exposing it to a large strain (500%). We observe a substantial drop in moduli (Figure 4-2 A-D). Re-healing was then monitored by following the moduli buildup at a low strain (in the LVE region) of 1%. We observe an instantaneous increase in G', which is now larger than G'', and approximately at the same value at which it was prior to sample breaking. Except in the last case shown in Figure 4-2D, all samples reflect self-healing. The unusual features observed in Figure 4-2D has not be probed further as this was outside the scope of the present work. As presented in this figure all samples except 1:1 1 show self- healing property. The reason for not showing self-healing property in the 1:1, 1 sample could be explained by high concentration of graphene oxide and HCA that interact with chitosan differently. HCA has repulsive interactions and GO improve crosslinking between chitosan chains. In Damage cycles, our samples are not damaged totally. After 3 cycles of damaging and healing, it seems our sample is going to show some level of damage (after t= 360

s). By increasing one more cycle of damaging/healing we may get some level of self-healing property (see Figure 7-2). Results of visual evidence for self-healing property for one of the samples (1: 0.5, 0.5) is presented in Figure 4-2E. As shown in Figure 4-2E after healing the hydrogel stays uniform. Hydrogen bonding and π-π stacking could be two main mechanisms for intrinsic self-healing property. Frequency sweep for one of the samples (1:0.5,1) has been performed at T= 37 °C and 1% strain (frequency 0.1-10 HZ). As shown in Figure 4-1 G'>G" over entire frequency. It also showed all tan delta (G"/G') is relatively frequency independent. All this evidence showed our sample is gel at this condition.

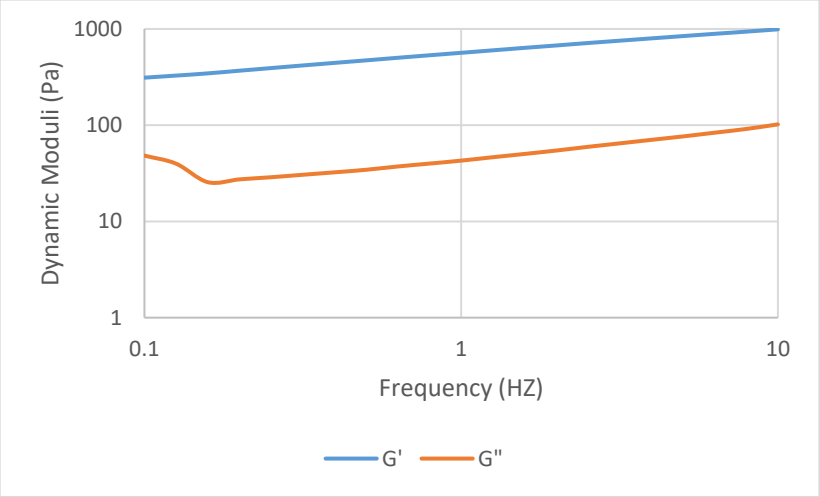

Figure 4-1. Frequency sweep test for 1:0.5, 1 sample at 37 C and 1% strain.

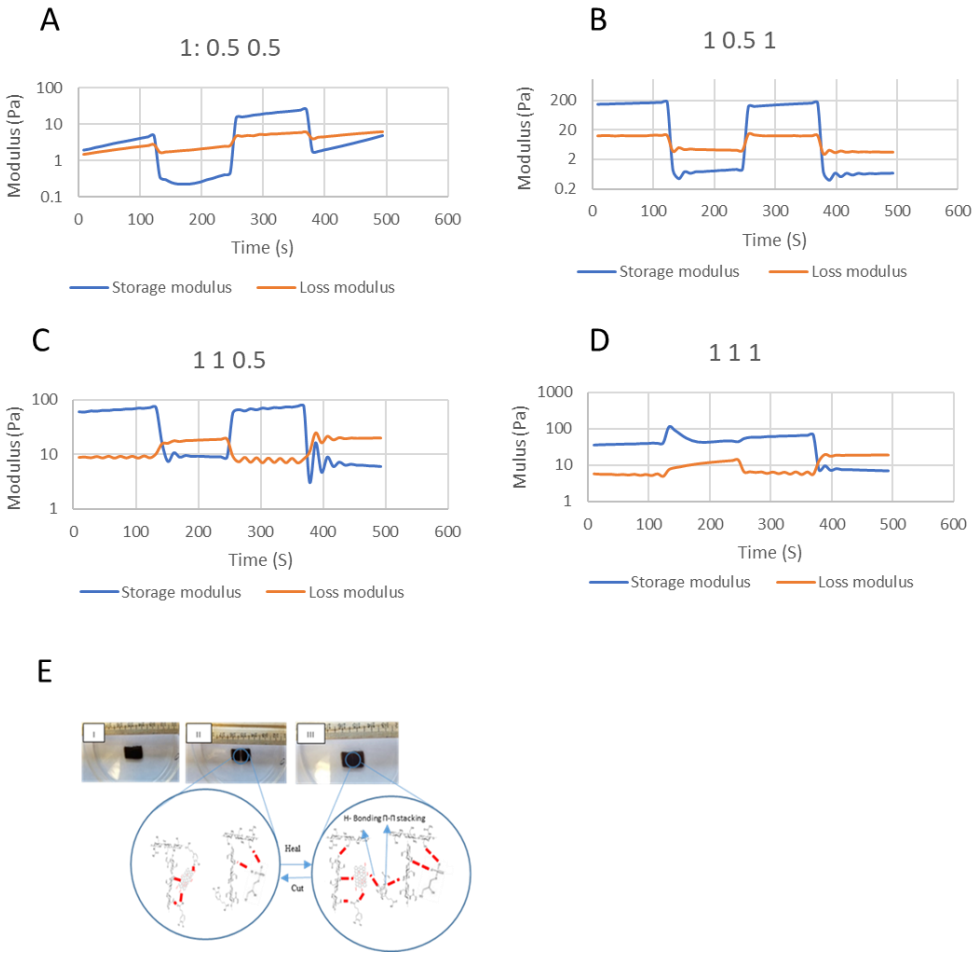

Figure 4-2 A-D) Self-healing properties of the hydrogels evaluated by rheological study and measuring G′ and G″ (log-Y axis) for network break and recovery at alternate 1 and 500% dynamic strains, respectively. Each step was processed for 120 s at 1 Hz frequency. E) Visual evidence for self- healing property of 1:0.5, 0.5 sample, I: before damage, II) damage, III) healing phase.

Rheological studies on samples' viscosities are presented in Figure 4-3A, all samples are shear thinning polymers. Meaning that increase in shear rate decreases viscosity. This property makes these samples good candidates for injection. In Figure 4-3B, their injectability is tested by injecting samples in PBS solution at room temperature through a needle (G20) as well. Visual evidence of samples injection shows smooth release from needle. Also, there is not Newtonian plateau in all these viscosity graphs that could be due to the presence of Graphene Oxide microstructures in the polymer.

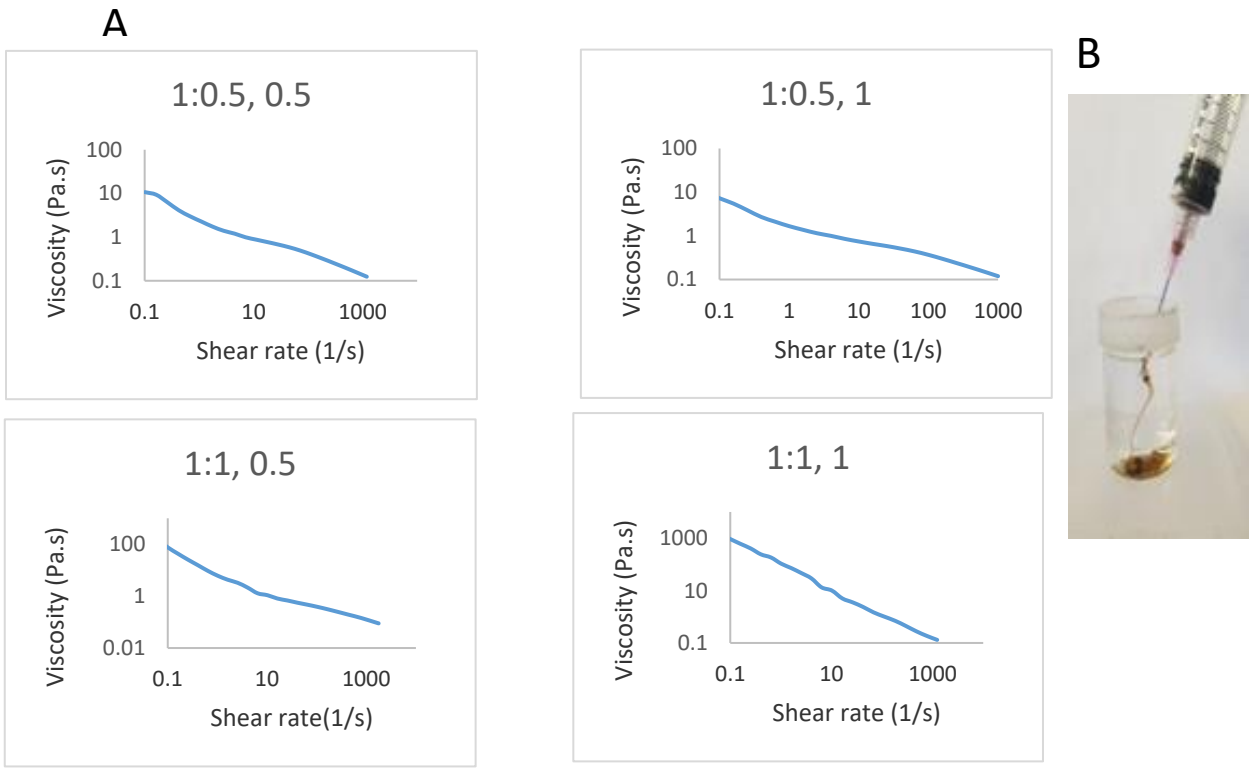

Figure 4-3.A) Changes in viscosity indifferent shear rate at 20 °C, B) injectability of 1:0.5, 0.5 through needle (G20)

4-3 FTIR:

As presented in Figure 4-4 A, band at 1010 cm^{-1} in Chitosan/Beta Glycerophosphate (CS/BG) is characteristic of glycerophosphate and indicates aliphatic P-O-C stretching. The band at 1060 cm^{-1} is characteristic of the PO_4^{2-} group, whereas the band at 960 cm^{-1} may indicate the presence of the HPO_4^{-} group. The FTIR spectrum of Chitosan (CS) has one broad band at 660 cm−1 which is connected with vibrations of the O=C-N group. The band at 780 cm^{-1} in the CS/BG spectra is characteristic of GP (aliphatic stretching of P-O-C). [204] Lowering of wavenumbers of amide I from 1740 and 1,580 cm^{-1} in Chitosan (CS) to 1640 and 1470 cm^{-1} in Chitosan/HCA/Graphene Oxide/ Beta Glycerophosphate (CS/HCA/GO/BG) spectra could be due to the electrostatic interaction between negatively charged beta glycerophosphate and protonated Chitosan. For the

hydrogels containing Graphene Oxide, the disappearing of the peak at 1,730 cm^{-1} which is related to C=O stretch could be explained by the synergistic effect of H-bonding between Chitosan and the oxygen containing groups in Graphene Oxide and electrostatic interaction between polycationic Chitosan and the negatively charged Graphene Oxide. [205] In the spectra of CS/HCA/GO/BG, the success of functionalization of HCA was confirmed by the presence of two bands at 1400 cm^{-1} the C=C aromatic stretching and at 783 cm^{-1} the C-H aromatic bending which is related to the aromatic ring of HCA.

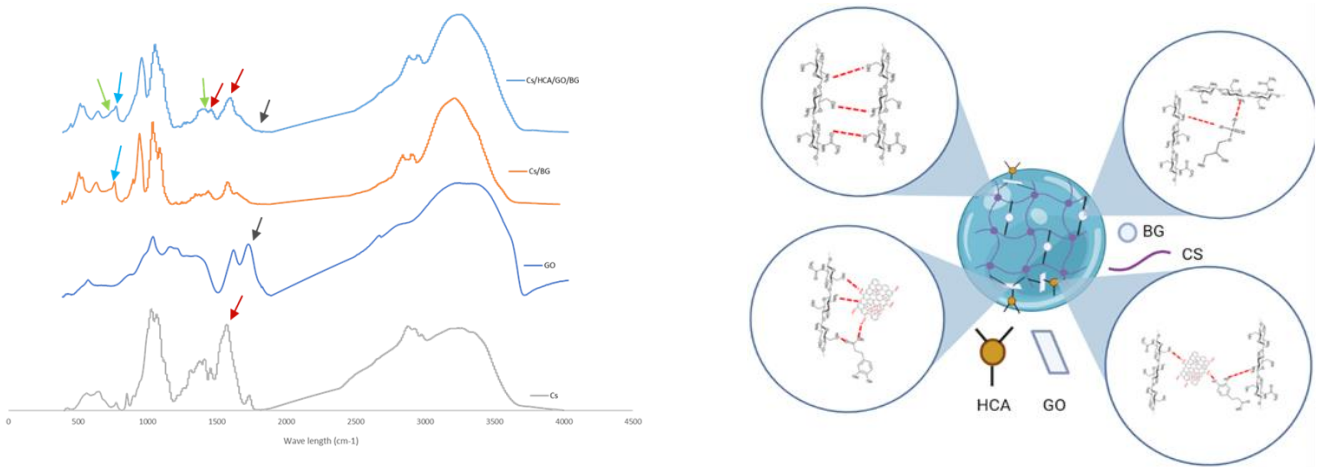

Figure 4-4 A) FT-IR spectra of Cs, GO, Cs/BG, Cs/HCA/GO/BG, b) Schematic of possible molecular interactions based on FTIR test

4-4 Lap shear test:

As described before, a key functional group of HCA is the o-dihydroxyphenyl group (catechol), which forms strong covalent and noncovalent bonds with various surfaces. The amino groups on CS backbones and the catechol groups on the HCA interact with tissues by various mechanisms such as electrostatic interactions, intermolecular and interatomic interactions (such as hydrogen bonding, π−π stacking and cation−π interactions). Schematic of these interactions are presented in Figure 7-3. To measure the effect of different factors on adhesiveness and cohesiveness, various content combinations of precursor hydrogels were prepared.

The effect of HCA on adhesive property in wet condition (submerge samples in PBS solution at 37 °C) is presented in Figure 4-5A. HCA addition has significant effect on detachment force (see 1:0, 0.5 vs 1:0.5 0.5). Increase in HCA concentration does not have significant effect on adhesive property (Figure 4-5B)

.

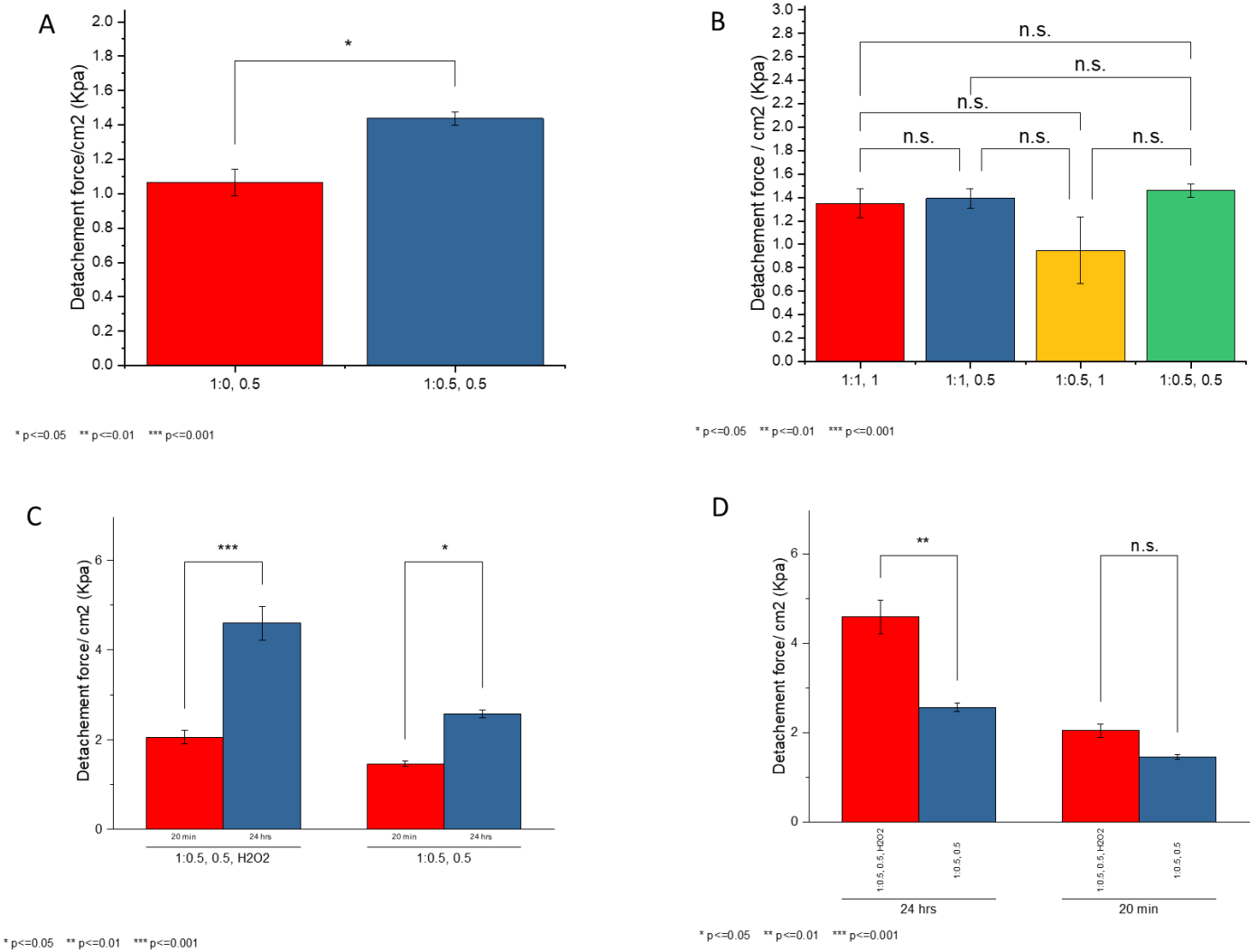

Figure 4-5. A) The effect of HCA on detachment force in wet condition after 20 mints contact between adherent and adhesive polymer. III) The effect of increase in HCA and GO concentration on detachment force C, D) The effect of catechol oxidization on detachment force after 20 mints and 24 hrs. In wet condition with H2O2 and without H2O2 as an oxidizer agent.

As presented in Figure 4-6, 1:0.5, 0.5 sample is more hydrophobic than 1:0, 0.5 It could be concluded that due to the presence of HCA, hydrophobicity of hydrogel increases. Hydrophobic interaction between HCA and water molecules avoids gap formation between adherent and adhesive polymer. Accordingly, interactions between catechol groups of HCA and amine groups of tissue are more productive.

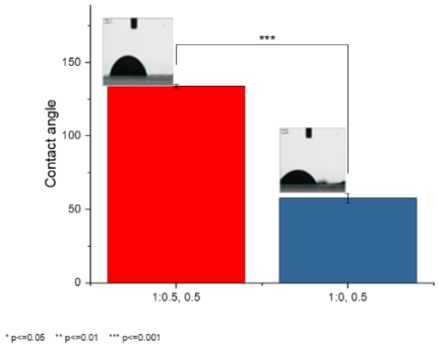

Figure 4-6. Contact angle of different polymer combinations to see the effect of GO and HCA on hydrogel hydrophobicity property

Moreover, GO could improve mechanical property of the hydrogel (Cohesiveness). However, as presented in Figure 4-5B adhesive property of 1:0.5, 0.5 vs. 1:0.5, 1 does not change significantly. It could be concluded the hydrophilic effect of GO that decrease adhesive property and cancel out the effect of cohesiveness.

Catechol oxidization is another important factor on adhesive property. To study this factor, H_2O_2 is added as an oxidizing agent to accelerate oxidation process (catechol groups are oxidized by H_2O_2). Lap shear test measured after 20 mints and 24 hrs. of pigskins contact in wet condition. The results are shown in Figure 4-5 C, D. Those containing H_2O_2 had significant improvement in adhesive property (after 24 hrs). Another studied factor is time. 1:0.5, 0.5, H_2O_2 hydrogel had higher degree of oxidization after 24 hrs due to the presence of the H_2O_2 as an oxidizer and accordingly higher adhesive property (2-3 times more than (1:0.5, 0.5)). Oxidized HCA contributes to strong adhesion to biological surfaces, through the formation of covalent bonds with

available nucleophile groups on their surfaces such as $–NH_2$, –SH, –OH, and –COOH. However, adding HCA into the polymeric structure has some level of oxidization in atmosphere and alkaline condition. [206] To provide this condition (higher pH condition) in this study, BG has added to the polymer solution before HCA addition.

4-5 In vitro degradability:

Biodegradation is important for wound dressing design. It can provide space for neo-tissue. As shown after 10 days both samples lost 90% of their original weigh. At first day all samples lost 80% of their weight. In our experiment one of our samples without graphene oxide (1:0, 0) totally dissolved in PBS after 24 hours, while other samples kept their structure after 10 days. It could be concluded, due to the presence of graphene oxide in samples, they keep their polymer networks and they do not dissolve in PBS even after losing 80% of their weight.

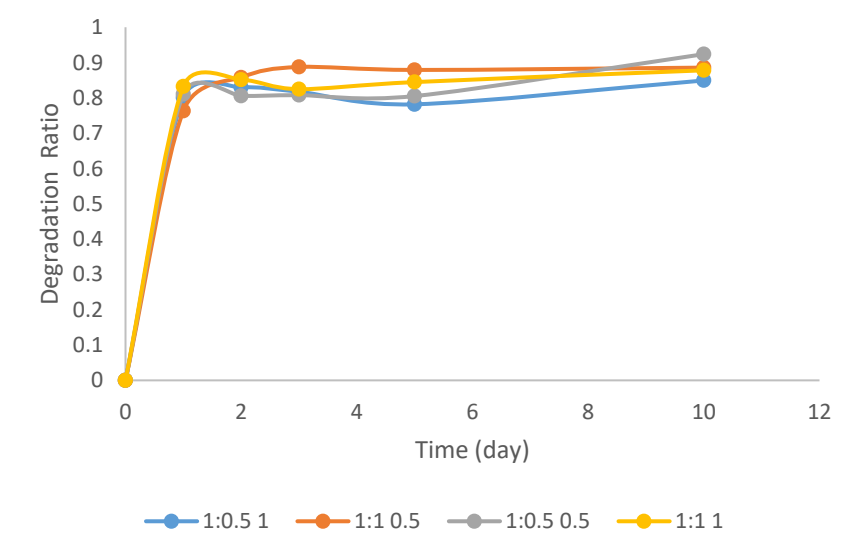

Figure 4-7. In vitro biodegradation in PBS solution at 37 °C

4-6 Morphology

As demonstrated in Figure 4-8, addition of Graphene oxide increases cross-linking. this is concluded from the presence of different functional groups such as graphene oxide and chitosan in all samples. These functional groups provide electrostatic interactions and hydrogen bonding for cross-linking between polymeric networks. HCA and chitosan have repulsive interactions. By adding HCA, this interaction provide a beehive shape in the 1:0.5, 0.5 sample. More addition of HCA damages some of the polymeric network crosslinking. This means, in 1:1, 0.5 there must be fewer interconnections between polymeric networks. Having bigger pore size enables better cell migration. Pore sizes required for the regeneration of various tissues varied depending on the size and the origin of transplanted cell and regenerating tissue. Optimum pore size for fibroblast cells migration is 50-160 μm [207]. By using Image J, average pore size of our samples are presented in Table 4-2. Increase in GO concentration improve crosslinking and increase crosslinking thickness. GO concentration increased in 4 and 8 v/v% and the effect of such increase is presented in Figure 7-5. As expected, crosslinks are even thicker, while pores are smaller.

Table 4-2. Average pore size (μm) in different samples

Sample	1:0.5, 0.5	1:1, 0.5	1:0.5, 1	1:1, 1
Average pore size (μm)	123	135	129	86

Optimum pore size of a sample enable better oxygen and chemoattractant transfer and consequently better directional cell migrations, while very big pore size may affect other wound dressing properties like water vapor transmission rate. A combination of different images that is taken by Zeiss Xradia Xray nano CT scanner in a video format (Movie 1) 3D view of (1:0.5, 0.5)

is presented to give us a better view of interconnections and porosity distribution. For better understanding of this uniformity, three different cross sections of sample (1:0.5, 0.5) are selected and pore size are measured Figure 7-6. The porosity of the sample is the same as porosity that is measured by SEM.

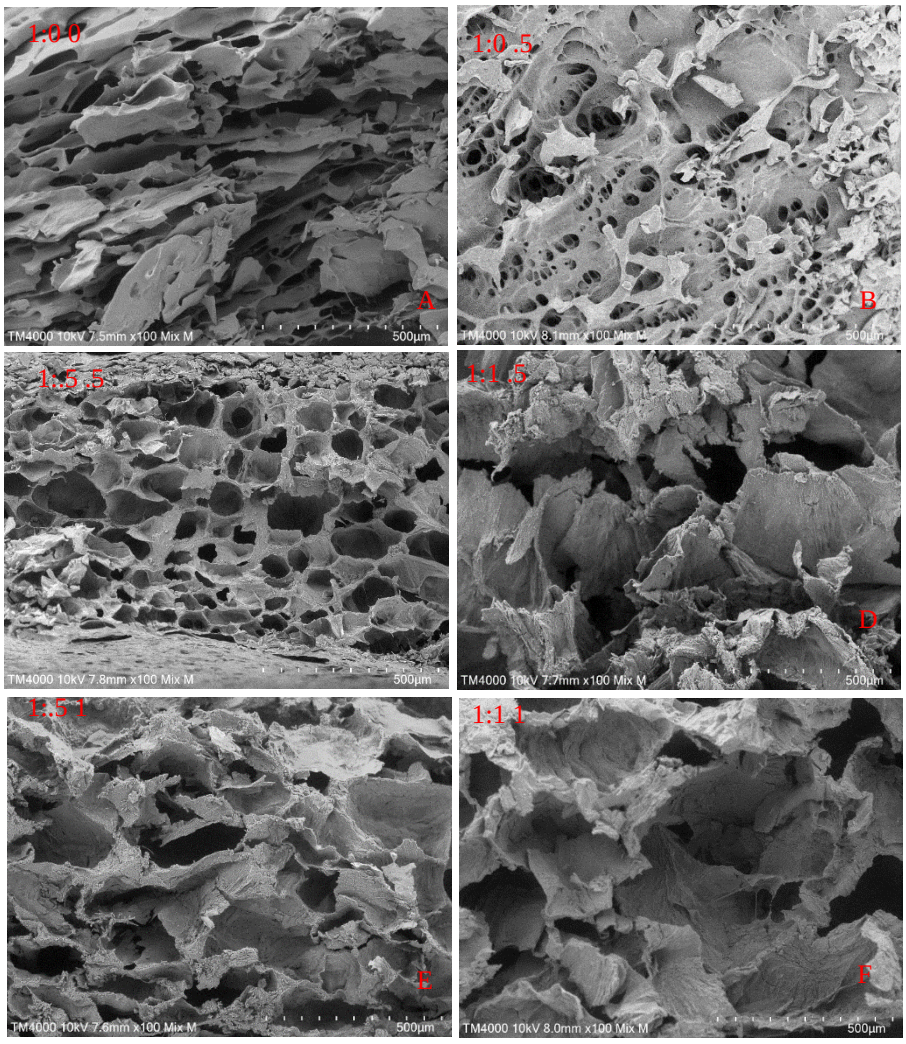

Figure 4-8.Morphology of different samples by SEM

4-7 Water vapor transmission rate (WVTR) and Swelling ratio:

Controlling the water loss from wound surface in order to prevent excessive dehydration is an essential factor for an ideal wound dressing. R. Xu [208] recommended a rate of 1790–2265 gr/m^2/day of WVTR should maintain an appropriate moisture level without wound dehydration.

Very high WVTR could cause wound dehydration and adhesion of wound dressing to the wound site and the chance of secondary injury of new skin in wound site during wound dressing renovation would increase. Very low WVTR could cause the accumulation of exudate in wound site. As presented in Table 4-3, our samples have WVTR of 1813- 2670 gr/m^2/day. The reason for increasing WVTR by increasing in HCA concentration in low concentration of GO (1:0.5, 0.5 vs, 1:1, 0.5) cold be explained by repulsive interactions of HCA and Chitosan. Increases in HCA concentration damages some of polymeric network. However, WVTR of all samples are in an acceptable range or slightly higher than acceptable range (1:0.5, 1) keeping moist environment for wound healing and avoiding exudate accumulation in wound site. There are some commercial wound dressings such as Geliperms (Geistlich Ltd, Switzerland) and Vigilons (Bard Ltd, Crawley, UK) that have a WVTR of 9009±319 and 9360±34 gr/ m2/day, respectively, which would dehydrate the wound surface and make the dressing adhere to the wound surface. [30].

Table 4-3. Water Vapor Transmission Rate for different samples

Sample	1:0.5, 0.5	1:1 0.5	1:1, 1	1:0.5, 1
WVTR (gr/m^2/day)	1813	2183	2291	2670

Wound exudate includes water, electrolytes, nutrients, inflammatory mediators, white cells, protein, digesting enzymes, growth factors and waste products. High level of wound exudate could be a problem in wound healing process due to leakage onto the periwound skin. This may overhydrate the periwound [209]. Having a wound dressing with exudate removal property is very helpful to accelerate wound healing process. As presented in Figure 4-9, in first 2-6 hours of the test, samples reach a maximum swelling ratio that could help to manage exudates immediately after applying wound dressing. De-swelling happens in 6-24 hrs. One reason for deswelling could

be degradation processes happening in the samples which is in good agreement with degradation tests. De-swelling in 1:1, 0.5 sample is much lower than other samples. It could be due to its larger pores that keep more water molecules. This conclusion is in good agreement with SEM test (Table 4-2) where 1:1, 0.5 sample has bigger pore size. 1:1 1 has lowest swelling ratio that could be explained by lower pore size. Moreover, de-swelling in 1:1, 1 is much lower than other samples (see the slope of graphs in Figure 4-9 after 6 hrs.) It is due to higher concentration of GO that provides this sample with better mechanical property.

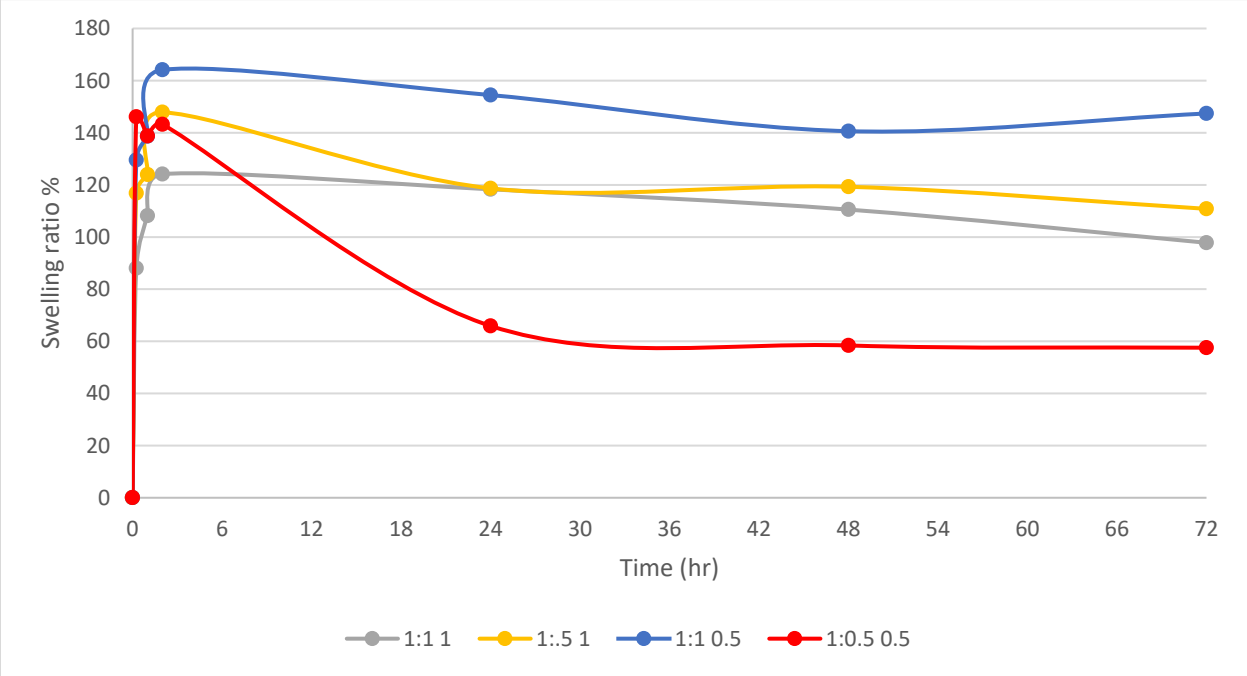

Figure 4-9. Swelling ratio for different samples

4-8 Antibacterial test

As shown in Figure 4-10, almost all samples do not show antibacterial activity against gram-negative and gram-positive bacteria. The main reason for not getting antibacterial property could be explained by pH. Chitosan has antibacterial property, but its antibacterial property is pH dependent. The most generally accepted hypothesis for chitosan antibacterial activity is that positively-charged amine groups (NH3+) of glucosamine interact with the negatively charged

surface of bacteria, causing leakage of intracellular constituents that results in cell death [210]. This mechanism needs high number of protonated amine groups and consequently low pH, while in this project we used betaglycerophosphate to improve solubility of chitosan at high pH (pH= 7.0+). Increase in pH decreases antibacterial activity of chitosan.

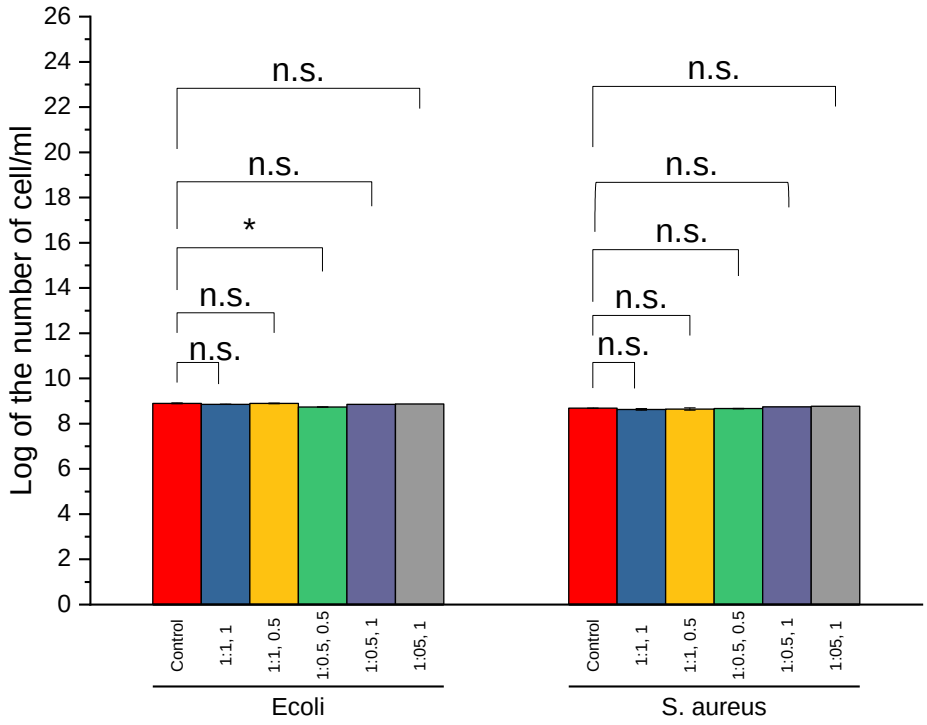

* p<=0.05 ** p<=0.01 *** p<=0.001

Figure 4-10. Quantitative amount of survival Bacteria left: Ecoli, right: S. aureus

4-9 Cell cytotoxicity and cell morphology

Biocompatibility of wound dressings is one of the most important properties. As presented in Figure 4-11A cell activity at day 1 for all samples is above 100%. Cell activity of 1:1, 0.5 sample drop to 75% at day 3, while other samples keep their cell activity above 100%. According to GB/T 16886.5-2003 (ISO 10993-5: 1999), samples with cell viability larger than 75% can be considered as non-cytotoxic material, so all samples except 1:1, 0.5 could be considered as biocompatible

materials. The main reason for the differences in cell cytotoxicity of these samples could be explained by the effect of HCA concentration on cell cytotoxicity. In the previous studies cell cytotoxicity of the catechol moiety on different cell lines are presented [211, 212]. R. Ahmadi et al [213] showed beta glycerophosphate concentration below 15% (W/V) in 2% (W/V) Chitosan hydrogel could promote cell proliferations that is in good agreements with our results. Increase in HCA concentration in the 1:1, 0.5 sample cancel out the effect of beta glycerophosphate and decrease cell proliferation. Cell attachment and live dead assay for all samples at day3 was done and are presented in Figure 7-7 and Figure 7-8. As presented in Figure 7-7 cell proliferated on all samples except 1:1, 0.5 and their spindle shapes are obvious. Cell circularity and cell density is measured by analyzing SEM images (3 images for each samples) by ImageJ software and results are presented in Figure 4-11B. As presented in this image 1:1,0.5 has the lowest cell density ($p<0.05$). Figure 4-11 C shows samples 1:1, 0.5 and 1:0.5 1 have less cell circularity in comparison with 1:1, 1 and 1:0.5, 0.5 ($p<0.05$).

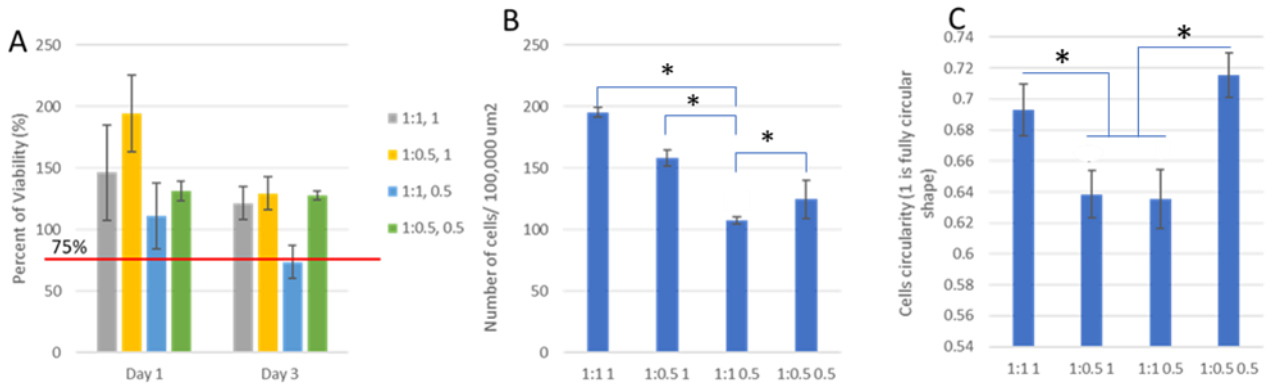

Figure 4-11. A) In vitro study on cell metabolic activity in Day 1 and Day 3 with Alamarblue assay, B) Number of cells in 100k µm^2, C) Cell circularity (1 is fully circular)

4-10 Angiogenisis assay on HUVEC

Results show samples 1:1, 1 is not compatible with HUVEC in day 1 and day 3. While 1:0.5, 0.5 and 1:1, 0.5 are biocompatible in day 1 and day3. Sample 1:0.5, 1 is at the edge of

biocompatibility at day 3. As it is clear in Figure 4-12, GO could promote HUVEC proliferation at some concentration. S. Mukherjee et. al results showed the production of Nitric Oxide (NO) inside HUVECs in presence of GO may improve angiogenesis properties [214]. Their results showed Reactive oxygen species (ROS) affect on NO production in HUVEC. GO concentration has direct effect on ROS production. However, high concentration of GO may have negative effect on HUVEC proliferation. This effect is presented in Figure 4-12. This result is in good agreement with previous studies on the GO effect on HUVEC.

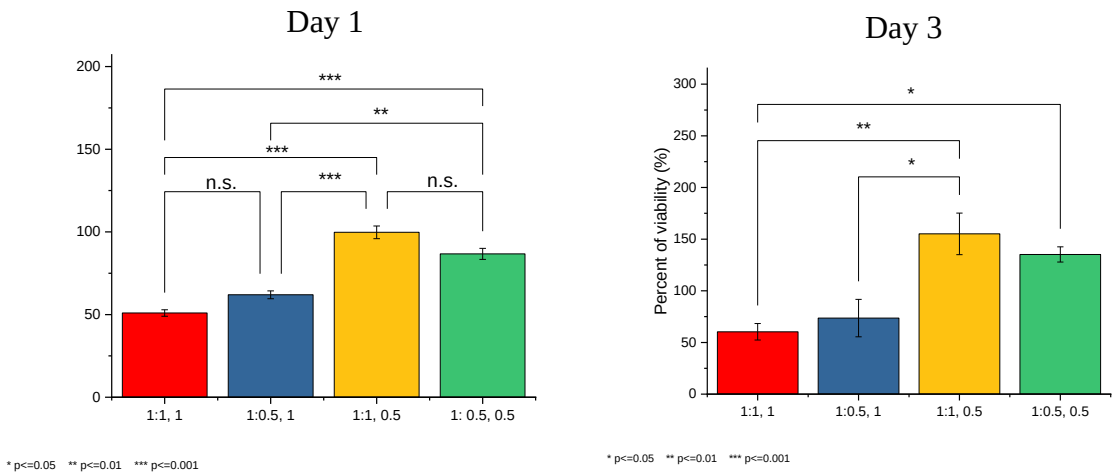

Figure 4-12. Cell viability assay (alamarblue) on HUVEC at Day 1 and Day 3

4-11 Cell migration

As presented in Figure 4-13, cell migration increases significantly in presence of 1:1, 1 and 1:0.5, 0.5 samples. Visual evidence for decreasing in closure area of the scratched area in presence of 1:0.5, 0.5 and control are shown in Figure 7-9. ROS are formed continuously in cells because of both oxidative biochemical reactions and external factors. ROS formed may cause cellular damage. HCA as an antioxidant could remove ROS and consequently improve cell metabolic activity [215]. In summary HCA balance ROS and consequently improve cell migration. Some researchers showed, antioxidants could stimulate some genes that are vital for wound dressing

[216] . Moreover GO could improve cell differentiation. One of the most interesting properties of GO is capturing differentiation cues, like growth factors from culture media and accumulate them onto their surface. It is one common reason for enhanced cell differentiation in several studies [217] [218]. Balance in both GO and HCA play a critical role in cell migration.

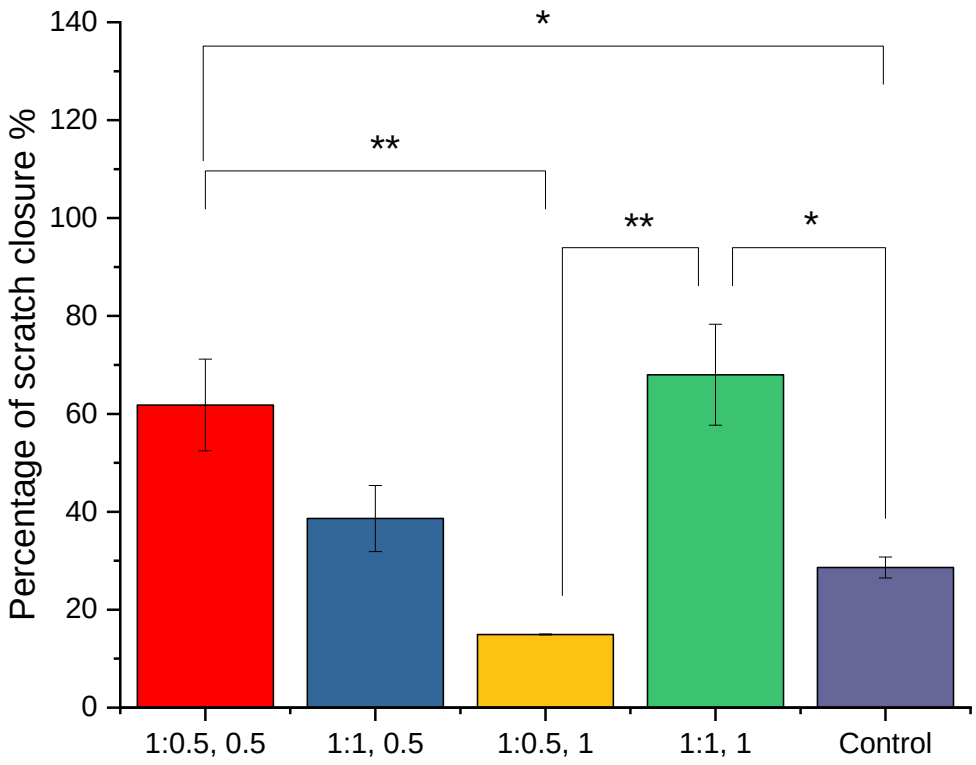

Figure 4-13. Results of cell migration assay after 12 hrs. of applying samples on the top of the scratched area

4-12 Clotting time and whole blood clotting kinetics:

As shown in Figure 4-14A clotting time of all samples are lower than control sample (activated blood). Zhang Hu et. al [219] study showed chitosan has hemostasis properties and the main mechanism for hemostasis properties could be explained by interaction between chitosan and

erythrocytes and linking them together to establish a cellular clot or hemostatic plug. 1:1, 1 and 1:0.5, 1 samples have significant decrease in blood clotting time. GO has positive effect on immediate blood clotting. It is due to absorbance capacity of GO for whole blood proteins. Order of blood proteins absorbance on GO is fibrinogen > immunoglobulin > transferrin. [220]. Fibrinogen responsible for blood clotting, Fibrinogen binds to activated αIIbβ3 integrin on the platelet surface, forming bridges responsible for platelet aggregation in hemostasis.

Result of whole blood clotting kinetic is presented in Figure 4-14B. This test is used to evaluate whole blood clotting efficiency of the samples. As shown in this figure 1:0.5, 0.5 and 1:0.5,1 have sharper change in first five minutes in comparison with 1:1, 0.5 and 1:1, 1 sample. It seems higher concentration of GO does not have that much effect on blood clotting efficiency. It could be explained by hemolysis effect of GO on red blood cells that destroy their membrane and release their contents (in this case, they release in DI water). Catechol moieties in HCA molecule has Anticoagulant properties. Its effect is visible in Figure 4-14B, where 1:1, 1 and 1:1, 0.5 (high HCA contents) have lower blood clotting efficiency.

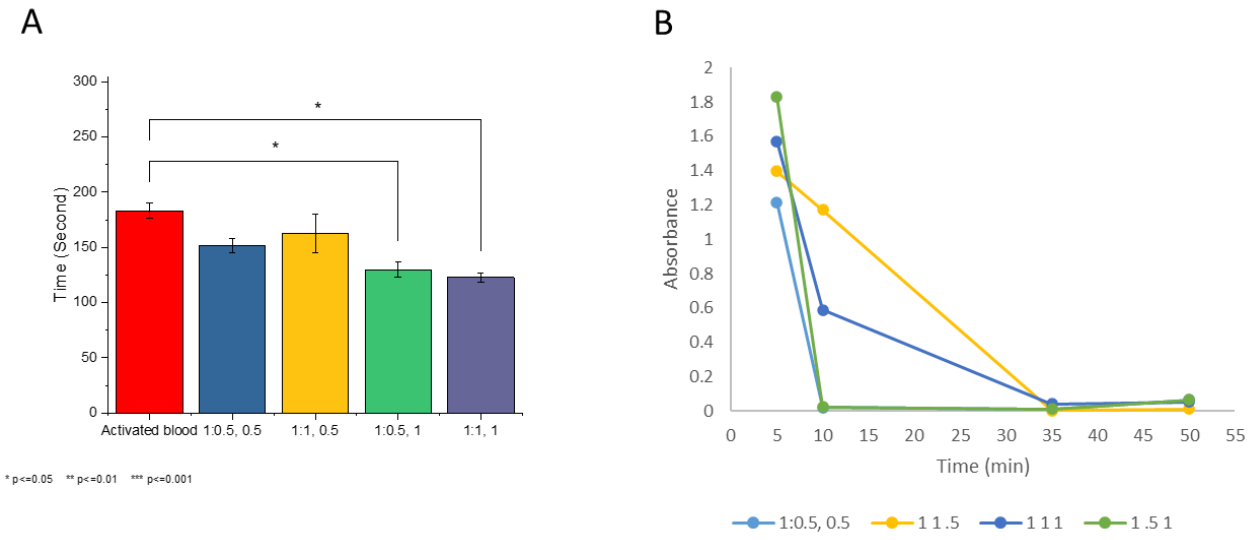

Figure 4-14. A)Blood Clotting time in presence of samples. B) Whole blood clotting kinetics of samples

4-13 Real time polymer chain reaction (PCR)

Based on results obtained from real time PCR test (Figure 4-15) level of TGFβ1 at day 1 is eight times higher than control sample (without polymer). TGF-β is involved in a number of processes in wound healing: inflammation, stimulating angiogenesis, fibroblast proliferation, collagen synthesis and deposition and remodeling of the new extracellular matrix. Interestingly chronic, non-healing wounds often show a loss of TGFβ1 signaling [221].

TGF-β is a chemotaxis for fibroblasts and activate their proliferation. Interactions between TGF-β and fibroblasts is a key factor for wound healing. TGF-β promote fibroblasts to proliferate and migrate into a wound while producing extra cellular matrix (ECM). This ECM allows other healing processes such as epithelialization and angiogenesis to occur. Moreover, by TGF-β stimulation, fibroblasts turn to myofibroblasts, which causes wound contraction and maturation

[222]. It is in good agreement with cell migration assay (Figure 4-13). The level of bFGF at day 1 is not higher than control, while its level at day 7 is twelve times higher than control.

bFGF has probably the broadest range of target cells involved in wound healing. A X. Zhang et. al [223] study showed bioinspired hydrogels with basic fibroblast growth factor improved in vitro wound closure 2.5 times better than control samples without any treatment. Their results (in vitro and in vivo) indicate the bioinspired hydrogels with bFGF accelerate wound healing process that might be due to the bFGF effect on wound re-epithelialization, collagen deposition, and contraction. HCA is an antioxidants that can control the level of ROS in wound sites and improve cell metabolic activity, moreover it can provide signaling pathway for growth factor productions of bFGF and TGF-β [224].

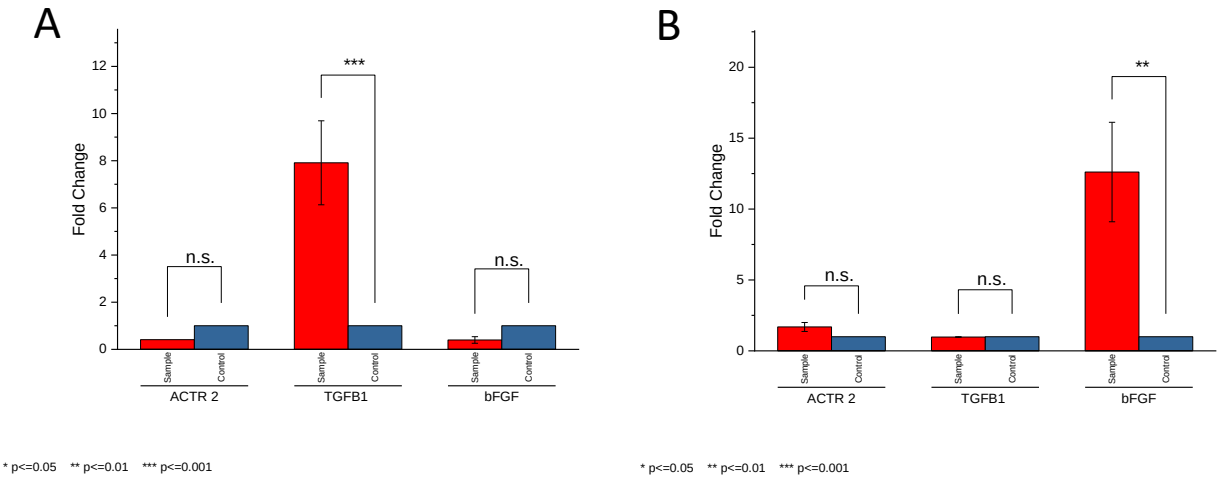

Figure 4-15. PCR results for 1:1, 1sample at A) Day 1, B) Day 7

5. CHAPTER FIVE: CONCLUSIONS & RECOMMENDATIONS

In this project, we took advantage of biomechanical and biochemical properties of a thermoresponsive bioadhesive polymer to accelerate the wound healing process. Chitosan was selected as a base polymer for this project due to its excellent specifications in wound healing such as biocompatibility, biodegradability and hemostatic properties. Chitosan has a lack of adhesive property in wet condition as well as cohesiveness. Addition of graphene oxide and HCA could improve other properties of chitosan. HCA has repulsive interactions with chitosan, so increase in HCA molar ratio increase gelation time (avoid of chain entanglements and hydrophobic interactions), while increase in GO decrease gelation time. Gelation time for all samples is less than 5 minutes, though. This gelation time is in good agreement with current design on thermoresponsive polymers. An appropriate porosity and pore size provide an acceptable water permeability and exudate removal properties that are very important for wound healing process, all samples are in a good range of water vapor transmission rate (water permeability). SEM images indicate increase in GO decreases pore size and improve cross-links. Addition of HCA improved chitosan adhesion in wet (bloody) condition. Our polymer composites showed self-healing property without external stimuli, meaning that after damaging it could heal its self. This property is very helpful when wound dressing is applied on moving tissues that has a chance of tearing and damaging. Viscosity of the samples was measured and results showed viscosity of all samples decreased by increasing the shear rate. Meaning that they are shear-thinning polymers that are ideal for injectable wound dressings and active agent delivery. Degradation test showed almost 80% of samples weight were lost in first two days. However, our samples kept their structure after this loss.

Presence of different functional groups in polymer composites provide an optimum porosity (90-140 μm) for cell migration. Our study showed, cell cytotoxicity of chitosan based thermoresponsive bioadhesive on fibroblast cells (NIH 3T3) is dose dependent and the interactions between GO and HCA on cells. Cell migration for 1:0.5, 0.5 and 1:1, 1 improved significantly. PCR test on 1:1, 1 showed bFGF and TGF-β1 are two main growth factors that are responsible for this improvement in NIH 3T3 cell migration. Our results showed samples with lower concentration of GO could promote HUVEC proliferation. While, high concentration of GO decrease HUVEC metabolic activity. Clotting assay showed all samples could improve whole blood clotting times. Efficiency of blood clotting was evaluated by whole blood clotting kinetic assay. Results showed high concentration of GO may improve blood clotting time in first 5 minutes, while due to hemolysis effect of GO on red blood cells clotting efficiency decrease with time. In general, this study open new window for chitosan based thermoresponsive bioadhesive for wound dressings and showed its potential for other biomedical applications.

We classified our aims of this project in two level, basic objective and detail objective. Regarding our results, we achieved to the basic design, In basic objective, we aimed to find a composition that shows an appropriate bioadhesive property and gelation time. In the detail objective, we aimed to work on different combinations of components to find an efficient design for wound healing. Regarding our results and considering some key features for an appropriate wound dressing like; good adhesiveness, gelation time, swelling ratio, WVTR, biocompatibility , angiogenesis property and clotting time. It seems 1:0.5, 0.5 is a good candidate among four designs as a wound dressing. The only concerns is antibacterial property. Our samples do not show antibacterial activity. It means secondary additives are needed as antibacterial agents to be applied in wound site with this design.

Recommendations:

As presented in result, this design does not have antibacterial property. In a future project, an antibacterial agent could be encapsulated and release study could be conducted. Moreover, the effect of this antibacterial agent on adhesion and gelation time should be addressed.

This study could open new window for future studies on chitosan based thermoresponsive bioadhesives applications in biomedical engineering. Localized active agent delivery could be studied in future projects. Due to bioadhesive property, this polymer could adhere to the tissue site for active agent delivery. Moreover, it is a shear thinning polymer that make it good candidate as an injectable polymer.

GO is a Near Infrared Region responsive material (NIR). NIR could permeate through skin and excite GO. We can take advantage of this property for localized drug delivery and cancer therapy. More studies on this potential could open new avenue for effective localized delivery.

Robotic surgery is drawing much attentions these days. This design may find some applications in robotic surgery. One of the main problem in robotic surgery is suturing the surgical site. To suture the surgical site, it needs to follow a very complicated algorithm, while applying an injectable bioadhesive could circumvent this issue. This application of chitosan based thermoresponsive bioadhesive needs more study.

The effect of different additives on cell behavior and signaling pathway could be other recommendation for the future works.

6. REFERENCES

[1] X. Liu, T. Lin, J. Fang, G. Yao, H. Zhao, M. Dodson, X. Wang, "In vivo wound healing and antibacterial performances of electrospun nanofibre membranes," *Wiley InterScience,* vol. 508, p. 499, 2009.

[2] H. Liu et. al, "A functional chitosan-based hydrogel as a wound dressing and drug delivery system in the treatment of wound healing," *RSC Advances,* no. 14, 2018.

[3] S. Dhivya, V. V. Padma, E. Santhini, "Wound dressings – a review," *BioMedicine,* vol. 5, pp. 24-28, 2015.

[4] S. O. Blacklow, J. Li, B. R. Freedman, M. Zeidi, C. Chen, D. J. Mooney, "Bioinspired mechanically active adhesive dressings to accelerate wound closure," *science advance,* 2019.

[5] J. H. Ryu, Y. Lee, W. H. Kong, T. G. Kim, T. G. Park,H. Lee, "Catechol-Functionalized Chitosan/Pluronic Hydrogels for Tissue Adhesives and Hemostatic Materials," *bio macromolecules,* p. 2653–2659, 2011.

[6] B. Balakrishnan, D. Soman, U. Payanam, A. Laurent, D. Labarree, A. Jayakrishnan, "A novel injectable tissue adhesive based on oxidized dextran and chitosan," *Acta Biomaterialia,* pp. 343-354, 2017.

[7] J. Zeng, D. Shi,Y. Gu, T. Kaneko, L. Zhang, H. Zhang, D. Kaneko, M. Chen, "Injectable and Near-Infrared-Responsive Hydrogels Encapsulating Dopamine-Stabilized Gold Nanorods with Long Photothermal Activity Controlled for Tumor Therapy," *Biomacromolecules,* p. 3375–3384, 2019.

[8] X. Jing, H. Y. Mi, B. N. Napiwocki, X. F. Peng, L. S. Turng, "Mussel-inspired electroactive chitosan/graphene oxide composite hydrogel with rapid self-healing and recovery behavior for tissue engineering," *Carbon,* pp. 557-570, 2017.

[9] E. Bellotti, A. L.Schilling, S. R.Little, P. Decuzzi, "Injectable thermoresponsive hydrogels as drug delivery system for the treatment of central nervous system disorders: A review," *Journal of controlled release,* vol. 329, pp. 16-35, 2021.

[10] H. Hamedi, S. Moradi, S. M. Hudson, A. E. Tonelli, "Chitosan based hydrogels and their applications for drug delivery in wound dressings: A review," *Carbohydrate Polymers,* vol. 199, pp. 445-460, 2018.

[11] H. Hamedi, S. Moradi, S. M. Hudson, A. E. Tonelli, M. W.King, "Chitosan based bioadhesives for biomedical applications: A review," *Carbohydrate Polymers,* 2022.

[12] S. Moradi, H. Hamedi, A. E. Tonelli, M. W. King , "Chitosan/Graphene Oxide Composite Films and Their Biomedical and Drug Delivery Applications: A Review," *Appl. Sci.,* 2021.

[13] M. Mehdizadeh, J. Yang, "Design Strategies and Applications of Tissue Bioadhesives," *Macromol. Biosci,* vol. 13, p. 271–288, 2013.

[14] N. M. Baouche, P. H. Elchinger, H. Baynast, G. Pierre, C. Delattre, P. Michaud, "Chitosan as an adhesive," *European Polymer Journal,* pp. 198-212, 2014.

[15] T. M. D. Le, H. T. T. Duong, T. Thambi, V.H. Giang Phan, J. H. Jeong, D. S. Lee, "Bioinspired pH- and Temperature-Responsive Injectable Adhesive Hydrogels with

Polyplexes Promotes Skin Wound Healing," *Bio Macromolecules,* vol. 19, p. 3536−3548, 2018.

[16] F.S. Rezaei, F. Sharifianjazi, A. Esmaeil khanian, E. Salehi, "Chitosan films and scaffolds for regenerative medicine applications: A review," *Carbohydrate Polymers,* vol. 273, p. 118631, 2021.

[17] E. Salehi, P. Daraei, A. Arabi Shamsabadi, "A review on chitosan-based adsorptive membranes," *Carbohydrate Polymer,* vol. 152, pp. 419-432, 2016.

[18] S. Islam, M. A. Rahman Bhuiyan, M. N. Islam , "Chitin and Chitosan: Structure, Properties and Applications in Biomedical Engineering," *Journal of Polymers and the Environment,* p. 854–866, 2017.

[19] M. Rinaudo, "Chitin and chitosan: Properties and applications," *Progress in Polymer Science,* vol. 31, no. 7, pp. 603-632, 2006.

[20] F. Arrouze, M. Essahli, M. Rhazi, J. desberieres, A. Tolaimate, "Chitin and chitosan: Study of the possibilities of their production by valorization of the waste of crustaceans and cephalopods rejected in Essaouira," *Journal of Materials and Environmental Sciences,* pp. 2251-2258, 2017.

[21] A. Shanmugam, K. Kathiresan, L. Nayak, "Preparation, characterization and antibacterial activity of chitosan and phosphorylated chitosan from cuttlebone of sepia kobiensis (hoyle, 1885)," *Biotechnology Reports,* vol. 9, pp. 25-30, 2016.

[22] S.C. Tan, T.K. Tan, S.M. Wong, E. Khor, "The chitosan yield of zygomycetes at their optimum harvesting time," *Carbohydrate Polymers,* vol. 30, pp. 239-242, 1996.

[23] S.A. White, P.R. Farina, I. Fulton, "Production and isolation of chitosan from mucor rouxii," *Applied and Environmental Microbiology,* vol. 38, pp. 323-328, 1979.

[24] S. Arcidiacono, D.L. Kaplan, "Molecular weight distribution of chitosan isolated from mucor rouxii under different culture and processing conditions," *Biotechnology and Bioengineering,* vol. 39, no. 3, pp. 281-286, 1992.

[25] F. Tajdini, M.A. Aminia, N. Nafissi-Varcheh, M.A. Faramarzi, "Production, physiochemical and antimicrobial properties of fungal chitosan from rhizomucor miehei and mucor racemosus," *International Journal of Biological Macromolecules,* vol. 47, p. 2010, 180-183.

[26] R. Kumria, B.E. Al-Dhubiab, J. Shah, A.B. Nair , "Formulation and Evaluation of Chitosan-Based Buccal Bioadhesive Films of Zolmitriptan," *Journal of Pharmaceutical Innovation,* vol. 13, pp. 133-143, 2018.

[27] C. Guyot, M. Cerruti, S. Lerouge, "Injectable, strong and bioadhesive catechol-chitosan hydrogels physically crosslinked using sodium bicarbonate," *Materials Science and Engineering: C,* vol. 118, p. 111529, 2021.

[28] Ameeduzzafar, N. Khan, N.K. Alruwaili, S.N.A. Bukhari, B. Alsuwayt, M.Afzal, S. Akhter, M. Yasir, M. Elmowafy, K. Shalaby, A. Ali, "Improvement of Ocular Efficacy of Levofloxacin by Bioadhesive Chitosan Coated PLGA Nanoparticles: Box-behnken Design, In-vitro Characterization, Antibacterial Evaluation and Scintigraphy Study," *Iranian Journal of Pharmaceutical Research,* vol. 19, no. 1, pp. 292-311, 2020.

[29] C.V. Pardeshi, V.S. Belgamwar, "Controlled synthesis of N,N,N-trimethyl chitosan for modulated bioadhesion and nasal membrane permeability," *International Journal of Biological Macromolecules,* vol. 82, pp. 933-944, 2016.

[30] S. Moradi, A. Barati, E. Salehi, A. Tonelli, H. Hamedi, "Preparation and Characterization of Chitosan Based Hydrogels Containing Cyclodextrin-Inclusion Compounds or Nanoemulsions of Thyme oil," *Polymer International,* vol. 68, pp. 1891-1902, 2019.

[31] H. Hamedi, S. Moradi, A. Tonelli, S. Hudson, "Preparation and Characterization of Chitosan–Alginate Polyelectrolyte Complexes Loaded with Antibacterial Thyme Oil Nanoemulsions," *Applied Science,* vol. 9, no. 18, p. 3933, 2019.

[32] S. Moradi, A. Barati, A.E. Tonelli, H. Hamedi, "Chitosan-based hydrogels loading with thyme oil cyclodextrin inclusion compounds: From preparation to characterization," *European Polymer Journal,* vol. 122, p. 109303, 2020.

[33] S. Moradi, A. Barati, A.E. Tonelli, H. Hamedi, "Effect of clinoptilolite on structure and drug release behavior of chitosan/thyme oil γ-Cyclodextrin inclusion compound hydrogels," *Journal of Applied Polymer Science,* vol. 138, no. 6, p. 49822, 2021.

[34] J.W. Lee, J.H. Park, J.R. Robinson, "Bioadhesive-Based Dosage Forms: The Next Generation," *Journal of Pharmaceutical Sciences,* vol. 89, no. 7, pp. 850-866, 2000.

[35] E. Lih, J. S. Lee, K. M. Park, K. D. Park, "Rapidly curable chitosan–PEG hydrogels as tissue adhesives for hemostasis and wound healing," *Acta Biomaterialia,* vol. 8, pp. 3261-3269, 2012.

[36] W. Nie, X. Yuan, J. Zhao, Y. Zhou, H. Bao, "Rapidly in situ forming chitosan/ε-polylysine hydrogels for adhesive sealants and hemostatic materials," *Carbohydrate Polymers,* vol. 96, no. 1, pp. 342-348, 2013.

[37] Y. Shou, J. Zhang, Sh. Yan, P. Xia, P. Xu, G. Li, K. Zhang, J. Yin, "Thermoresponsive Chitosan/DOPA-Based Hydrogel as an Injectable Therapy Approach for Tissue-Adhesion and Hemostasis," *ACS Biomaterial Science Engineering,* vol. 6, no. 6, p. 3619–3629, 2020.

[38] J.H. Ryu, Y. Lee, M. Jae Do, S. Duk Jo, J.S. Kim, B. Kim, G. Im, T.G. Park, H. Lee, "Chitosan-g-hematin: Enzyme-mimicking polymeric catalyst for adhesive hydrogels," *Acta Biomaterialia,* vol. 10, no. 1, pp. 224-233, 2014.

[39] J. Xu, G. M. Soliman, J. Barralet, M. Cerruti, "Mollusk Glue Inspired Mucoadhesives for Biomedical Applications," *Langmuir,* vol. 28, no. 39, pp. 14010-14017, 2012.

[40] K. Yamada, T. Chen, G. Kumar, O Vesnovsky, L. D. T. Topoleski, G. F. Payne, "Chitosan Based Water-Resistant Adhesive. Analogy to Mussel Glue," *Biomacromolecules,* vol. 1, no. 2, pp. 252-258, 2000.

[41] A.Martinac, J. Filipović-Grčić, D. Voinovich, B. Perissutti, E. Franceschinis, "Development and bioadhesive properties of chitosan-ethylcellulose microspheres for nasal delivery," *International Journal of Pharmaceutics,* vol. 291, no. 1-2, pp. 69-77, 2005.

[42] R.A. Fitaihi, F.S. Aleanizy, S. Elsamaligy, H.A. Mahmoud, M.A. Bayomia, "Role of chitosan on controlling the characteristics and antifungal activity of bioadhesive fluconazole vaginal tablets," *Saudi Pharmaceutical Journal,* vol. 26, no. 2, pp. 151-161, 2018.

[43] T.I. Shalaby, W.M. El-Refaie, "Bioadhesive Chitosan-Coated Cationic Nanoliposomes With Improved Insulin Encapsulation and Prolonged Oral Hypoglycemic Effect in Diabetic Mice," *Journal of Pharmaceutical Sciences,* vol. 107, no. 8, pp. 2136-2143, 2018.

[44] H. P. James,R. John, A. Alex,K. R. Anoop, "Smart polymers for the controlled delivery of drugs - A concise overview," *Acta Pharm. Sin. B,* pp. 120-127, 2014.

[45] M. L. Bruschi, B. F. Borghi-Pangoni, M. V. Junqueira, S. B. de Souza Ferreira, "NANOSTRUCTURED THERAPEUTIC SYSTEMS WITH BIOADHESIVE AND THERMORESPONSIVE PROPERTIES," in *Nanostructures for Novel Therapy*, 2017, pp. 325-327.

[46] S. Gunasekaran, T. Wang, C. Chai, "Swelling of pH-sensitive chitosan–poly(vinyl alcohol) hydrogels," *Applied polymer science,* pp. 4665-4671, 2006.

[47] L. Liu, Q. Gao, Xuemin. Lu, H. Zhou, "In situ forming hydrogels based on chitosan for drug delivery and tissue regeneration," *Asian Journal of Pharmaceutical Sciences,* pp. 673-683, 2016.

[48] A. R. Dudhani, S. L. Kosaraju, "Bioadhesive chitosan nanoparticles: Preparation and characterization," *Carbohydrate Polymers,* pp. 243-251, 2010.

[49] N. Shrestha, M. A. Shahbazi, F. Araújo, E. Mäkilä, J. Raula, E. I.Kauppinen, J. Salonen, B. Sarmento, J. Hirvonen, H. A.Santos, "Multistage pH-responsive mucoadhesive nanocarriers prepared by aerosol flow reactor technology: A controlled dual protein-drug delivery system," *Biomaterials,* pp. 9-20, 2015.

[50] B. Fan, Y. Xing, Y. Zheng, C. Sun, G. Liang, "pH-responsive thiolated chitosan nanoparticles for oral low-molecular weight heparin delivery: in vitro and in vivo evaluatio," *Drug delivery*, p. 238–247, 2016.

[51] Y. H. Chen, Y. C. Chung, I. J. Wang, T. H. Young, "Control of cell attachment on pH-responsive chitosan surface by precise adjustment of medium pH," *Biomaterials,* vol. 33, pp. 1336-1342, 2012.

[52] H. Chang, N. Cheng, Y. Ethan, L.Wang, T. Young, "pH-responsive characteristics of chitosan-based blends for controlling the adhesivity of cells," *Journal of the Taiwan Institute of Chemical Engineers,* vol. 111, pp. 34-43, 2020.

[53] C. Yen, T. Young, M. Hsieh, L. Liao, T. Huang , "Increased Cell Detachment Ratio of Mesenchymal-Type Lung Cancer Cells on pH-Responsive Chitosan through the β3 Integrin," *Marine Drugs,* vol. 17, no. 12, p. 659, 2019.

[54] C. H. Yen, S. T. Li, N. C. Cheng, Y. R. Ji, J. H. Wang, T. H. Young, "Label-free platform on pH-responsive chitosan: Adhesive heterogeneity for cancer stem-like cell isolation from A549 cells via integrin β4," *Carbohydrate Polymers,* vol. 239, 2020.

[55] Y. Liang, X. Zhao, P.X. Mad, B. Guo, Y. Du, X. Han, "pH-responsive injectable hydrogels with mucosal adhesiveness based on chitosan-grafted-dihydrocaffeic acid and oxidized pullulan for localized drug delivery," *Journal of Colloid and Interface Science,* vol. 536, pp. 224-234, 2019.

[56] C. Wang, X. Wang, K. Dong, J. Luo, Q. Zhang, Y. Cheng, "Injectable and responsively degradable hydrogel for personalized photothermal therapy," *Biomaterials,* pp. 129-137, 2016.

[57] P. C. P. C. K. P. H. Zhu, "Recent progress in the development of near-infrared organic photothermal and photodynamic nanotherapeutics," *Biomaterials Science,* 2018.

[58] R. Xing, K. Liu, T. Jiao, N. Zhang, K. Ma, R. Zhang, Q. Zou, G.Ma, X. Yan, "An Injectable Self-Assembling Collagen–Gold Hybrid Hydrogel for Combinatorial Antitumor Photothermal/Photodynamic Therapy," *Advanced material,* pp. 3669-3676, 2016.

[59] K. Shi, Z. Liu, Y. Y. Wei, W. Wang, X. J. Ju, R. Xie, L. Y. Chu, "Near-Infrared Light-Responsive Poly(N-isopropylacrylamide)/Graphene Oxide Nanocomposite Hydrogels with Ultrahigh Tensibility," *ACS Appl. Mater. Interfaces,* vol. 7, no. 49, p. 27289–27298, 2015.

[60] R. L. Sousa, D. M. Diogo, C. G. Alves, E. C.Costa, P. Ferreira, R. O.Louro, I. J.Correia, "Hyaluronic acid functionalized green reduced graphene oxide for targeted cancer photothermal therapy," *Carbohydrate Polymers,* vol. 200, pp. 93-99, 2018.

[61] P. Matteini, F. Ratto, F. Rossi, S. Centi, L. Dei, R. Pini, "Chitosan Films Doped with Gold Nanorods as Laser-Activatable Hybrid Bioadhesives," *Advanced Materials,* vol. 22, pp. 4313-4316, 2010.

[62] P. Matteini, F. Ratto, F. Rossi, M. de Angelis, L. Cavigli, R. Pini, "Hybrid nanocomposite films for laser-activated tissue bonding," *Journal of Biophotonics,* vol. 5, pp. 868-877, 2012.

[63] R. Xu, S. Ma, Y. Wu, H. Lee, F. Zhou, W. Liu , "Adaptive control in lubrication, adhesion, and hemostasis by Chitosan–Catechol–pNIPAM," *Biomater. Sci.,* vol. 7, pp. 3599-3608, 2019.

[64] V. Stoyneva, D. Momekova, B. Kostova, P. Petrova, "Stimuli sensitive super-macroporous cryogels based on photo-crosslinked 2-hydroxyethylcellulose and chitosan," *Carbohydrate Polymers,* pp. 825-830, 2014.

[65] F. Ahmadi, Z. Oveisi, S. M. Samani, Z. Amoozgar, "Chitosan based hydrogels: characteristics and pharmaceutical applications," *Res Pharm Sci,* pp. 1-16, 2015.

[66] K. Ono et. al, "Experimental evaluation of photocrosslinkable chitosan as a biologic adhesive with surgical applications," *Surgery,* vol. 130, pp. 844-850, 2001.

[67] B. Chatterjee, N. Amalina, P. Sengupta, U. K. Mandal, "Mucoadhesive Polymers and Their Mode of Action: A Recent Update," *Journal of Applied Pharmaceutical Science ,* pp. 195-203, 2017.

[68] L. Kaur, I. Singh, "Chitosan-Catechol Conjugates–A Novel Class of Bioadhesive Polymers: A Critical Revie," *Rev. Adhesion Adhesives,* vol. 7, pp. 51-67, 2019.

[69] D. W. Lee, C. Lim, J. N. Israelachvili, D. S. Hwang, "Strong Adhesion and Cohesion of Chitosan in Aqueous Solutions," *Langmuir,* p. 14222–14229, 2013.

[70] M. C. van der Leeden, G. Frens, "Surface Properties of Plastic Materials in Relation to Their Adhering Performance," *Advanced engineering Materials,* vol. 4, no. 5, pp. 280-289, 2002.

[71] H. Ruprai et. al , "Porous chitosan adhesives with L-DOPA for enhanced photochemical tissue bonding," *Acta Biomaterialia,* vol. 101, pp. 314-326, 2020.

[72] D .Depan, B.Girase, J.S.Shah, R.D.K.Misra, "Structure–process–property relationship of the polar graphene oxide-mediated cellular response and stimulated growth of osteoblasts

on hybrid chitosan network structure nanocomposite scaffolds," *Acta Biomaterialia,* vol. 7, no. 9, pp. 3432-3445, 2011.

[73] Y. Ai, J. Nie, G.Wu, D. Yang, "The DOPA-functionalized bioadhesive with properties of photocrosslinked and thermoresponsive," *Applied polymer science,* vol. 131, no. 22, 2014.

[74] T. A. Sonia, M. R. Rekha, C. P. Sharma, "Bioadhesive hydrophobic chitosan microparticles for oral delivery of insulin: In vitro characterization and in vivo uptake studies," *Applied Polymer science,* vol. 119, no. 5, 2010.

[75] I. A. Sogias, A. C. Williams, V. V. Khutoryanskiy, "Why is Chitosan Mucoadhesive," *Biomacromolecules,* p. 1837–1842, 2008.

[76] E.M.Petrie, "Adhesive bonding of textiles: principles, types of adhesive and methods of us," in *Joining Textiles Principles and Applications*, Woodhead Publishing, 2013, pp. 225-274.

[77] E. M. Lund, C. M. Westergaard, C. Sander, P. Madelung, J. Jacobsen, "A mechanistic based approach for enhancing buccal mucoadhesion of chitosan," *International Journal of Pharmaceutics,* vol. 461, no. 1-2, pp. 280-285, 2014.

[78] Y. H. William, L. A. Foss, N. APeppas, "Molecular aspects of muco- and bioadhesion:: Tethered structures and site-specific surfaces," *Journal of Controlled Release,* vol. 65, no. 1-2, pp. 63-71, 2000.

[79] K. Suknuntha, V. Tantishaiyakul, N. Worakul, W. Taweepreda, "Characterization of muco- and bioadhesive properties of chitosan, PVP, and chitosan/PVP blends and release of amoxicillin from alginate beads coated with chitosan/PVP," *Drug Development and Industrial Pharmacy,* vol. 37, no. 4, p. 408–418, 2011.

[80] L. Kumar, S. Verma, B. Vaidya, V. Gupta, "Chapter 10 - Bioadhesive Polymers for Targeted Drug Delivery," in *Nanotechnology-Based Approaches for Targeting and Delivery of Drugs and Genes*, Academic Press, 2017, pp. 322-362.

[81] K.C. Ugoeze, "Bioadhesives in Drug Delivery," in *Chapter 2: Bioadhesive Polymers for Drug Delivery Applications*, Scrivener Publishing LLC, 2020, pp. 29-56.

[82] D. Brahmbhatt, "Bioadhesive drug delivery systems: Overview and recent advances," *International Journal of Chemical and Lifesciences,* vol. 6, no. 3, pp. 2016-2024, 2017.

[83] G. Tan, S. Yu, H. Pan, J. Li, D. Liu, K. Yuan, X. Yang, W. Pana, "Bioadhesive chitosan-loaded liposomes: A more efficient and higher permeable ocular delivery platform for timolol maleate," *International Journal of Biological Macromolecules,* vol. 94A, pp. 355-363, 2017.

[84] L. Plapied, G. Vandermeulen, B. Vroman, V. Préat, A. Rieux, "Bioadhesive nanoparticles of fungal chitosan for oral DNA delivery," *International Journal of Pharmaceutics,* vol. 398, no. 1-2, pp. 210-218, 2010.

[85] S. Zeynep Ay, K. Sinem Yaprak, E. Bayri, G. Özge, L. Mine Hosgör, et al., "Evaluation of chitosan based vaginal bioadhesive gel formulations for antifungal drugs," *Acta Pharmaceutica,* vol. 64, no. 2, pp. 139-156, 2014.

[86] A.A. Elzatahry, M.S. Mohy Eldin, E.A. Soliman, E.A. Hassan, "Evaluation of alginate–chitosan bioadhesive beads as a drug delivery system for the controlled release of theophylline," *Journal of Applied Polymer Science,* vol. 111, no. 5, pp. 2452-2459, 2009.

[87] C. Sander, H.M. Nielsen, J. Jacobsen, "Buccal delivery of metformin: TR146 cell culture model evaluating the use of bioadhesive chitosan discs for drug permeability enhancement," *International Journal of Pharmaceutics,* vol. 458, no. 2, pp. 254-261, 2013.

[88] P. Agrawal, Sonali, R.P. Singh, G. Sharma, A.K. Mehata, S. Singh, C.V. Rajesh, B.L. Pandey, B. Koch, M.S. Muthu, "Bioadhesive micelles of d-α-tocopherol polyethylene glycol succinate 1000: Synergism of chitosan and transferrin in targeted drug delivery," *Colloids and Surfaces B: Biointerfaces,* vol. 152, no. 1, pp. 277-288, 2017.

[89] I. Modhia, A. Mehta, R. Patel, C. Patel, "Development of Bioadhesive Chitosan Superporous Hydrogel Composite Particles Based Intestinal Drug Delivery System," *BioMed Research International,* p. Article ID 563651, 2013.

[90] B. Luppi, F. Bigucci, A. Abruzzo, G. Corace, T. Cerchiara, V. Zecchia, "Freeze-dried chitosan/pectin nasal inserts for antipsychotic drug delivery," *European Journal of Pharmaceutics and Biopharmaceutics,* vol. 75, no. 3, pp. 381-387, 2010.

[91] J. Xu, S. Strandman, J. X.X.Zhu, J. Barralet, M. Cerruti, "Genipin-crosslinked catechol-chitosan mucoadhesive hydrogels for buccal drug delivery," *Biomaterials,* vol. 37, pp. 395-404, 2015.

[92] I. Ayensu, J. C. Mitchell. J.S. Boatenga, "Development and physico-mechanical characterisation of lyophilised chitosan wafers as potential protein drug delivery systems via the buccal mucosa," *Colloids and Surfaces B: Biointerfaces,* vol. 91, pp. 258-265, 2012.

[93] T.S. Anirudhan, S.S. Nair, A.S. Nair, "Fabrication of a bioadhesive transdermal device from chitosan and hyaluronic acid for the controlled release of lidocaine," *Carbohydrate Polymers,* vol. 152, pp. 687-698, 2016.

[94] J. Varshosaz, H. Sadri, A. Heidari, "Nasal Delivery of Insulin Using Bioadhesive Chitosan Gels," *Drug Delivery,* vol. 13, no. 1, pp. 31-38, 2006.

[95] M. C.García, A. A. Aldan, L. I.Tártara, F. Alovero, M. C.Strumia, R. H. Manzo, M. Martinelli, A. F. J. Kairuz, "Bioadhesive and biocompatible films as wound dressing materials based on a novel dendronized chitosan loaded with ciprofloxacin," *Carbohydrate Polymers,* vol. 175, no. 1, pp. 75-86, 2017.

[96] S. Wittaya-areekula, C. Prahsarn, "Development and in vitro evaluation of chitosan–polysaccharides composite wound dressings," *International Journal of Pharmaceutics,* vol. 313, no. 1-2, pp. 123-128, 2006.

[97] T. A. Khan, K. K. Peh, H. S. Chng, "Mechanical, Bioadhesive Strength and Biological Evaluations of Chitosan films for Wound Dressing," *Journal of Pharmacy & Pharmaceutical Sciences,* pp. 303-311, 2000.

[98] V. A. M. Gonzaga, A. L. Poli and et. al, "Chitosan-laponite nanocomposite scaffolds for wound dressing application," *J Biomed Mater Res,* p. 1388–1397, 2020.

[99] A. D. Sezer, F. Hatipoğlu, E. Cevher, Z. Oğurtan, A. L. Baş, J. Akbuğa, "Chitosan Film Containing Fucoidan as a Wound Dressing for Dermal Burn Healing: Preparation and In Vitro/In Vivo Evaluation," *AAPS PharmSciTech,* vol. 8, no. 2, 2007.

[100] S. Wittaya-areekul, C. Prahsarn, S. Sungthongjeen, "Development and In Vitro Evaluation of Chitosan–Eudragit RS 30D Composite Wound Dressings," *AAPS PharmSciTech,* vol. 7, no. 1, 2007.

[101] H. J. Hong, S. E. Jin, J. S. Park, W. S. Ahn, C. K. Kim, "Accelerated wound healing by smad3 antisense oligonucleotides-impregnated chitosan/alginate polyelectrolyte complex," *Biomaterials,* vol. 29, no. 36, pp. 4831-4837, 2008.

[102] A. H. S. A. A. Mahmoud, "Norfloxacin-loaded collagen/chitosan scaffolds for skin reconstruction: Preparation, evaluation and in-vivo wound healing assessment," *European Journal of Pharmaceutical Sciences,* vol. 83, no. 15, pp. 155-165, 2016.

[103] S. Ternullo, L. V. S. Werning, A. M. Holsæter, N. Š. Basnet , "Curcumin-In-Deformable Liposomes-In-Chitosan-Hydrogel as a Novel Wound Dressing," *Pharmaceutics,* vol. 12, no. 1, 2020.

[104] X. Du, Y. Liu, H. Yan, M. Rafique, S. Li, X. Shan, L. Wu, M. Qiao,D. Kong, L. Wang, "Anti-Infective and Pro-Coagulant Chitosan-Based Hydrogel Tissue Adhesive for Sutureless Wound Closure," *Biomacromolecules,* vol. 21, no. 3, p. 1243–1253, 2020.

[105] M. Ishihara, K. Nakanishi, K. Ono, M. Sato, M. Kikuchi, Y. Saito, H. Yura, T. Matsui, H. Hattori, M. Uenoyama, A. Kurita, "Photocrosslinkable chitosan as a dressing for wound occlusion and accelerator in healing process," *Biomaterials,* vol. 23, no. 3, pp. 833-840, 2002.

[106] Y. Huang, Y. Chou, Y. Lin, W. Chen, C. Chen, H. Lin, "Polyurethane modified by oxetane grafted chitosan as bioadhesive," *International Journal of Polymeric Materials and Polymeric Biomaterials,* vol. 70, no. 15, pp. 1100-1114, 2021.

[107] R. Wang, J. Zhu, G. Jiang, Y. Sun, L. Ruan, P. Li, H. Cui, "Forward Wound Closure with Regenerated Silk Fibroin and Polylysine-Modified Chitosan Composite Bioadhesives as Dressings," *ACS Applied Bio Materials,* vol. 3, no. 11, pp. 7941-7951, 2020.

[108] M. J. Barton, J. W. Morley, M. A. Stoodley, A. Lauto, D. A. Mahns , "Nerve repair: toward a sutureless approach," *Neurosurgical Review volume ,* p. 585–595, 2014.

[109] H. Ruprai, S. Romanazzo, J. Ireland, K. Kilian, D. Mawad, L. George, R. Wuhrer, J. Houang, D. Ta, S. Myers, A. Lauto, "Porous Chitosan Films Support Stem Cells and Facilitate Sutureless Tissue Repair," *CS Appl. Mater. Interfaces,* p. 32613–32622, 2019.

[110] A. Lauto, L. J. Foster, A. Avolio, D. Sampson, C. Raston, M. Sarris, G. M. Kenzie, M. Stoodley, "Sutureless Nerve Repair with Laser-Activated Chitosan Adhesive: A Pilot in Vivo Study," *Photomedicine and Laser Surgery,* vol. 26, p. 227–234, 2008.

[111] A. Lauto, "Integration of Extracellular Matrix With Chitosan AdhesiveFilm for Sutureless Tissue Fixation," *Lasers in Surgery and Medicine,* p. 366–371, 2009.

[112] M. Shokrollahi, S. H. Bahrami, M. Haghbin Nazarpak, A. Solouk, "Biomimetic double-sided polypropylene mesh modified by DOPA and ofloxacin loaded carboxyethyl chitosan/polyvinyl alcohol-polycaprolactone nanofibers for potential hernia repair applications," *International Journal of Biological Macromolecules,* vol. 165, no. A, pp. 902-917, 2020.

[113] T. Gratieri, G. M. Gelfuso, E. M. Rocha, V. H. Sarmento, O. Freitas, R. F. V. Lopez, "A poloxamer/chitosan in situ forming gel with prolonged retention time for ocular delivery," *European Journal of Pharmaceutics and Biopharmaceutics,* pp. 186-193, 2010.

[114] J. Shahbazi, H. Marçal, S. Watson, D. Wakefield, M. Sarris, L. J. R. Foster , "Sutureless sealing of penetrating corneal wounds using a laser-activated thin film adhesive," *Lasers in Surgery and Medicine,* p. 490–498, 2011.

[115] M. Barton, J. W. Morley, M. A. Stoodley, K. S. Ng, S. C. Piller, H. Duong, D. Mawad, D. A. Mahns, A. Lauto, "Laser-activated adhesive films for sutureless mediannerve anastomosis," *J. Biophotonics* , p. 938–949, 2013.

[116] N. T. Phuong, V. A. Ho, D. H. Nguyen, N. C. Khoa, T. N. Quyen, Y. Lee, K. D. Park , "Enzyme-mediated fabrication of an oxidized chitosan hydrogel as a tissue sealant," *Journal of Bioactive and Compatible Polymers,* vol. 30, no. 4, p. 412–423, 2015.

[117] X. Du, L. Wu, H. Yan, L. Qu, L. Wang, X. Wang, S. Ren, D. Kong,, "Multifunctional Hydrogel Patch with Toughness, Tissue Adhesiveness, and Antibacterial Activity for Sutureless Wound Closure," *ACS Biomater. Sci. Eng,* vol. 5, p. 2610−2620, 2019.

[118] G. Singh, A. Nayal, S. Malhotra, V. Koul, "Dual functionalized chitosan based composite hydrogel for haemostatic efficacy and adhesive property," *Carbohydrate Polymer,* vol. 247, p. 116757, 2020.

[119] C. Sun, X. Zeng, S. Zheng, Y. Wang, Z. Li, H. Zhang, L. Nie, Y. Zhang, Y. Zhao, X. Yang, "Bio-adhesive catechol-modified chitosan wound healing hydrogel dressings through glow discharge plasma technique," *Chemical Engineering Journal,* vol. 427, p. 130843, 2022.

[120] J. Hoque, R.G. Prakash, K. Paramanandham, B.R. Shome, J. Haldar, "Biocompatible Injectable Hydrogel with Potent Wound Healing and Antibacterial Properties," *Molecular Pharmaceutics,* vol. 14, no. 4, pp. 1218-1230, 2017.

[121] P. Zhang, S. Li. Zhang, X. Zhang, L. Wan, Z. Yun, S. Ji, F. Gong, M. Huang, L. Wang, X. Zhu, Y. Tan, Y. Wan, "GRGDS-functionalized chitosan nanoparticles as a potential intravenous hemostat for traumatic hemorrhage control in an animal model," *Nanomedicine: Nanotechnology, Biology and Medicine,* vol. 14, no. 8, pp. 2531-2540, 2018.

[122] N.D. Sanandiya, S. Lee, S. Rho, H. Lee, I. S. Kim, D. SooHwang, "Tunichrome-inspired pyrogallol functionalized chitosan for tissue adhesion and hemostasis," *Carbohydrate Polymer,* vol. 208, pp. 77-85, 2019.

[123] E. Park, J. Lee, K.M. Huh, S.H. Lee, H. Lee, "Toxicity-Attenuated Glycol Chitosan Adhesive Inspired by Mussel Adhesion Mechanisms," *Advanced Healthcare Materials* , vol. 8, no. 14, p. 1900275, 2019.

[124] W. Huang, S. Cheng, X. Wang, Y. Zhang, L. Chen, L. Zhang, "Noncompressible Hemostasis and Bone Regeneration Induced by an Absorbable Bioadhesive Self-Healing Hydrogel," *Advanced Functional Materials,* vol. 31, no. 22, p. 2009189, 2021.

[125] M. Fuente, B. Seijo, M.J. Alonso , "Bioadhesive hyaluronan–chitosan nanoparticles can transport genes across the ocular mucosa and transfect ocular tissue," *Gene therapy,* vol. 15, pp. 668-676, 2008.

[126] S. Mirza, I. Zia, R. Jolly, S. Kazmi, M. Owais, M. Shakira, "Synergistic combination of natural bioadhesive bael fruit gum and chitosan/nano-hydroxyapatite: A ternary bioactive nanohybrid for bone tissue engineering," *International Journal of Biological Macromolecules,* vol. 119, pp. 215-224, 2018.

[127] B. Hoffmann, E. Volkmer, A. Kokott, P. Augat, M. Ohnmacht, N. Sedlmay, M. Schieker, L. Claes, W. Mutschler, G. Ziegler, "Characterisation of a new bioadhesive system based on polysaccharides with the potential to be used as bone glue," *Journal of Material Science: Material Medicine,* vol. 20, pp. 2001-2009, 2009.

[128] Y. Liu, Y. Zhai, X. Han, X. Liu, W. Liu, C. Wu, L. Li, Y. Du, H. Lian, Y Wang, Z. He, J. Sun , "Bioadhesive chitosan-coated cyclodextrin-based superamolecular nanomicelles to enhance the oral bioavailability of doxorubicin," *Journal of Nanoparticle Research,* vol. 16, p. 2587, 2014.

[129] J.G. Vargas Villanueva, P.A. Sarmiento Huertas, F. Salcedo Galan, R.J. Esteban Rueda, J.C. Briceño Triana, J.P. Casas Rodriguez, "Bio-adhesion evaluation of a chitosan-based bone bio-adhesive," *International Journal of Adhesion and Adhesives,* vol. 92, pp. 80-88, 2019.

[130] T.A. Rickett, Z. Amoozgar, C.A. Tuchek, J. Park, Y.Yeo, R. Shi, "Rapidly Photo-Cross-Linkable Chitosan Hydrogel for Peripheral Neurosurgeries," *Biomacromolecules,* vol. 12, no. 11, pp. 57-65, 2011.

[131] B. Sayın, S. Somavar, X.W. Li, M. Thanou, D. Sesardi, H.O. Alpar, S. Şenela, "Mono-N-carboxymethyl chitosan (MCC) and N-trimethyl chitosan (TMC) nanoparticles for non-invasive vaccine delivery," *International Journal of Pharmacutics,* vol. 363, no. 1-2, pp. 139-148, 2008.

[132] Y.L. Uscátegui, S.J. Arévalo-Alquichire, J.A. Gómez-Tejedor, A. Vallés-Lluch, L.E. Díaz, M.F. Valero, "Polyurethane-based bioadhesive synthesized from polyols derived from castor oil (Ricinus communis) and low concentration of chitosan," *Journal of Materials Research ,* vol. 23, no. 19, pp. 3699-3711, 2019.

[133] H. Abd-Allah, R.T.A. Abdel-Aziz, M. Nasra, "Chitosan nanoparticles making their way to clinical practice: A feasibility study on their topical use for acne treatment," *Macromolecules,* vol. 156, pp. 262-270, 2020.

[134] L.Y. Ashri, A. El S. F.Abou El Ela, M.A. brahima, D.H. Alshora, M.j. Naguibd, "Optimization and evaluation of chitosan buccal films containing tenoxicam for treating chronic periodontitis: In vitro and in vivo studies," *Journal of Drug Delivery Science and Technology,* vol. 57, p. 101720, 2020.

[135] H. Akıncıbay, S. Şenel, Z.Y. Ay, "Application of chitosan gel in the treatment of chronic periodontitis," *Journal of Biomedical Materials Research Part B: Applied Biomaterials,* vol. 80B, no. 2, pp. 290-296, 2007.

[136] H. Pavis, A. Wilcock, J. Edgecombe. Carr, C. Manderson, N. Church, A. Fisher, "Pilot Study of Nasal Morphine-Chitosan for the Relief of Breakthrough Pain in Patients With Cancer," *Journal of Pain and Symptom Management,* vol. 24, no. 6, pp. 598-602, 2002.

[137] P. Aksungur, A. Sungur, S. Ünal, A. Bİskit, C.A. Squier, S. Şenel, "Chitosan delivery systems for the treatment of oral mucositis: in vitro and in vivo studies," *Journal of Controlled Release,* vol. 98, no. 2, pp. 269-279, 2004.

[138] P. Dubeya, P. Gopinath, "PEGylated graphene oxide-based nanocomposite-grafted chitosan/polyvinyl alcohol nanofiber as an advanced antibacterial wound dressing," *RSC Advances,* vol. 6, pp. 69103-69116, 2016.

[139] S. Chen, H. Wang, Z. Jian, G. Fei, W. Qian, G. Luo, Z. Wang, H. Xia, "Novel Poly(vinyl alcohol)/Chitosan/Modified Graphene Oxide Biocomposite for Wound Dressing Application," *Macromolecular Bioscience,* vol. 20, no. 3, p. 1900385, 2020.

[140] Y. He, N. Zhang, Q. Gong, H. Qiu, W. Wang, Y. Liu, J. Gao, "Alginate/graphene oxide fibers with enhanced mechanical strength prepared by wet spinning," *Carbohydrate Polymers,* vol. 88, no. 3, pp. 1100-1108, 2012.

[141] Y. Chen, Y. Qi, X. Yan, H. Ma, J. Chen, B. Liu, Q. Xue, "Green fabrication of porous chitosan/graphene oxide composite xerogels for drug delivery," *Journal of applied polymer Science,* vol. 131, no. 6, pp. 1-11, 2014.

[142] C. Chung, Y. Kim, D. Shin, S. Ryoo, B.H. Hong, D. Min, "Biomedical Applications of Graphene and Graphene Oxide," *Account of Chemical Reseach,* vol. 46, no. 10, pp. 2211-2224, 2013.

[143] M. Lin, Z.L. Wang, P.W. Yang, P. Li, "Micro- structure and rheological properties of graphene oxide rubber asphalt," *Nanotechnology Reviews,* vol. 8, no. 1, pp. 227-235, 2019.

[144] Y. Chang, S. Yanga, J. Liua, E. Dong, Y. Wang, A. Cao, Y. Liua, H. Wang, "In vitro toxicity evaluation of graphene oxide on A549 cells," *Toxicology Letters,* vol. 200, no. 3, pp. 201-210, 2011.

[145] C LiQiang, H. PingPing, Z. Li, H. SiZhou, L. LingFei, H. ChengZhi, "Toxicity of graphene oxide and multi-walled carbon nanotubes against human cells and zebrafish," *SCIENCE CHINA, Chemistry,* vol. 55, no. 10, pp. 2209-2216, 2012.

[146] H. J. Majidi, A. Babaei, Z. Arab Bafrani, D. Shahrampour, E. Zabihi, S.M. Jafaric, "Investigating the best strategy to diminish the toxicity and enhance the antibacterial activity of graphene oxide by chitosan addition," *Carbohydrate Polymers,* vol. 225, p. 115220, 2019.

[147] K. Liao, Y. Lin, C.W. Macosko, C.L. Haynes, "Cytotoxicity of Graphene Oxide and Graphene in Human Erythrocytes and Skin Fibroblasts," *ACS Applied Materials and Interfaces,* vol. 3, no. 7, pp. 2607-2615, 2011.

[148] A.B. Seabra, A.J. Paula, R. de Lima, O.L. Alves, Ne. Durán, "Nanotoxicity of Graphene and Graphene Oxide," *Chemical Research in Toxicology,* vol. 27, no. 2, pp. 159-168, 2014.

[149] K. Wang, J. Ruan, H. Song, J. Zhang, Y. Wo, S. Guo, D. Cui , "Biocompatibility of graphene oxide," *Nanoscale Reseach letters,* vol. 6, pp. 1-8, 2011.

[150] X. Zhang, J. Yin, C. Peng, W. Hu, Z. Zhu, W. Li, C. Fan, Q. Huang, "Distribution and biocompatibility studies of graphene oxide in mice after intravenous administration," *Carbon,* vol. 49, no. 3, pp. 986-995, 2011.

[151] S.F. Kiew, L.V. Kiew, H.B. Lee, T. Imae, L.Y. Chung, "Assessing biocompatibility of graphene oxide-based nanocarriers: A review," *Release,* vol. 226, pp. 217-228, 2016.

[152] S.P. Mukherjee, K. Kostarelos, B. Fadeel, "Cytokine Profiling of Primary Human Macrophages Exposed to Endotoxin-Free Graphene Oxide: Size-Independent NLRP3 Inflammasome Activation," *Advanced Healthcare Materials,* vol. 7, no. 4, p. 1700815, 2018.

[153] H. Lee, J. Kim, J. Lee, H. Park, Y. Park, S. Jung, J. Lim, H.C. Choi, W.J. Kim, "In vivo self-degradable graphene nanomedicine operated by DNAzyme and photo-switch for controlled anticancer therapy," *Biomaterials,* vol. 263, p. 120402, 2020.

[154] Y. Li L. Feng X. Shi, X. Wang Y. Yang, K. Yang T. Liu, G. Yang, Z. Liu, "Surface Coating-Dependent Cytotoxicity and Degradation of Graphene Derivatives: Towards the Design of Non-Toxic, Degradable Nano-Graphene," *Nano.Micro Small,* vol. 10, no. 8, pp. 1544-1554, 2014.

[155] S. Gurunathan, J.W. Han, A.A. Dayem, V. Eppakayala, J. Kim, "Oxidative stress-mediated antibacterial activity of graphene oxide and reduced graphene oxide in Pseudomonas aeruginosa," *International Journal of Nanomedicine,* vol. 7, pp. 5901-5914, 2012.

[156] S. Liu, M. Hu, T.H. Zeng, R. Wu, R. Jiang, J. Wei, L. Wang, J. Kong, Y. Chen, "Lateral Dimension-Dependent Antibacterial Activity of Graphene Oxide Sheets," *Langmuir,* vol. 28, no. 33, pp. 12364-12372, 2012.

[157] S. Liu, T.H. Zeng, M. Hofmann, E. Burcombe, J. Wei, R. Jiang, J. Kong, Y. Chen, "Antibacterial Activity of Graphite, Graphite Oxide, Graphene Oxide, and Reduced Graphene Oxide: Membrane and Oxidative Stress," *ACS Nano,* vol. 5, no. 9, pp. 6971-6980, 2011.

[158] S. R. Rehman, R. Augustine, A. A. Zahid, R. Ahmed, M. Tariq, A. Hasan, "Reduced Graphene Oxide Incorporated GelMA Hydrogel Promotes Angiogenesis For Wound Healing Applications," *Int J Nanomedicine,* p. 9603–9617, 2019.

[159] P. Chhabra, G. Chauhan, A. Kumar, "Augmented healing of full thickness chronic excision wound by rosmarinic acid loaded chitosan encapsulated graphene nanopockets," *Drug Development and Industrial Pharmacy,* p. 878–888, 2020.

[160] B.C. Ozkan,T. Soganci, H. Turhan, M. Akb, "Investigation of rGO and chitosan effects on optical and electrical properties of the conductive polymers for advanced applications," *Electrochimica Acta,* vol. 295, pp. 1044-1051, 2019.

[161] X. Wang, H. Bai, Z. Yao, A. Liua, G. Shi, "Electrically conductive and mechanically strong biomimetic chitosan/reduced graphene oxide composite films," *Journal of Materials Chemistry,* vol. 20, no. 41, pp. 9032-9036, 2010.

[162] L. Jiang, D. Chen, Z. Wang, Z. Zhang, Y. Xia, H. Xue, Y. Liu , "Preparation of an Electrically Conductive Graphene Oxide/Chitosan Scaffold for Cardiac Tissue Engineering," *Applied Biochemistry and Biotechnology* , vol. 188, pp. 952-964, 2019.

[163] M. Zhou, Y. Zhai, S. Dong, "Electrochemical Sensing and Biosensing Platform Based on Chemically Reduced Graphene Oxide," *Analytical Chemistry,* vol. 81, no. 14, pp. 5603-5613, 2009.

[164] D. Zhang, J. Tong, B. Xia, "Humidity-sensing properties of chemically reduced graphene oxide/polymer nanocomposite film sensor based on layer-by-layer nano self-assembly," *Sensors and Actuators B: Chemical,* vol. 197, pp. 66-72, 2014.

[165] S. Zhao, H. Zhang, J. Luo, Q. Wang, B. Xu, S. Hong, Z. Yu, "Highly Electrically Conductive Three-Dimensional Ti3C2Tx MXene/Reduced Graphene Oxide Hybrid Aerogels with Excellent Electromagnetic Interference Shielding Performances," *ACS Nano,* vol. 12, no. 11, pp. 11193-11202, 2018.

[166] Z.J. Li, B.C. Yang, S.R. Zhang, C.M. Zhao, "Graphene oxide with improved electrical conductivity for supercapacitor electrodes," *Applied Science Surface,* vol. 258, no. 8, pp. 3726-3731, 2012.

[167] S.R. Shin, C. Zihlmann, M. Akbari, P. Assawes, L. Cheung, K. Zhang, V. Manoharan, Y.S. Zhang, M. Yüksekkaya. K. Wan, M. Nikkhah, M.R. Dokmeci, X. Tang, A. Khademhosseini, "Reduced Graphene Oxide-GelMA Hybrid Hydrogels as Scaffolds for Cardiac Tissue Engineering," *Nano-Micro Small,* vol. 12, no. 27, pp. 3677-3689, 2016.

[168] M.H. Norahan, M. Amroon, R. Ghahremanzadeh, M. Mahmoodi, N. Baheiraei, "Electroactive graphene oxide-incorporated collagen assisting vascularization for cardiac tissue engineering," *Journal of Biomedical Materials Research Part A,* vol. 107, no. 1, pp. 204-219, 2019.

[169] L. Fan, J. Yi, J. Tong, X. Zhou, H. Ge, S. Zou, H. Wen, M. Nie, "Preparation and characterization of oxidized konjac glucomannan/carboxymethyl chitosan/graphene oxide hydrogel," *International Journal of Biological Macromolecules,* vol. 91, pp. 358-367, 2016.

[170] Y. Zhang, M. Zhang, H. Jiang, J. Shi, F. Li, Y. Xia, G. Zhang, H. Li, "Bio-inspired layered chitosan/graphene oxide nanocomposite hydrogels with high strength and pH-driven shape memory effect," *Carbohydrate Polymers,* vol. 177, pp. 116-125, 2017.

[171] N. Nowroozi, S. Faraji, A. Nouralishahi, M. Shahrousvand, "Biological and structural properties of graphene oxide/curcumin nanocomposite incorporated chitosan as a scaffold for wound healing application," *Life Science,* vol. In press, p. 118640, 2020.

[172] A. Konwar, S. Kalita, J. Kotoky, D. Chowdhury, "Chitosan–Iron Oxide Coated Graphene Oxide Nanocomposite Hydrogel: A Robust and Soft Antimicrobial Biofilm," *ACS Applied Material Interfaces,* vol. 8, no. 32, pp. 20625-20634, 2016.

[173] K. Kosowska, P. Domalik-Pyzik, M. Nocuń, J. Chłopek, "Chitosan and graphene oxide/reduced graphene oxide hybrid nanocomposites – Evaluation of physicochemical properties," *Materials Chemistry and Physics,* vol. 216, pp. 28-36, 2018.

[174] Y. Chen, H. Wang, J. Yu, Y. Wang,, J. Zhu, Z. Hu, "Mechanically strong and pH-responsive carboxymethyl chitosan/graphene oxide/polyacrylamide nanocomposite hydrogels with fast recoverability," *Journal of Biomaterials Science-Polymer Edition,* vol. 28, no. 16, pp. 1899-1917, 2017.

[175] B. Zhang, J. He, M. Shi, Y. Liang, B. Guoabc, "Injectable self-healing supramolecular hydrogels with conductivity and photo-thermal antibacterial activity to enhance complete skin regeneration," *Chemical Engineering Journal,* vol. 400, p. 125994, 2020.

[176] M. Yang, Y. Tseng, K. Liu, Y. Cheng, W. Chen, W. Chen, C. Hsiao, M. Yung, C. Hsu, T. Liu, "Preparation of Amphiphilic Chitosan–Graphene Oxide–Cellulose Nanocrystalline Composite Hydrogels and Their Biocompatibility and Antibacterial Properties," *Applied Science,* vol. 9, no. 5, p. 3051, 2019.

[177] R. Khalili, P. Zarrintaj, S.H. Jafari, H. Vahabi, M.R. Saeb, "Electroactive poly (p-phenylene sulfide)/r-graphene oxide/chitosan as a novel potential candidate for tissue engineering," *Macromolecules,* vol. 154, pp. 18-24, 2020.

[178] S. Yang, X. Zhang, D. Zhang, "Electrospun Chitosan/Poly (Vinyl Alcohol)/Graphene Oxide Nanofibrous Membrane with Ciprofloxacin Antibiotic Drug for Potential Wound

Dressing Application," *International Journal of Molecular Science,* vol. 20, no. 18, p. 4395, 2019.

[179] S. Yang, P. Lei, Y. Shan, D. Zhang, "Preparation and characterization of antibacterial electrospun chitosan/poly (vinyl alcohol)/graphene oxide composite nanofibrous membrane," *Applied Surface Science,* vol. 435, pp. 832-840, 2018.

[180] N, Mahmoudi, A. Simchi , "On the biological performance of graphene oxide-modified chitosan/polyvinyl pyrrolidone nanocomposite membranes: In vitro and in vivo effects of graphene oxide," *Materials Science and Engineering: C,* vol. 70, no. 1, pp. 121-131, 2017.

[181] C. Yang, Z. Yan, Y. Lian, J. Wang, K. Zhang, "Graphene oxide coated shell-core structured chitosan/PLLA nanofibrous scaffolds for wound dressing," *Journal of Biomaterials Science, Polymer Edition,* vol. 31, no. 5, pp. 622-641, 2020.

[182] Y. Liu, M. Park, H.K. Shin, B. Pant, J. Choi, Y.W. Park, J.Y. Lee, S. Park, H. Kim, "Facile preparation and characterization of poly(vinyl alcohol)/chitosan/graphene oxide biocomposite nanofibers," *Journal of Industrial and Engineering Chemistry,* vol. 20, no. 6, pp. 4415-4420, 2014.

[183] A. Azarniya, N. Eslahi, N. Mahmoudi, A. Simchi, "Effect of graphene oxide nanosheets on the physico-mechanical properties of chitosan/bacterial cellulose nanofibrous composites," *Composites Part A: Applied Science and Manufacturing,* vol. 85, pp. 113-122, 2016.

[184] A.F. de Faria, F. Perreault, E. Shaulsky, L.H. Arias Chavez, M. Elimelech, "Antimicrobial Electrospun Biopolymer Nanofiber Mats Functionalized with Graphene Oxide–Silver Nanocomposites12751-12759," *ACS Applied Material Interfaces,* vol. 7, no. 23, pp. 12751-12759, 2015.

[185] N. Cai, H. Zeng, J. Fu, V. Chan, M. Chen, H. Li, F. Yu, "Synergistic effect of graphene oxide-silver nanofillers on engineering performances of polyelectrolyte complex nanofiber membranes," *Journal of Applied Polymer Science,* vol. 135, no. 19, p. 46238, 2018.

[186] L. Shao, X. Chang, Y. Zhang, Y. Huang, Y. Yao, Z. Guo, "Graphene oxide cross-linked chitosan nanocomposite membrane," *Applied Surface Science,* vol. 280, pp. 989-992, 2013.

[187] Y. Yang, Z. Dong, M. Li, L. Liu, H. Luo, P. Wang, D. Zhang, X. Yang, K. Zhou, S. Lei, "Graphene Oxide/Copper Nanoderivatives-Modified Chitosan/Hyaluronic Acid Dressings for Facilitating Wound Healing in Infected Full-Thickness Skin Defects," *International Journal of Nanomedicine,* vol. 15, pp. 8231-8247, 2020.

[188] T. Figueroa, S. Carmona, S. Guajardo, J. Borges, C. Aguayo, K. Fernández, "Synthesis and characterization of graphene oxide chitosan aerogels reinforced with flavan-3-ols as hemostatic agents," *Colloids and Surfaces B: Biointerfaces,* vol. 197, p. 111398, 2021.

[189] A.K. Mahanta, D.K. Patel, P. Maiti, "Nanohybrid Scaffold of Chitosan and Functionalized Graphene Oxide for Controlled Drug Delivery and Bone Regeneration," *ACS Biomaterials Science and Engineering,* vol. 5, no. 10, pp. 5139-5149, 2019.

[190] J. Li, N. Ren, J. Qiu, X. Mou, H. Liu, "Graphene oxide-reinforced biodegradable genipin-cross-linked chitosan fluorescent biocomposite film and its cytocompatibility," *International of Nanomedicine,* vol. 8, pp. 3415-3426, 2013.

[191] V.K. Rana, M. Choi, J. Kong, G.Y. Kim, M.J. Kim, S. Kim, S. Mishra, R.P. Singh, C. Ha, "Synthesis and Drug-Delivery Behavior of Chitosan-Functionalized Graphene Oxide Hybrid Nanosheets," *Macromolecular Materials and Engineering,* vol. 296, no. 2, pp. 131-140, 2011.

[192] R. Justin, B. Chen, "Strong and conductive chitosan–reduced graphene oxide nanocomposites for transdermal drug delivery," *Journal of Materials Chemistry B,* vol. 2, no. 24, pp. 3759-3770, 2014.

[193] J. Jia, Y. Gai, W. Wang, Y. Zhao, "Green synthesis of biocompatiable chitosan–graphene oxide hybrid nanosheet by ultrasonication method," *Ultrasonics Sonochemistry,* vol. 32, pp. 300-306, 2016.

[194] J. Chabbi, A. Aqil, N. Katir, B. Vertruyen, C. Jerôme, M. Lahcini, A. El Kadib, "Aldehyde-conjugated chitosan-graphene oxide glucodynamers: Ternary cooperative assembly and controlled chemical release," *Carbohydrate Polymers,* vol. 230, p. 115634, 2020.

[195] H. Mianehrow, R. Afshari, S. Mazinani, F. Sharif, M. Abdouss, "Introducing a highly dispersed reduced graphene oxide nano-biohybrid employing chitosan/hydroxyethyl cellulose for controlled drug delivery," *International Journal of Pharmaceutics,* vol. 509, no. 1-2, pp. 400-407, 2016.

[196] T. Figueroa, C. Aguayo, K. Fernández , "Design and Characterization of Chitosan-Graphene Oxide Nanocomposites for the Delivery of Proanthocyanidins," *International Journal of Nanomedicine* , vol. 15, pp. 1229-1238, 2020.

[197] N. Mahmoudi, N. Eslahi, A. Mehdipour, M. Mohammadi, M. Akbari, A. Samadi kuchaksaraei, A. Simchi, "Temporary skinskin grafts based on hybrid graphene oxide-natural biopolymer nanofibers as effective wound healing substitutes: pre-clinical and pathological studies in Animal Models," *Journal of Material Science: Material Medicine,* vol. 28, p. 73, 2017.

[198] T. Liu, W. Dan, N. Dan, X. Liu, X. Liu, X. Peng, "A novel grapheme oxide-modified collagen-chitosan bio-film for controlled growth factor release in wound healing applications," *Materials Science and Engineering: C,* vol. 77, pp. 202-211, 2017.

[199] Y. Zhang, J. Guan, J. Wu, S. Ding, J. Yang, J. Zhang, A. Dong, L. Deng, "N-alkylated chitosan/graphene oxide porous sponge for rapid and effective hemostasis in emergency situations," *Carbohydrate Polymer,* vol. 219, pp. 405-413, 2019.

[200] C. Mellado, T. Figueroa, R. Baez, R. Castillo, M. Melendrez, B. Schulz, K. Fernandez, "Development of Graphene Oxide Composite Aerogel with Proanthocyanidins with Hemostatic Properties As a Delivery System," *ACS Appl. Mater. Interfaces,* vol. 10, pp. 7717-7729, 2018.

[201] M. V. Deshpande, A. J. West, S. H. Bernacki, K. Luan, M. W. King , "Poly(ε-Caprolactone) Resorbable Auxetic Designed Knitted Scaffolds for Craniofacial Skeletal Muscle Regeneration," *Bioengineering,* 2020.

[202] C. C. Liang, A. Y. Park, J. L. Guan, "In vitro scratch assay: a convenient and inexpensive," Nature Publishing Group, 2007.

[203] X. Sun, Z. Tang, M. Pan, Z. Wang, H. Yang, H. Liu, "Chitosan/kaolin composite porous microspheres with high hemostatic efficacy," *Carbohydrate Polymers,* vol. 177, pp. 135-143, 2017.

[204] A. Skwarczynska ,M. Kaminska, P. Owczarz, N. Bartoszek, B. Walkowiak, Z. Modrzejewska, "The structural (FTIR, XRD, and XPS) and biological studies ofthermosensitive chitosan chloride gels with b-glycerophosphatedisodium," *Journal of applied Polymer science,* 2018.

[205] H. Qin, J. Wang, T. Wang, X. Gao, Q. Wan, X. Pei, "Preparation and Characterization of Chitosan/β-Glycerophosphate Thermal-Sensitive Hydrogel Reinforced by Graphene Oxide," *Front. Chem,* vol. 6, 2018.

[206] C. Shi, X. Chen, Z. Zhang, Q. Chen, D. Shi, D. Kaneko, "Mussel inspired bio-adhesive with multiinteractions for for tissue repair," *Journal of Biomaterials Science, Polymer Edition,* vol. 31, p. 491–503, 2019.

[207] I. Bružauskaitė, D. Bironaitė, E. Bagdonas, E. Bernotienė, "Scaffolds and cells for tissue regeneration: different scaffold pore sizes—different cell effects," *Cytotechnology,* p. 355–369, 2016.

[208] R. Xu et. al, "Controlled water vapor transmission rate promotes wound-healing via wound re-epithelialization and contraction enhancement," *Scientific reports,* 2016.

[209] P. Chadwick, J. McCardle, "Exudate management using a gelling fibre dressing," *The Diabetic Foot Journal ,* vol. 18, 2015.

[210] M. P. Ž. K. M. L. G. Kravanja, "Chitosan-Based (Nano)Materials for Novel Biomedical Applications," *Molecules,* 2019.

[211] D. Oliveira et. al, "Catechol cytotoxicity in vitro Induction of glioblastoma cell death by apoptosis," *Human and Experimental Toxicology,* p. 199–212, 2010.

[212] Y. Soh, M. H. Shin, J. S. Lee, J. H. Jang, O. H. Kim, H. Kang, Y. J. Surh, "Oxidative DNA damage and glioma cell death induced by tetrahydropapaveroline," *Mutation Research,* p. 129–142, 2003.

[213] R. Ahmadi, J. D. Bruijn, "Biocompatibility and gelation of chitosan–glycerolphosphate hydrogels," *Journal of Biomaterial Science,* vol. 68A, no. 3, pp. 824-832, 2008.

[214] S. Mukherjee , P. Sriram , A. K. Barui, S. K. Nethi, V. Veeriah, S. Chatterjee , K. I. Suresh, C. R. Patra , "Graphene Oxides Show Angiogenic Properties," *Adv. Healthcare Mater,* p. 1722–1732, 2015.

[215] A. Russo, R. Longo, A. Vanella, "Antioxidant activity of propolis: role of caffeic acid phenethyl ester and galangin," *Fitoterapia,* vol. 73, pp. 21-29, 2002.

[216] Y. RiPark. T. Sultan, H. J. Park, J. M. Lee, H. W. Ju, O. J. Lee, D. J. Lee, D. L. Kaplan, C. H. Park, "NF-κB signaling is key in the wound healing processes of silk fibroin," *Acta Biomaterialia,* pp. 183-195, 2018.

[217] T.R. Nayak et. al, "Graphene for controlled and accelerated osteogenic differentiation of human mesenchymal stem cells," *ACS Nano,* pp. 4670-4678, 2011.

[218] M. Zhou et. al, "Graphene oxide: A growth factor delivery carrier to enhance chondrogenic differentiation of human mesenchymal stem cells in 3D hydrogels," *Acta Biomaterialia,* pp. 271-280, 2019.

[219] Z. Hu , S. Lu, Y. Cheng, S. Kong, S. Li, Ch. Li, L Yang, "Investigation of the Effects of Molecular Parameters on the Hemostatic Properties of Chitosan," *Molecules,* vol. 23, 2018.

[220] V. Palmieri, G. Perini, M. De Spirito, M. Papi, "Graphene oxide touches blood: in vivo interactions of bio-coronated 2D materials," *Nanoscale Horiz*, pp. 273-290, 2019.

[221] J. W Penn, A. O Grobbelaar, K. J Rolfe, "The role of the TGF-β family in wound healing, burns and scarring: a review," *Int J Burn Trauma*, pp. 18-28, 2012.

[222] B. J. Faler, "Transforming Growth Factor-B and Wound healing," *Perspectives in Vascular Surgery and Endovascular Therapy,* vol. 18, 2006.

[223] X. Zhang, X. Kang, L. Jin, J. Bai, W. Liu, Z. Wang, "Stimulation of wound healing using bioinspired hydrogels with basic fibroblast growth factor (bFGF)," *International Journal of Nanomedicine,* vol. 13, p. 3897–3906, 2018.

[224] P. V. Mendieta, M. L. Sanchez, J. Benavides, "Rational selection of bioactive principles for wound healing applications: Growth factors and antioxidants," *Int Wound J*, 2021.

[225] L. S. Soares et. al, "Insights on physicochemical aspects of chitosan dispersion in aqueous solutions of acetic, glycolic, propionic or lactic acid," *International Journal of Biological Macromolecules*, pp. 140-148, 2019.

APPENDICES

7. APPENDIX A

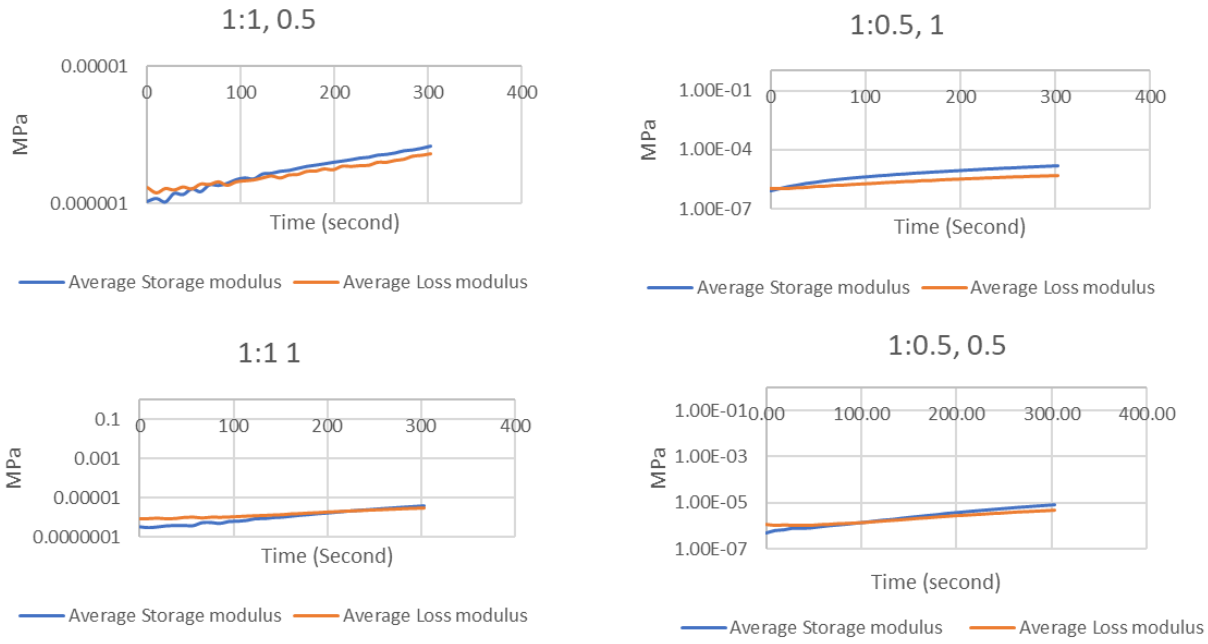

Figure 7-1 Rheological analyses of different samples showing the storage moduli (G′) and loss moduli (G″) of the samples at 1 Hz frequency and 1% dynamic strain against the gelling time

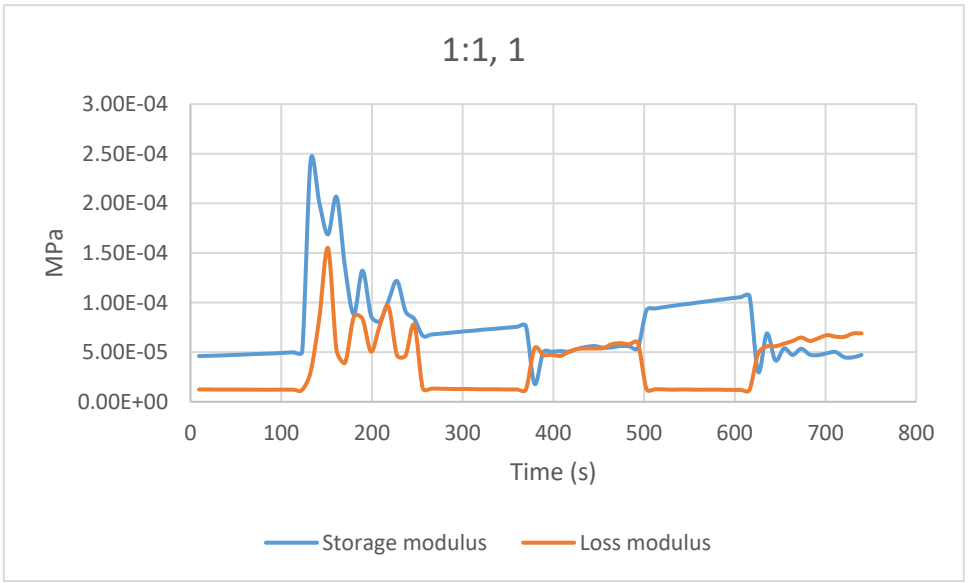

Figure 7-2. Increase number of damaging / healing cycles

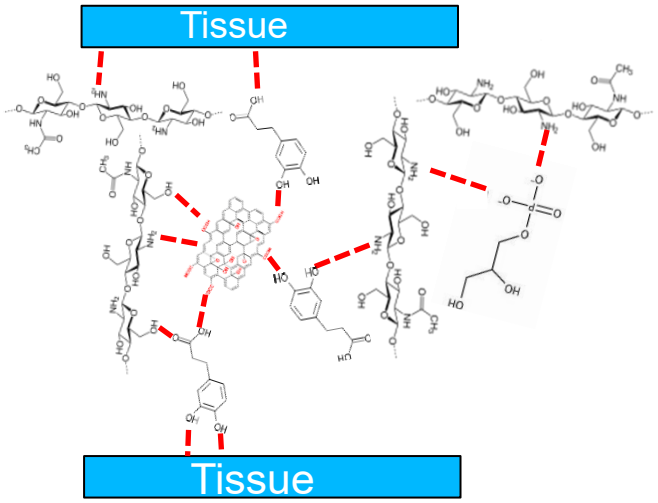

Figure 7-3. Schematic of intermolecular interactions of samples and their interactions with tissue

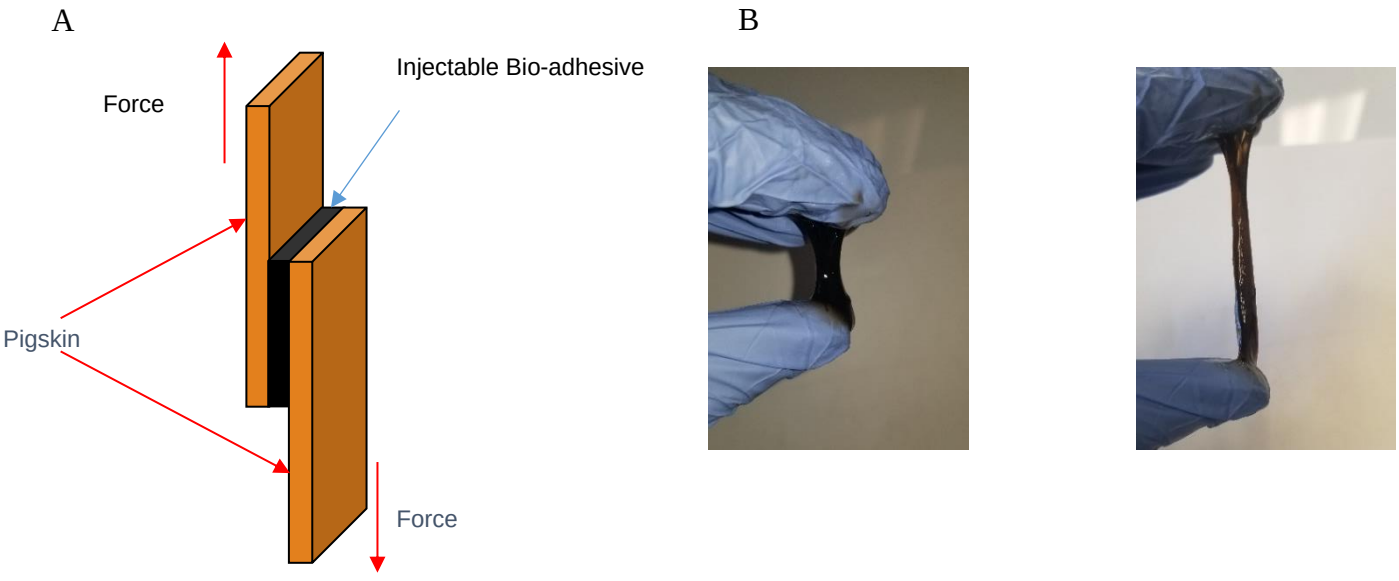

Figure 7-4. A. Schematic of lap shear test setup, B) Visual evidence of adhesive property of 1:.05, 0.5 sample

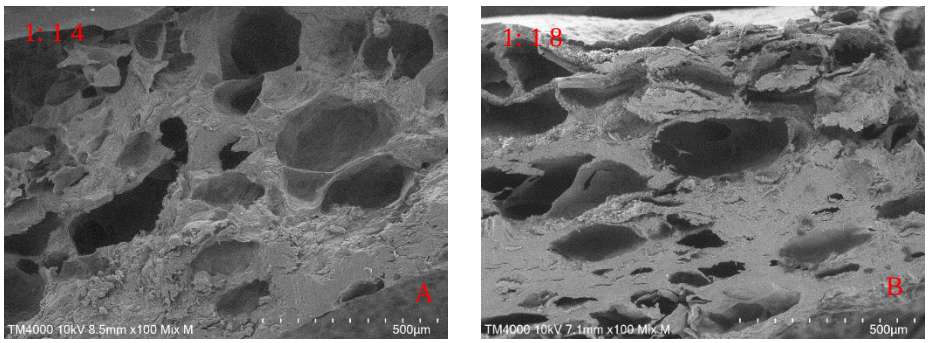

Figure 7-5. Increase GO concentration to see its effect on crosslinks and pore sizes in A) GO concentration 4 v/v%, B) 8 v/v %

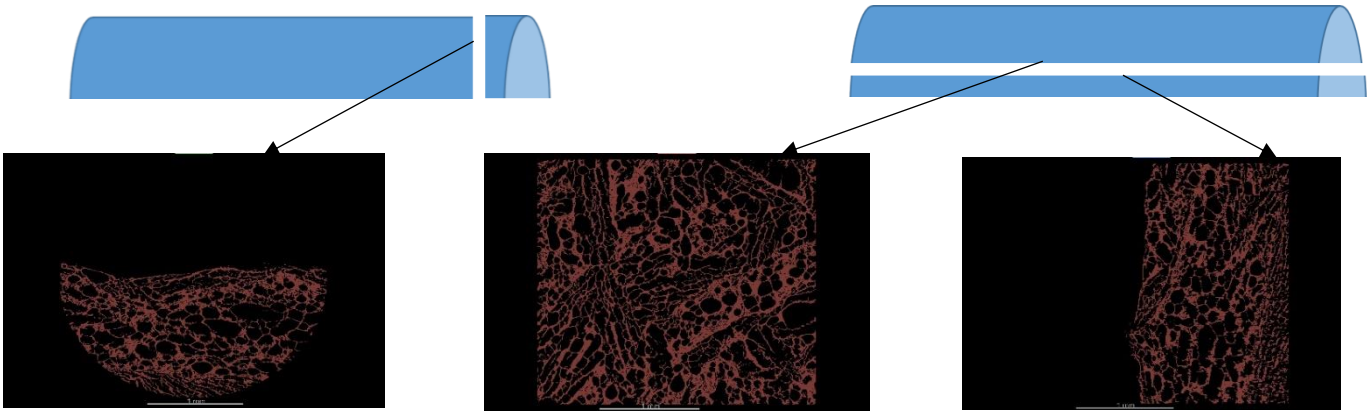

Figure 7-6. Porosity of CS/GO/HCA/BG (1:0.5, 0.5) in different cross sections taken by a Nano CT scanner

Figure 7-7. Cell attachment assay at Day 3 for all samples. Scale bars for big pictures are 500µm and for small ones are 50µm.

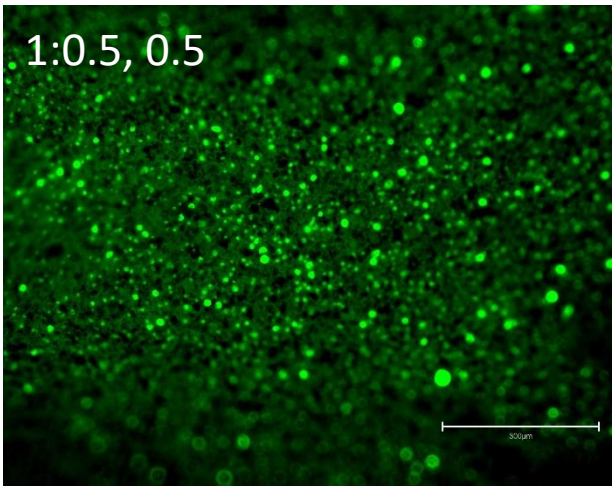

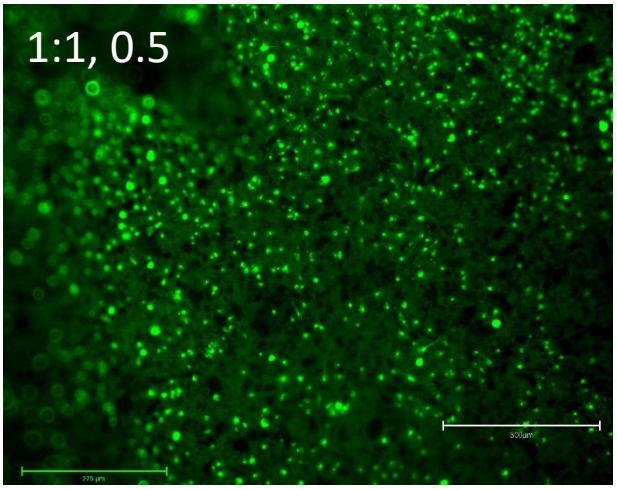

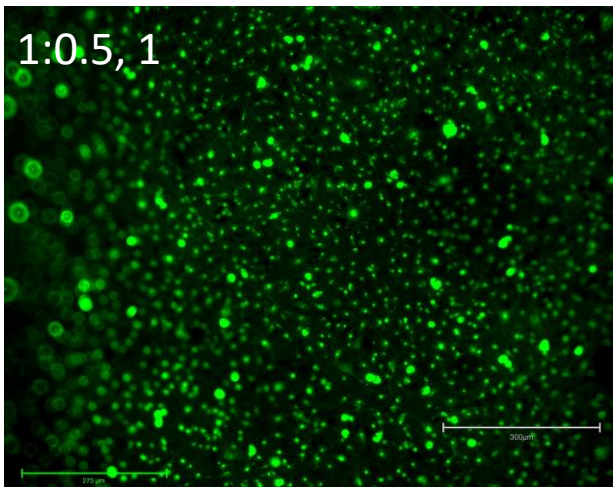

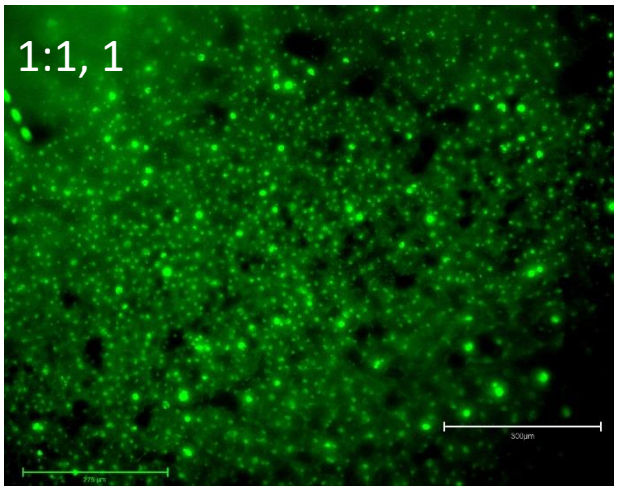

Figure 7-8. Live/Dead assay for all samples

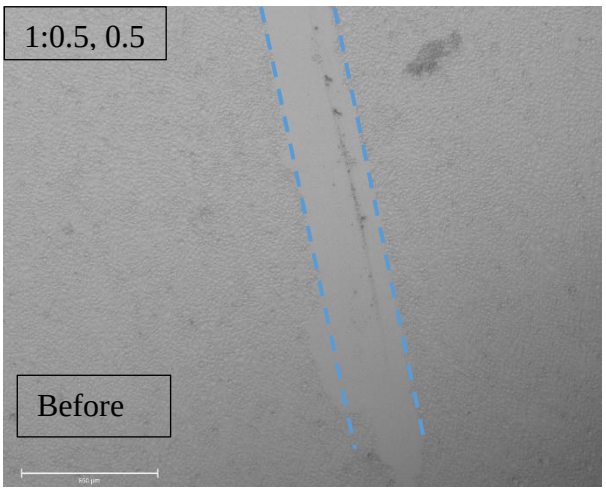

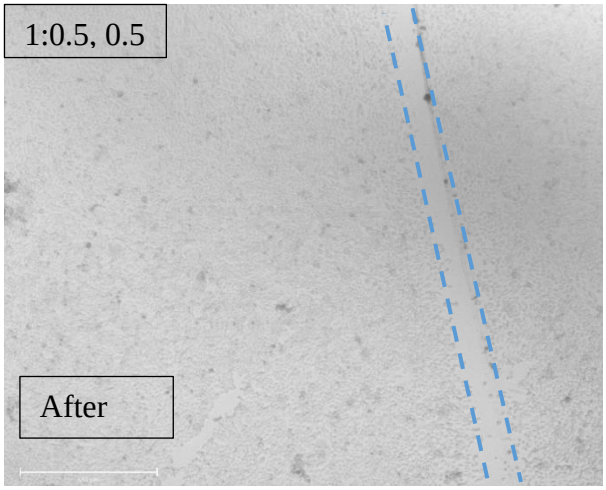

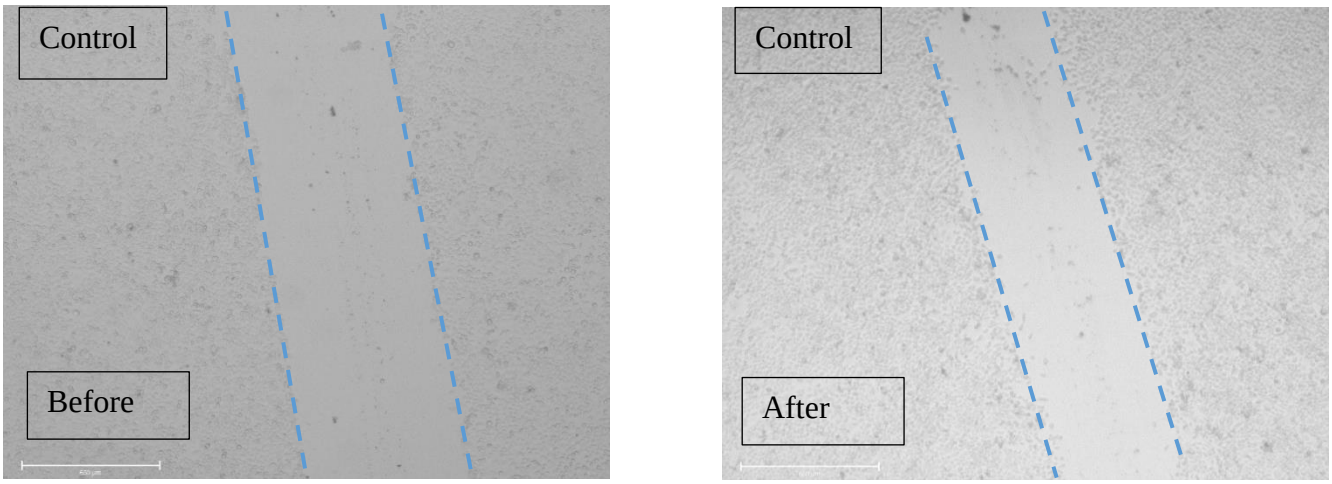

Figure 7-9. Cell migration assay for 1:0.5, 0.5 sample and control after 12 hrs.